Online Theses and Dissertations   Student Scholarship

January 2012

Deuterium Tracer Studies Of The Mechanism Of Cobalt Catalyzed Fischer-Tropsch Synthesis

Chunfen Jin
Eastern Kentucky University

Follow this and additional works at: https://encompass.eku.edu/etd

Part of the Organic Chemistry Commons

DEUTERIUM TRACER STUDIES OF THE MECHANISM OF COBALT CATALYZED FISCHER-TROPSCH SYNTHESIS
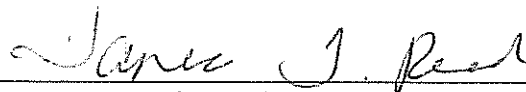
By

CHUNFEN JIN

Thesis Approved:

_____

Chair, Advisory Committee

_____

Member, Advisory Committee

_____

Member, Advisory Committee

_____

Dean, Graduate School

STATEMENT OF PERMISSION TO USE

In presenting this thesis in partial fulfillment of the requirements for a Master's degree at Eastern Kentucky University, I agree that the Library shall make it available to borrowers under rules of the Library. Brief quotations from this thesis are allowable without special permission, provided that accurate acknowledgment of the source is made. Permission for extensive quotation from or reproduction of this thesis may be granted by my major professor, or in [his/her] absence, by the Head of Interlibrary Services when, in the opinion of either, the proposed use of the material is for scholarly purposes. Any copying or use of the material in this thesis for financial gain shall not be allowed without my written permission.

Signature _____

Date _____5/10/2012_____

DEUTERIUM TRACER STUDIES OF THE MECHANISM OF COBALT CATALYZED FISCHER-TROPSCH SYNTHESIS

By

CHUNFEN JIN

Bachelor of Science
Liaoning University of Technology
Jinzhou, China

2009

Submitted to the Faculty of the Graduate School of
Eastern Kentucky University
in partial fulfillment of the requirements
for the degree of
MASTER OF SCIENCE
August, 2012

DEDICATION

This thesis is dedicated to my parents Mr. Jizheng Jin and Mrs. Mingyu Piao, who have given me unwavering educational opportunities.

ACKNOWLEDGMENTS

ABSTRACT

Since the Fischer-Tropsch (FT) catalytic polymerization reaction has been discovered in 1920s, many kinds of possible mechanisms have been reported. However, there is still debate because there is a lacking of experimental evidence to discriminate the validity of each mechanism. To define the mechanism of Fischer-Tropsch-Synthesis (FTS), we must define the C-C formation pathways as well as the structure of initiator species in the process, and finally provide an explanation in mechanistic detail as to how branched hydrocarbon compounds are formed in the reaction sequence.

In order to understand the cobalt catalyzed mechanism of FTS, we conducted H_2/D_2 switching and competition experiments, and found that there is an inverse isotope effect during FTS and there is deuterium enrichment in the hydrocarbon products. The presence of the inverse isotope effect was indicated from the H_2/D_2 switch experiments by an increase in CO conversion by changing the syngas reagent from hydrogen to deuterium during the cobalt catalyzed FTS. The inverse isotope effect was again confirmed by performing the H_2/D_2 competition experiments, and we also observed deuterium was enriched with the increasing carbon number in the FT hydrocarbon products. The findings of inverse isotope effect and deuterium enrichment, led us to propose a modified alkylidene mechanism for cobalt catalyzed FT reactions.

In order to understand structure of the C_2, C_3 species, we performed the deuterium tracer experiments, and found that the structure of C_2 and C_3 resembles ethene and propene in the Co/SiO_2 catalyzed FTS, but not alcohol.

According to the modified alkylidene mechanism, the mono-methyl branched hydrocarbons should be formed but not ethyl or dimethyl branched hydrocarbons. Branched hydrocarbons with identification of carbon number 8, 10, 11 confirmed this conclusion.

TABLE OF CONTENTS

LIST OF TABLES

LIST OF FIGURES

xiii

LIST OF SYMBOLS AND ABBREVIATIONS

α ....chain growth probability

ASF .... Anderson-Schulz-Flory

FT ....Fischer-Tropsch

FTS ....Fischer-Tropsch-Synthesis

k ....rate constant

m ....mass (g)

O ....olefin

P ....paraffin

T ....temperature

FBR ....Fixed Bed Reactor

CHAPTER 1

INTRODUCTION

Fischer-Tropsch Synthesis (FTS) was discovered in 1920s by Franz Fischer and

Hans Tropsch[1]. FTS is a catalytic reaction that converts carbon monoxide (CO) and

hydrogen (H_2) into a variety of chemicals and high quality fuel products. It became a

commercial scale industrial technique shortly after its invention despite incomplete

understanding of the underlying mechanism. This reaction attracted the attention of

governments from the very beginning due to geopolitical reasons. Large scale FT plants

were built in Germany and Japan during World War II in order to produce liquid fuel to

support the war; South Africa has employed the same technique to produce synthetic

fuels since 1950s from its abundant coal and to gain energy independence; the energy

crisis in 1970s revitalized research in synthetic fuel in most countries of the world.

Recently, there has been renewed interest in FT synthesis due to the environmental

concern and the declining supply of crude oil.

Because of the decreasing availability, and increasing demand of the fossil

energy source, to find an optimal alternative synthetic fuel formation pathway is

becoming a growing research and industry interest[2, 3]. Since the starting materials of

the reaction are carbon monoxide and hydrogen, FTS is becoming more important since

the FTS is an alternative way to convert the plenty source of biomass and coal to

1

valuable liquid fuel products[4] as shown in the Fig 1.1.This leads to understanding the

fundamentals of the FT mechanism rising in interest as well, as once the mechanism is

determined the process is likely to be more easily manipulated and more economical.
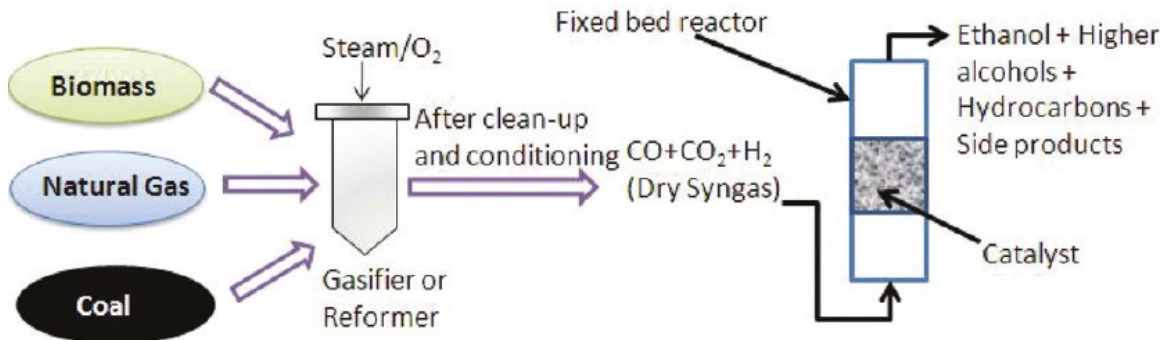
Figure 1.1: Schematic of thermochemical conversion of biomass, natural gas, and coal to valuable hydrocarbon products[5]

The FTS reaction is generally expressed as in eq. 1.1, where n is the carbon

number. The long chain hydrocarbons were synthesized by the polymerization of a C_1

species that derived from CO.

$$nCO + (2n + 1)H_2 \rightarrow C_nH_{2n+2} + nH_2O \qquad (1.1)$$
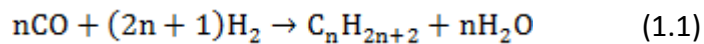
During the past 90 years, significant progresses have been made in

understanding the FT reactions. It has been used to produce fuels and chemicals in large

scale, for instance the Sasol FT process provides South Africa with about 50% of its oil

need, estimated at 60,000 barrels per day. Several transition metal catalysts are found

to be active for FTS reaction, such as iron, cobalt, ruthenium, and nickel[6-9]; different

reactors have been designed depending on the scale of the reaction. One of the most important development on the understanding of the FT reaction is FT long chain hydrocarbon product distribution follows the Anderson-Schulz-Flory (ASF) model in 1950s. The ASF eq. 1.2 was based on the Flory distribution that was developed for free-radical polymerization[10].

This equation usually leads to satisfactory correlation with the further assumption that unbranched 1-alkenes are the primary products[11]. In eq. 1.2, m_n is the mole fraction of compounds, n is a specific carbon number, and α is the chain growth probability factor, which is defined as eq. 1.3, where k_p and k_t are the rate constant of propagation and termination, respectively.

$$m_n = (1 - \alpha)\alpha^{n-1} \qquad (1.2)$$

$$\alpha = \frac{k_p}{k_p + k_t} \qquad (1.3)$$

Through decades of FT reaction studies, the following observations have been made: (1)The FT reaction is a polymerization reaction and the product distribution obeys the ASF kinetics with several exceptions[12]; (2) the major products are linear hydrocarbons[13]; (3) linear alkanes and 1-alkenes are the primary products of the reaction; (4) branched hydrocarbons can be produced; (5) oxygenates such as alcohols and aldehydes can be produced in the case of Fe catalyzed FT reactions; (6) the 1-alkenes produced can undergo the isomerization reaction to produce the corresponding trans- and cis-2-alkenes; (7) the alkenes can be readsorbed on the surface of the catalyst

and regrown; (8) a C_2 species can be considered as the initiator of this polymerization process; (9) a C_1 species derived from CO is the monomer of the FT reactions; (10) the amount of methane formed is always larger than expected from ASF kinetics; (11) the C_2 products are significantly lower than expected from the ASF equation leading to a "kick" in the product distribution diagram; (12) the relative amount of alkanes, alkenes, oxygenates and branched hydrocarbons produced through the FT reactions over different catalysts are different; and others. In order to explain these experimental facts, several mechanisms have been proposed.

Since significant amount of oxygenates (alcohols and aldehydes) are produced during Fe catalyzed FT reactions, the hydroxymethylene mechanism[13] was proposed in 1950s (Fig 1.2) to account for the formations of oxygenates as well as the long chain hydrocarbons. According to this mechanism, the monomer is M=CH(OH) which is produced in situ by reaction of CO and H_2 and the growing chain is M=C(OH)R.
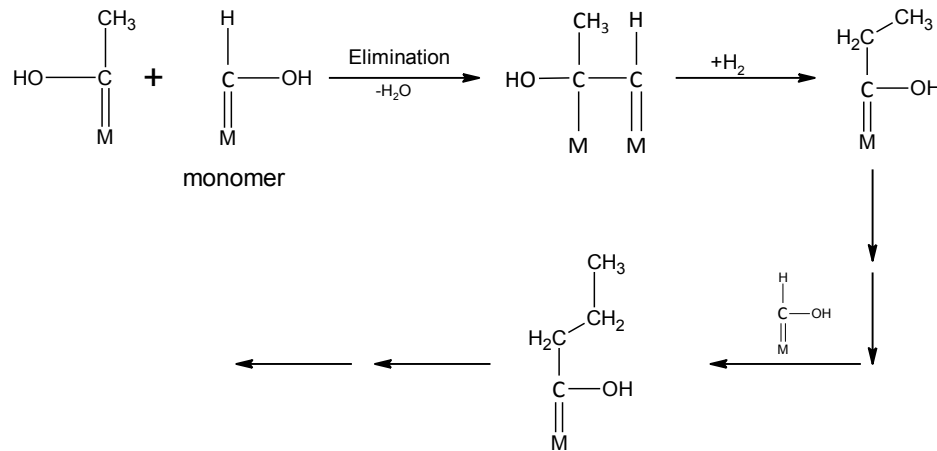
Figure 1.2: Hydroxymethylene mechanism[13]

4

A CO insertion mechanism[14] was also proposed for Fe catalyzed FT reactions (Fig 1.3). According to this mechanism, the CO is inserted into the M-C bond of a surface alkyl species M-CH₂R forming M-COCH₂R, which can then either be desorbed as oxygenates or form the surface alkyl species M-CH₂CH₂R.
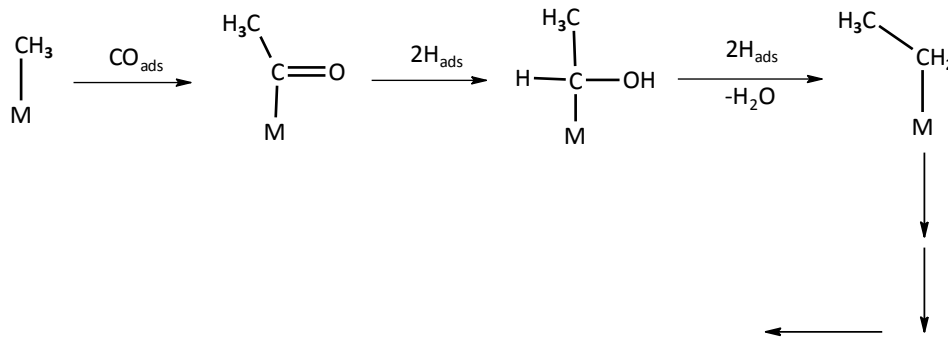
Figure 1.3: Oxygenate mechanism[14]

Based on the results of isotope tracer studies, the alkyl mechanism[15, 16] was proposed in early 1980s as shown in Fig 1.4. According to this mechanism, the monomer of this polymerization reaction is M=CH₂, which is produced in situ by reaction of CO and H₂ over catalyst. The hydrogenation of M=CH₂ produce M-CH₃, which can either react with H$_{ads}$ to produce methane or react with the monomer M=CH₂ to generate M-CH₂CH₃. Similar to M-CH₃, the M-CH₂CH₃ can either produce C_2 hydrocarbons or grow to form M-CH₂CH₂CH₃ through reaction with the monomer. This mechanism can explain the polymerization characteristics of the FT reaction but cannot explain the formation of oxygenates produced in Fe catalyzed FT reactions.

5
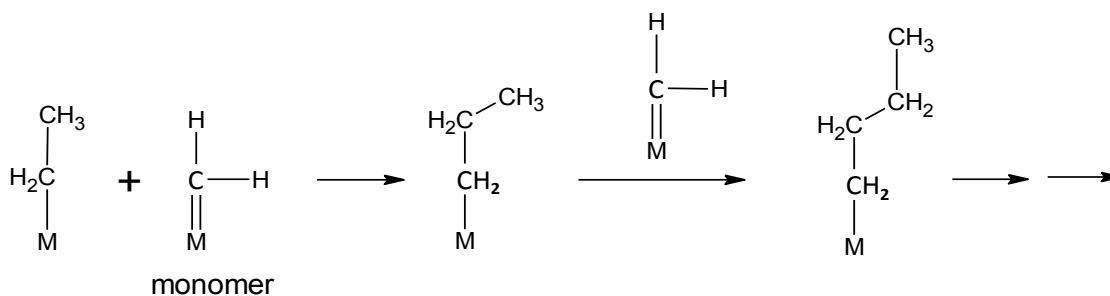
Figure 1.4: Alkyl mechanism[15, 16]

In 1990s, the alkenyl mechanism[17] was proposed as shown in Fig 1.5. This mechanism can explain not only the formation of normal alkanes and 1-alkenes but also the formation of cis- and trans-2-alkenes. According to this mechanism, the monomer of the FT reaction is $M=CH_2$ and the growing chain is M-CH=CHR. The coupling of the growing chain and monomer gives $M-CH_2CH=CH_2$, which can undergo the isomerization to generate a new growing chain by increasing one more carbon or terminate to produce the 2-alkenes.
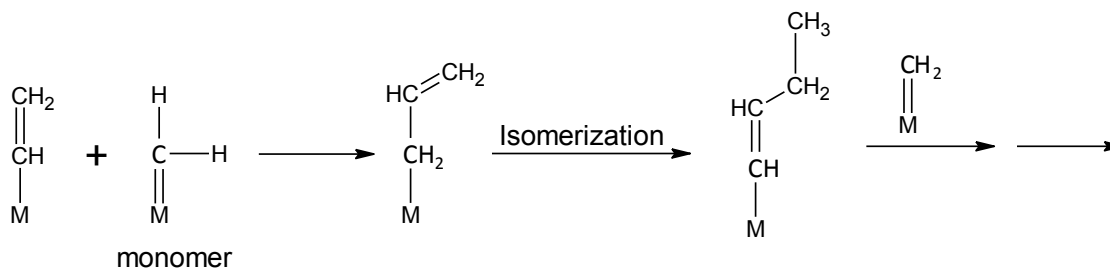
Figure 1.5: Alkenyl mechanism[17]

Other types of mechanisms, such as alkylidene mechanism[18], carbide mechanism[19] and modified carbide mechanisms[20-22] were proposed over the years in an attempt to explain the new experimental facts. All of the above mentioned mechanisms were proposed based on the solid scientific foundations and can to some extent explain the experimental facts accumulated over the years. Therefore, the mechanism for FTS remains unclear and without new experimental facts it is very difficult to distinguish these mechanisms.

Fischer-Tropsch process is also invoked to explain the formation of abiogenic hydrocarbons. It has been widely referred to explain the formation of abiogenic hydrocarbons in the micrometeorites[23, 24], interplanetary dust[25, 26], earth crust[27, 28], hydrothermal field[29-35], and solar nebula chemistry[36]; where transition metals are existent in each case. The formation pathway of abiogenic hydrocarbons has been suspected to be formed through FTS process because it has a similar trend of the Anderson-Schulz-Flory (ASF) distribution in the C_2-C_4 alkane compounds. However, whether or not the formation of abiogenic hydrocarbons is through the FTS is a hot topic of debating among geoscientists.

While Patzlaff and Liu's research group has reported that carbon dioxide and hydrogen can coexist for long intervals at temperatures and pressures as high as 400°C and 500bars[37], without a proper catalyst they cannot produce hydrocarbon compounds. The experiments under hydrothermal conditions showed that the product contents formed are similar to the FTS products. A recent study on abiogenic

hydrocarbon production at the Lost City indicated that the hydrocarbons from C_1 to C_4 found at the Lost City were produced by FT-type reactions, which could be a common pathway for producing precursors of life-essential building blocks in the ocean-floor environment. Therefore, the FT reaction is not only important in producing fuel to reach the goal of energy independence, it is also important in understanding the origins of life.

In geochemistry, the isotopic composition of oxidized and reduced forms of carbon (mainly CO_2 and CH_4) is one of the most important indicators of sources and fluxes of carbon on Earth. A limited and important part of the reduced carbon (CH_4 and higher hydrocarbons) may be products of FT-type synthesis from highly abundant (primary) magmatic CO_2 and/or (secondary) sedimentary carbonates under local or regional reduced conditions. Isotopic composition of such produced hydrocarbons showed that (i) there was ^{13}C depletion in alkanes from C_2 to C_4 relative to methane; (ii) there was deuterium enrichment in abiogenic alkanes from C_1 to C_4 and (iii) the deuterium enrichment in organic matters in meteorites was observed. Several mechanisms for the FT reaction have been used to explain these results but interpretations were not satisfactory. It seems clear that if the abiogenic hydrocarbons were indeed produced by the FT-type reactions, a new mechanism is needed to explain the isotope fractionations found in abiogenic hydrocarbons.

In the area of FT research, the inverse isotope effect in the formation of methane or light hydrocarbons has been reported. However, there is no report for the deuterium enrichment in hydrocarbons produced by the FT reaction. In this study, we

plan to answer the following questions: is there a hydrogen isotope effect during Co

catalyzed FT reaction? Is there deuterium enrichment in hydrocarbons produced by the

Co catalyzed FT reactions? What is the C_2 species during the FT reactions? How are the

branched hydrocarbons formed? The answers to these questions will provide new

insight into the mechanism for the FT reaction.

CHAPTER 2

INVERSE ISOTOPE EFFECT AND DEUTERIUM ENRICHMENT DURING THE COBALT

CATALYZED FISCHER-TROPSCH SYNTHESIS

2.1   INTRODUCTION

During nearly a century of FT mechanism studies, many kinds of possible

mechanisms have been proposed but it still remains a controversial topic [38-41]. In the

carbide mechanism[1], it involves C_1 monomer formation through the CO dissociation

and subsequent hydrogenation of absorbed carbon atom, but it does not involve

simultaneous methane and water formation process. The oxygenate mechanism[13, 42]

involves carbon-carbon formation through the water elimination steps on adjacent

hydroxycarbene groups, and this mechanism has received strong support by ^{14}C labeled

alcohol or alkene addition studies. In the carbon monoxide insertion mechanism[10], it

involves C-C formation via the CO insertion into the M-CH_3 bond. The main reason of the

FTS mechanism uncertainty is that there is still not enough evidence to prove the

complete validity of the currently proposed mechanisms. In many reports, it has been

suggested that the Fischer-Tropsch Synthesis is responsible for the natural abiogenic

hydrocarbon formations in the Earth's crust[27, 28, 43-45] and also the abiotic origin of

petroleum[46-48].

The carbon isotope and hydrogen isotope analyses have been widely performed for abiogenic hydrocarbon samples. The abiogenic hydrocarbon compounds have been analyzed based on their carbon and hydrogen isotopic compositions relative to their natural ratios in the atmosphere. Upon the carbon isotope analysis, the following trends have been found over the abiogenic hydrocarbon samples: (1)The abiogenic samples were found in natural gases in the Lost City[49]; it has been observed that the ^{13}C was increased with increasing carbon number in C_1-C_4 alkanes. (2) Abiogenic organic compounds in alkaline rocks[50, 51], natural gases from Precambrian crystalline shields[52], and mud volcanoes[53] have also been analyzed. In these samples, it has been found that the ^{13}C ratio was depleted with increasing carbon number from C_2-C_4 alkanes versus methane. This phenomenon has been considered as a signature of abiogenically derived hydrocarbon compounds. Opposing ^{13}C isotope distribution trends above from different abiogenic hydrocarbon sources led authors to suggest that the abiogenic hydrocarbon formation may have other pathways other than FTS. Upon the hydrogen isotope analysis of abiogenic hydrocarbon samples, it has been observed that the deuterium isotope ratio in C_1-C_4 alkanes was increased with increasing carbon number in the following sample sources: (1) gases from Precambrian crystalline shields[52]; (2) thermogenic gases[27]; (3) Canadian shield rocks[54].

The carbon and hydrogen isotope tracer studies have been widely used during the investigation of FTS mechanisms. In order to see whether there exists the deuterium

enrichment in hydrocarbons produced during Co catalyzed FT reaction, we conducted

H_2/D_2 competition and switching experiments.

2.2   EXPERIMENTAL

2.2.1   Reagents and Cobalt Catalysts

Reagents

The cobalt (II) nitrate and tartaric acid were purchased from the Sigma-Aldrich

company, the silica dioxide was purchased from the PQ Corporation and the tetra-

ammine-platinum (II) nitrate was purchased from Alfa Aesar Inc. The synthesis gas used

in this study was purchased from Scott-Gross Company, Inc. The synthesis gas was (CO:

H_2: N_2= 30%, 60%, 10%), (CO: D_2: N_2= 30%, 60%, 10%), and (CO: H_2: D_2: N_2=30%, 30%,

30%, 10%), respectively. The synthetic method of cobalt catalyst was obtained from the

literature [55, 56] without modification. The switch experiments were performed with

20% Co/Si catalyst, 16% Co/Si catalyst, and 16% Co/Si/Pt catalyst. The competition

experiments were performed with 20% Co/Si catalyst, 16% Co/Si catalyst, and 16%

Co/Si/Pt catalyst.

Synthesis of Co/SiO$_2$ Catalysts

20%Co/SiO$_2$(w/w) and 16%Co/SiO$_2$(w/w) catalysts were synthesized by the

method as reported in the literature[55] without modification. During the synthesis of

20%Co/SiO$_2$ catalyst, two steps of incipient-wetness impregnation were used to obtain

the catalyst. Initially, 13g of the cobalt nitrate hexahydrate was mixed with 60ml of distilled water, and it was impregnated on a SiO_2 solution. 16g of finely-ground SiO_2 and 50ml of distilled water were used in the SiO_2 solution preparation. Additional 20ml of distilled water was added into the cobalt catalyst container (500ml round bottom flask). When the Co-Si was evenly mixed, the mixture was stirred for an overnight under room temperature. Subsequently, water was evaporated out with a rotovapor, and the obtained sample was calcinated in an oven at 723K for 4hours. The 16%Co/SiO_2 catalyst was synthesized with similar method.

Synthesis of Pt promoted Cobalt Catalysts

A 0.5% Pt promoted 16%Co/SiO_2/Pt(w/w) and 16%Co/Al_2O_3/Pt(w/w) catalysts were synthesized by the method as reported in the literature[56] without modification. Three steps of incipient wetness impregnation method were used to synthesize the 0.5% Pt-promoted cobalt catalysts. During the synthesis of 16%Co/SiO_2/Pt catalyst, 13g of the cobalt nitrate hexahydrate was mixed with 60ml of distilled water. 16g of the SiO_2 was mixed with 50ml of distilled water. The cobalt and silica solution were combined into a 500ml round bottom flask and added additional 20ml of distilled water into it. When the Co-Si solution was completely mixed, the mixture was stirred for an overnight. Water was evaporated out with the rotavapor. Subsequently, the mixture of 0.12g of tetraammineplatinum (II) nitrate and 0.48g of tartaric acid was dissolved in 35ml of distilled water. The platinum solution was transferred into cobalt-silica sample, and the evenly mixed platinum promoted cobalt-silica solution was stirred for 12 hours.

Water was evaporated, and it was recalcinated at 673K for 4hours in an oven. The 16%Co/Al$_2$O$_3$/Pt was synthesized with similar method, but it was calcinated at 573K for 16hours.

2.2.2 Set up of The Fixed Bed Reactor

The FT reactions were carried out in a micro fixed-bed reactor (FBR) as shown in the Fig 2.1. One gram of cobalt catalyst and eight gram of white quartz sand was evenly mixed, and the mixture was placed in the center of the fixed-bed reactor. Above and below the catalyst, around 15g of white quartz sand was placed, and the rest space of the reactor was filled with glass wool. A thermocouple was located in the middle of the catalyst bed to measure the reaction temperature. The heavy liquid products were collected from the hot trap (60°C), and the oil products were collected from the cold trap (0°C). The gas products were collected with air bag, and analyzed by the Agilent 3000 Micro 4 channel gas chromatograph.
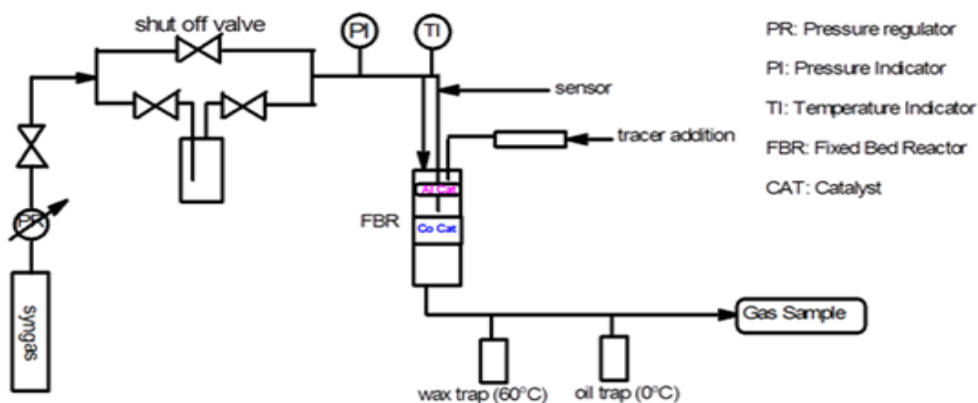
Figure 2.1: Set up of the Fixed Bed Reactor

2.2.3 General FT Experimental Procedures

Nitrogen gas was used to remove oxygen from the reactor, and gas tank was changed to the hydrogen when the gas analysis shows no oxygen component was left in the reaction system. The gas flow rate was checked under different partial pressures, and it was compared with the measured mass flow control rate in Table A-1. The gas leaking was checked by soap water at every tube connection under the pressure range from 50psi to 200psi. The flow rate was measured 6 times under different pressures ranging from 100psi up to 200psi, and the average flow rate was compared with mass flow control rate in Table A-1 to determine if there is gas leaking.

Catalyst was activated in situ with a flow of H_2 at 623K under atmospheric pressure for 12hours. The H_2 pressure was then gradually increased to the desired pressure of the reaction to make sure that there is no gas leaking at high pressure. Temperature was decreased to about 373K and the H_2 pressure was decreased to about 50Psi. The H_2 gas was then replaced by syngas (CO: H_2: N_2= 30%, 60%, 10%). At the same time, the heating and cooling systems for traps were turned on. Subsequently, the partial pressure and reactor temperature were slowly increased to 250Psi and 488K, respectively. The reaction was carried out in a synthesis gas flow control rate of 90%. Meanwhile, the hot trap temperature was increased to 333K. When the reaction conditions have reached a steady state (around 12hours), the wax and water mixture sample was collected in the hop trap (333K), and the oil and water mixture sample was collected in the cold trap (273K). The samples were combined and the top oil layer was

analyzed by a Focus gas chromatograph (GC) equipped with flame ionization detector. Gas samples were collected in every hour, and they were analyzed by an Agilent 3000 Micro 4 channel gas chromatograph. The carbon monoxide conversion was calculated for every gas sample.

2.2.4 H_2/D_2 Switching Experiment

The switch experiment was carried out with two different types of syngas CO: H_2: N_2= 30%, 60%, 10% and CO: D_2: N_2= 30%, 60%, 10%. The switch experiment was done by switching the two gasses above during the reaction process every 8 hours.

The reaction initiates with H_2/CO syngas as the reagent. When the CO conversion has reached a relatively stable condition, oil and wax traps were emptied, and the syngas was switched from (CO: H_2: N_2= 30%, 60%, 10%) to (CO: D_2: N_2= 30%, 60%, 10%). About 8 hours later, it was switched to D_2/CO syngas. After an additional 8 hours, it was switched back to the H_2/CO syngas. Wax and oil samples were collected as the syngases were switched every 8 hours. Gas samples were collected every one hour.

2.2.5 H_2/D_2 Competition Experiments

The competition experiment was carried out with the syngas (CO: H_2: D_2: N_2=30%, 30%, 30%, 10%) as the reagent of the FTS reaction. After the completion of the catalyst activation by hydrogen gas, the nitrogen gas was used to remove the hydrogen

remaining in the FBR before the syngas was introduced. After the H_2 was replaced by N_2, the syngas (CO: H_2: D_2: N_2=30%, 30%, 30%, 10%) was introduced into the reactor.

2.2.6   Product Analysis

The wax and oil liquid products obtained from competition experiments were analyzed by GC-FID and GC/MS. The mol percent of the isotopic isomers of an alkane was calculated based on the area of molecular ion of each isomer.

The relative amounts of gas products were analyzed every 1 hour using an offline Agilent 3000 Micro 4 channel gas chromatograph. The flow rates (ml/min) of H_2 gas from empty fixed bed reactor were measured under different temperatures and pressures at different percentage of the mass flow controler. The measured gas flow rates can be used to measure the volume of syngas introduced into the reactor during the reaction. For example, at $230^{\circ}C$ and 250Psi, the 90% of opening of mass flow controller gives flow rate of 125ml/min (Table A-1).

During the FTS, the gas flow rate was measured in ml/min while collecting each gas product. The gas sample was analyzed by the Agilent 3000 Micro 4 channel gas chromatograph. The percentage of CO in both syngas (provided by the manufacturer) and gas sample, the CO_{in} and CO_{out} can be calculated. The CO conversion can be calculated by eq. 2.1.

$$\text{CO conversion (\%)} = \frac{\text{volume of } CO_{in} \text{ (ml)/min} - \text{volume of } CO_{out} \text{ (ml)/min}}{\text{volume of } CO_{in} \text{ (ml)/min}} \times 100 \qquad (2.1)$$

According to the manufacturer, the CO in the syngas is 30%. At 230°C and

250Psi, the 90% of opening of the mass flow controller introduces syngas at a rate of

125ml/min. Therefore, the CO was introduced to the reactor at a rate of 37.5ml/min.

During the FT reaction, if the rate of CO coming out of the reactor is 20ml/min, the CO

conversion for this reaction will be 46.7%.

2.3   RESULTS OF H_2/D_2 SWITCHING AND COMPETITION EXPERIMENTS

2.3.1   Results of H_2/D_2 Switching Experiments

Results of the cobalt catalyzed H_2/D_2 switch experiments were shown in the

Table 2.1 with 6 different FTS runs. It summarized the results of cobalt catalyzed H_2/D_2

switching experiments with three different cobalt catalysts under different reaction

temperatures. The second column is the catalysts and component of cobalt in the

catalyst. The third column is the reaction temperatures in each run. The carbon

monoxide conversion percentages and standard deviations with each syngas were

shown. The CO conversion percentages are average number, which were calculated

based on analysis of around 6 gas samples. An example of detailed CO conversion

percentage result was shown in Fig 2.2.

Table 2.1 CO conversion during H_2/D_2 switching runs

Run	Catalyst	Temperature (°C)	CO Conversion (%) average			$[CO_{conv}]^H/[CO_{conv}]^D$
			H_2/CO	D_2/CO	H_2/CO	
1	20%Co/Si	215	28.9±1.1	34.9±1.5	29.6±1.7	0.83±0.01
2	20%Co/Si	230	42.7±1.1	45.9±1.0	41.7±0.0	0.93±0.01

Table 2.1 (continued)

3	16%Co/Si/Pt	215	28.1±1.1	41.5±1.5	25.7±1.7	0.68±0.02
4	16%Co/Si/Pt	230	43.0±0.0	55.7±2.2	39.9±2.1	0.77±0.02
5	16%Co/Al/Pt	215	17.3±2.2	18.9±2.3	13.7±1.5	0.91±0.01
6	16%Co/Al/Pt	240	52.1±1.3	55.0±1.3	51.9±1.0	0.95±0.01
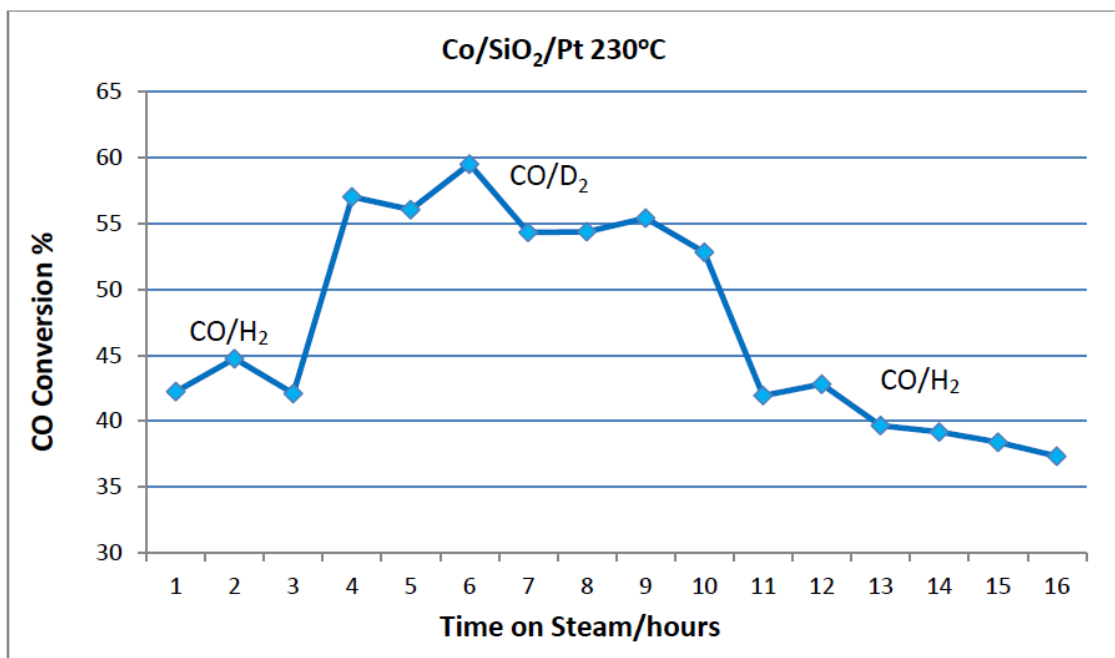
Figure 2.2: CO conversion during H_2/D_2 switching run using $Co/SiO_2/Pt$ catalyst

In the case of Co/SiO_2 catalyzed runs, the CO conversion at 215^oC was 28.9% when the syngas were CO/H_2, and it was increased to 34.9% when switching to CO/D_2. When the syngas was switched back to CO/H_2, the CO conversion was decreased to 29.6%. By the same catalyst, the CO conversions were increased to 42.7% when the temperature was increased to 230^oC if the syngas is CO/H_2. When switching to CO/D_2 at 230^oC, the CO conversion was measured to 45.9%. When syngas was switched back to CO/H_2, the CO conversion was decreased from 45.9% to 41.7%.

19

In the case of Co/SiO$_2$/Pt catalyzed H$_2$/D$_2$ switch experiment, the CO conversion at 215°C was 28.1% when the syngas were CO/H$_2$, and it was increased to 41.5% when switching to CO/D$_2$. When the syngas was switched back to CO/H$_2$, the CO conversion was decreased to 25.7%. By the same catalyst, the CO conversions were increased to 43.0% when the temperature was increased to 230°C if the syngas is CO/H$_2$ and 55.7% if the syngas was switched to CO/D$_2$.

In the case of Co/Al/Pt catalyzed H$_2$/D$_2$ switch experiment, the CO conversion at 215°C was 17.3% when the syngas were CO/H$_2$, and it was increased to 18.9% when switching to CO/D$_2$. When the syngas was switched back to CO/H$_2$, the CO conversion was decreased to 13.7%. By the same catalyst, the CO conversions were increased to 52.1% when the temperature was increased to 240°C if the syngas is CO/H$_2$ and 55.0% if the syngas was switched to CO/D$_2$.

The $[CO_{conv}]^H/[CO_{conv}]^D$ value was obtained based on the carbon monoxide conversions of the H$_2$/CO run and D$_2$/CO run. The ratios of $[CO_{conv}]^H/[CO_{conv}]^D$ are in the range of 0.68-0.95 for all runs.

2.3.2 Results of H$_2$/D$_2$ Competition Experiments

The H$_2$/D$_2$ Competition Experiments were conducted using equal amounts of H$_2$, D$_2$ and CO as the syngas. The liquid products were analyzed by GC/MS. The mol percent of each isotopic isomer of each alkane were determined. The example of nonaner is given in Fig 2.3.
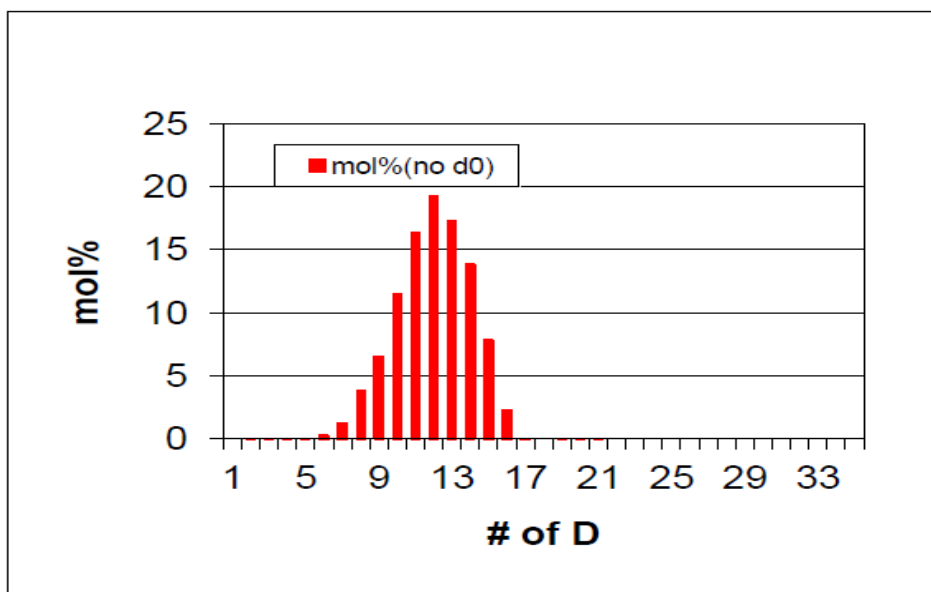
Figure 2.3: Deuterium distribution in Nonane isomers

Based on the mol% of the isotopic isomer, the H/D ratio of each alkane was calculated. The Table 2.2 summerized the results of cobalt catalyzed H_2/D_2 competition experiment with Co/Si/Pt catalyst.

Table 2.2 Ratio of H/D during H_2/D_2 competition experiment with Co/Si/Pt catalyst

Carbon Number	H/D Ratio	Carbon Number	H/D Ratio
8	0.89077	16	0.75593
9	0.84769	17	0.75520
10	0.82056	18	0.75364
11	0.79773	19	0.75003
12	0.78224	20	0.74901
13	0.77081	21	0.74579
14	0.76865	22	0.74207
15	0.76180	23	0.73580

Note: The H/D ratio was calculated based on the equation 2.2. The Co/Si/Pt catalyzed H_2/D_2 competition FT experiment was conducted once, and the product was analyzed by GC/MS only once that no experimental error can be provided.

In the Co/Si/Pt catalyzed H_2/D_2 competition FT experiment, the H/D ratios were smaller than 1, and it was decreased with increasing carbon number. The left side column is the carbon number of alkanes, and the right side column is the H/D ratio which was obtained by (eq. 2.2). The detailed results of deuterium distributions for carbon 8, 10, and 15 compounds were shown in the (Fig 2.4-Fig 2.6). The rest of carbon compounds were shown in the Appendix B (1-13).

$$\frac{H}{D} = \frac{\sum_{i=0}^{i=2n+2} i\, C_n^i}{\sum_{i=0}^{i=2n+2}(2n+2-i)\, C_n^i} \tag{2.2}$$
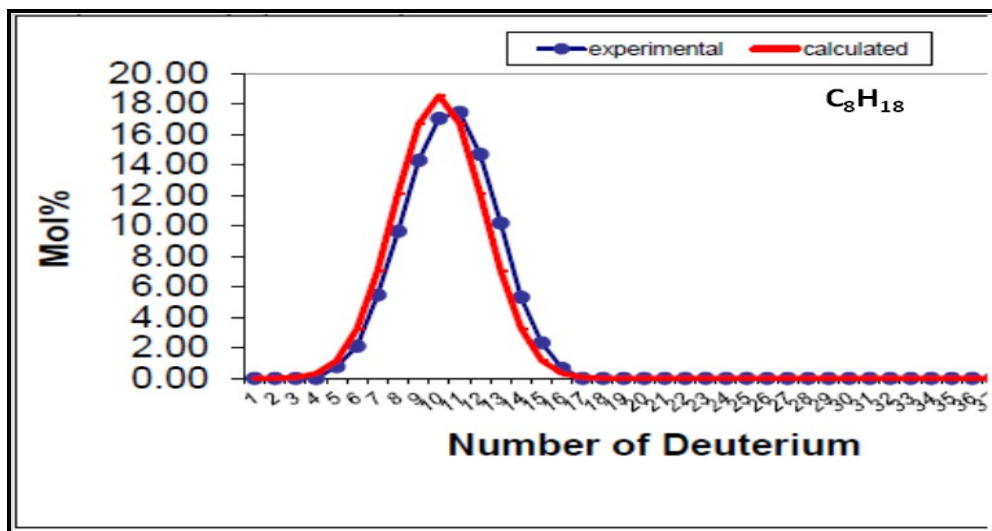
Figure 2.4: Deuterium distribution of n-Octane
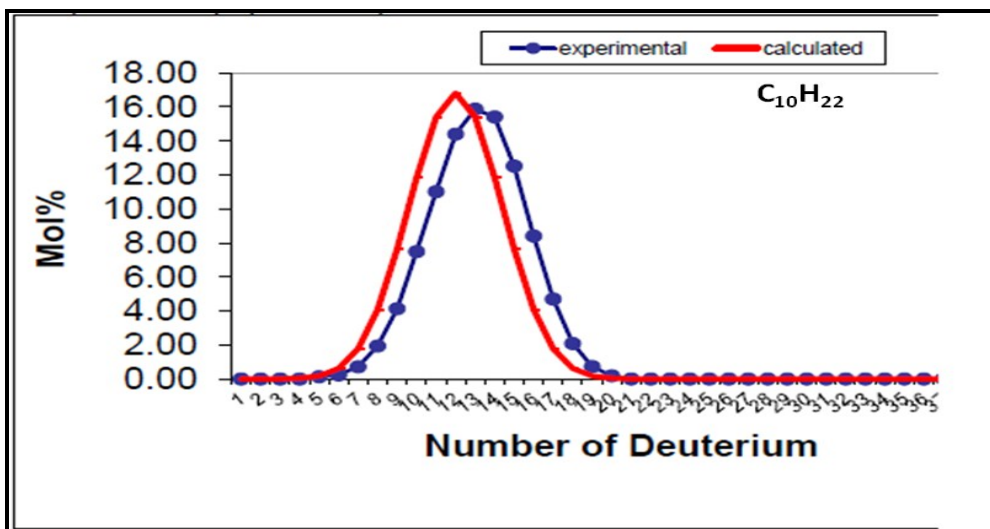
Figure 2.5: Deuterium distribution of n-Decane
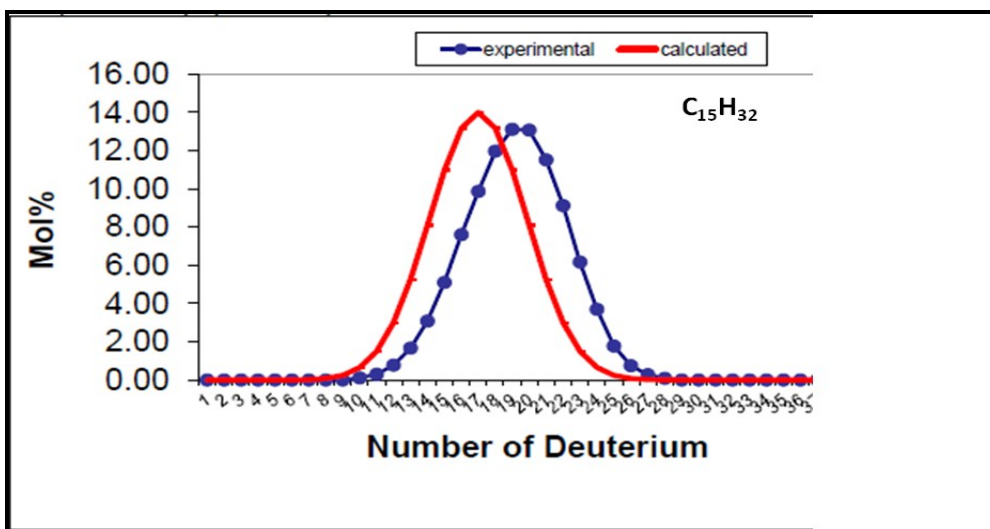
Figure 2.6: Deuterium distribution of n-Pentadecane

In the eq. 2.2, the i is the number of hydrogen in an isotopic isomer of paraffin, and n is the number of carbon, and C_n^i is the normalized value of mol% of an isotopic isomer with the carbon number of n paraffin compounds. The mol% of isotopmers of each alkane was calculated by given relative area at specific ion masses from GC/MS

data. The $\sum_{i=0}^{i=2n+2} i C_n^i$ is sum of mol% of all the hydrogen in the isotopic isomers of C_n paraffin compounds. The $\sum_{i=0}^{i=2n+2}(2n+2-i)C_n^i$ is sum of mol% of all the deuterium in the isotopic isomers of C_n paraffin products.

2.4   DISCUSSION

2.4.1   The Inverse Isotope Effect and Deuterium Enrichment in n-Alkanes

The results of cobalt catalyzed H_2/D_2 switch experiments in the Table 2.1 shows a higher CO conversion when the hydrogen was replaced by deuterium gas. The ratio of $[CO_{conv}]^H/[CO_{conv}]^D$ is at the range of 0.68-0.95 suggested that the deuterium and CO were reacted faster than hydrogen and CO, which is suggesting the presence of inverse isotope effect. Since the CO conversion is a measure of overall rate of the reaction, the results of these experiments suggest that the inverse isotope effect was originated from the rate-determining step of the FT reaction.

If the inverse isotope effect is originated from a single step of the reaction, there should be no deuterium enrichment in hydrocarbons since only one or two hydrogens (deuteriums) were involved in this step, leading to H/D equal to 1. However, if the inverse isotope effect was originated from multiple steps, the H/D will be less than 1, resulting in the deuterium enrichment.

If there is no isotope effect, the H/D ratio is equal to 1. If there is normal isotope effect and multiple steps were involved in generating the isotope effect, the deuterium distribution pattern in the H_2/D_2 competition experiment product can be represented as the Fig 2.7.
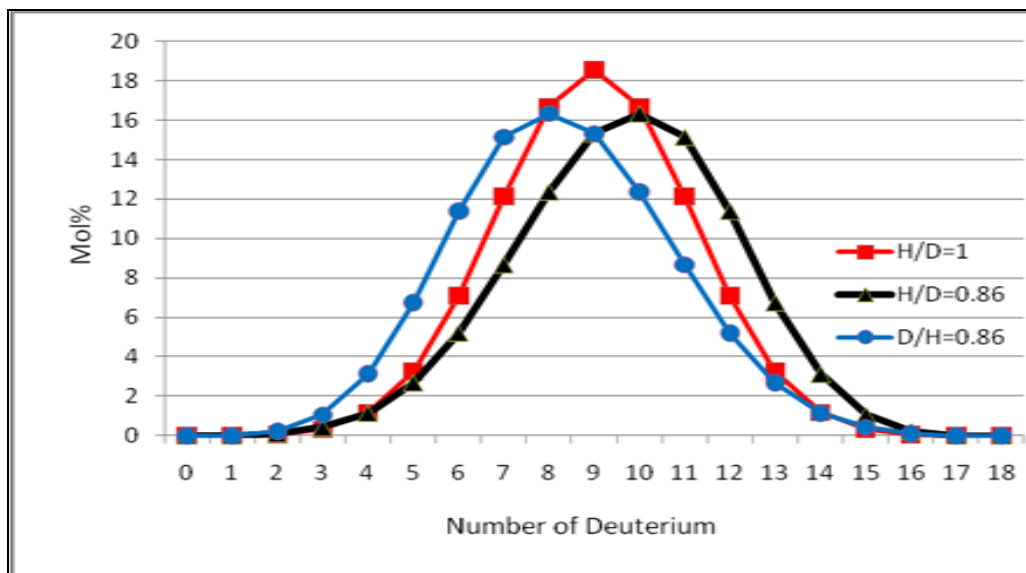
Figure 2.7: Theoretically calculated deuterium distribution of octane products

Notes: The red line is a deuterium distribution with no isotope effect, the blue line is primary isotope effect in the FTS, and the black line is the deuterium distribution pattern with the inverse isotope effect in the FTS.

Through the cobalt catalyzed H_2/D_2 competition experiments, it has clearly shown that the H/D ratio in each n-alkane is smaller than 1, and it has also shown that the ratio of H/D was decreased with increasing carbon number as shown in the Table 2.2. It also can be seen that the experimental deuterium distributions were shifted more to the right with the increasing carbon number in n-alkanes (Fig 2.4-Fig 2.6, and

Appendix B1-B13). In other words, the number of deuterium was enriched with increasing carbon number in n-alkanes.

The result of H/D ratio is smaller 1 in the cobalt catalyzed H_2/D_2 competition FT experiment in Table 2.2 is consistent with the result of inverse isotope effect obtained by H_2/D_2 switch experiments. Moreover, the decreasing in H/D ratio with increasing carbon number revealed that the inverse isotope effect is originated in each step of the chain propagations.

This Fig 2.8 clearly expresses the relationship of the H/D ratio and carbon number, which the H/D ratio is decreasing with increasing carbon number of each alkane. The correlation on the ratio of H/D and increasing carbon number indicating that the deuterium was enriched in the steps of C-C bond formation processes. This result indicates that the inverse isotope effect is generated by both of the monomer and growing chain during the chain propagation. Furthermore, since the inverse isotope effect is involved in both the monomer and the growing chain during the carbon-carbon bond formation, the number of deuterium will be increased in each carbon compound because it is reacting faster with the deuterium than hydrogen. This leads to the incorporation of more deuterium into longer hydrocarbons. If this were not the case then the ratio of H/D would remain constant.

The inverse isotope effect was considered to be result of a hybridization change of the carbon from sp^2 to sp^3 or from sp to sp^2[57]. In other words, if there is inverse isotope effect in a reaction, there is hybridization change of the carbon from sp^2 to sp^3

or from sp to sp^2. Since the steps generating inverse isotope effect are controlling the overall reaction rate during C-C formation with deuterium enrichment, the hybridization change is present not only on growing chain or monomer but both.
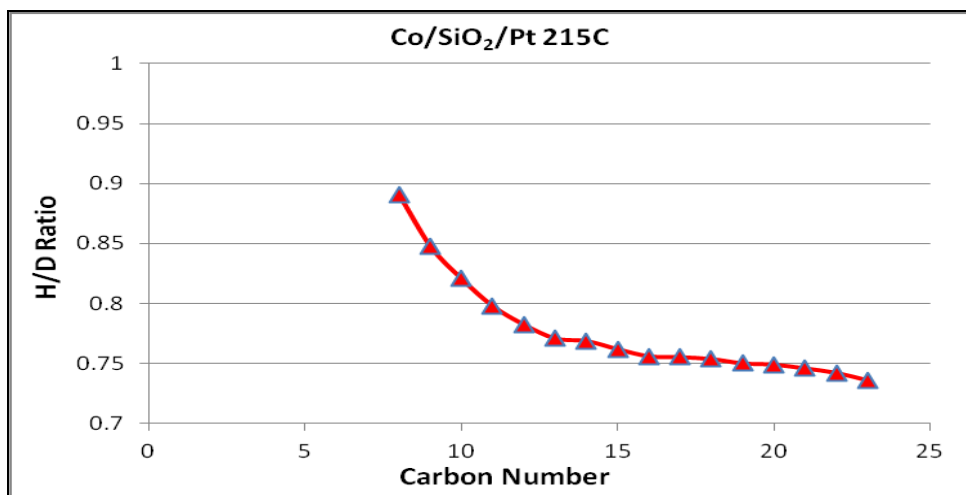
Figure 2.8: The H/D ratio versus carbon number

Notes: The H/D ratios were calculated by eq. 3.1. This result was obtained by analyzing the Co/SiO$_2$/Pt catalyzed liquid samples.

Above results indicate (1) there is an inverse isotope effect during cobalt catalyzed FT reaction; (2) this inverse isotope effect is originated from the propagation step of the FT reaction; (3) the inverse isotope effect is originated from each step of the propagation; and (4) both the monomer and the growing chain can produce the inverse isotope effect.

These new experimental facts need to be explained by a mechanism for the FT reaction. For the hydroxymethylene mechanism[58] as shown in Fig 2.9, the carbon-

carbon bond formation is through the dehydration process that it does not involve bond

order change by adding the monomer into the growing chain, which indicates that there

will be no inverse isotope effect during the propagation.
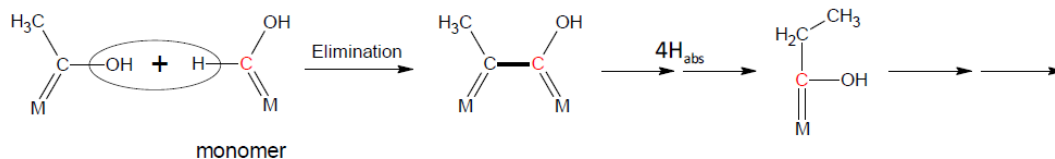
Figure 2.9: C-C bond formation in the Hydroxymethylene mechanism

For the alkyl mechanism[15, 16] as shown in the Fig 2.10, the formation of a

growing chain is involved a hybridization change of the monomer $M=CH_2$, which was

changed from a sp^2 carbon to a sp^3. This mechanism can explain the inverse isotope

effect obtained from switching experiments but cannot explain the H/D ratio decreasing

with increasing carbon number. According to this mechanism, the H/D ratio in

hydrocarbons should be less than 1 but the same for different hydrocarbons.
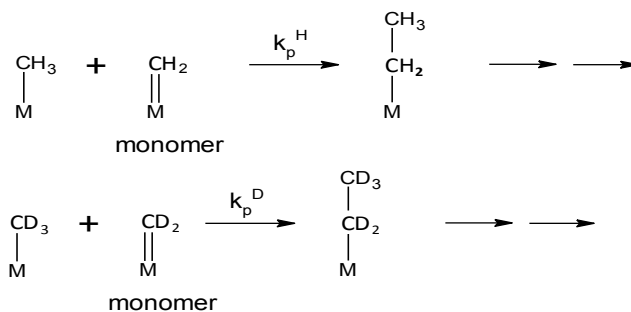
Figure 2.10: C-C bond formation in the Alkyl mechanism

28

Similar to Alkyl mechanism, the alkenyl mechanism (Fig 2.11) can explain the result of the inverse isotope effect by the hybridization change of the monomer as it changes from a sp^2 carbon to a sp^3 carbon, but it cannot explain the results of deuterium enrichment with the carbon number.
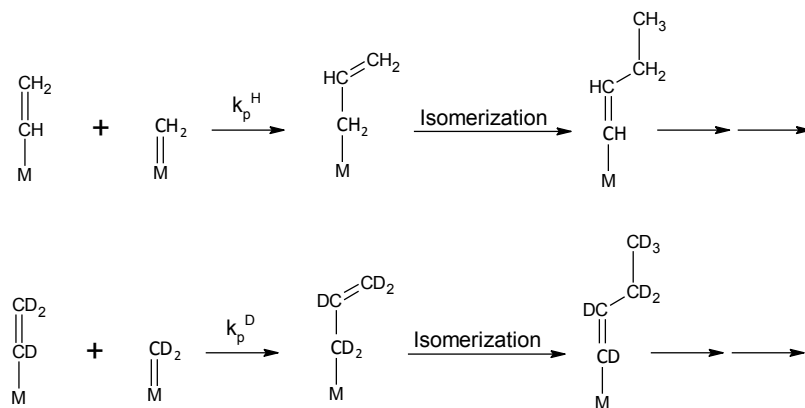
Figure 2.11: C-C bond formation in the Alkenyl mechanism

2.4.2 Modified Alkylidene Mechanism over the Co Catalyzed FTS

In order to explain the results of inverse isotope effect obtained from the H_2/D_2 switching and competition experiments, the modified alkylidene mechanism was proposed[59] as shown in the Fig 2.12 and Fig 2.13.
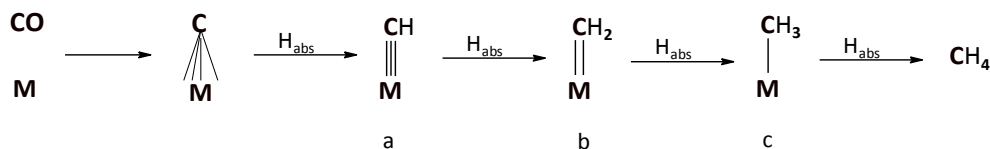
Figure 2.12: Catalyst surface C_1 species formation pathways
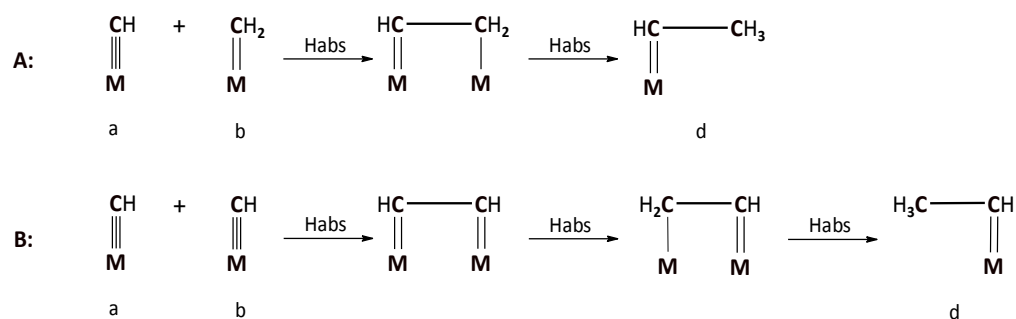
Figure 2.13: Catalyst surface C-C bond formation into C_2 species

The modified alkylidene mechanism utilizes an alkylidene growing chain and M≡CH as the monomer. During the carbon-carbon formation, the growing chain sp^2 carbon is hybridized into a sp^3 carbon and the monomer sp carbon is hybridized into a sp^2 carbon to generate the inverse isotope effect. In other words, the inverse isotope effect can be produced by both of the growing chain and the monomer during the C-C formation process, which will also result in the deuterium enrichment in alkanes produced by the FT reaction.

The formation of C_1 species has been shown in Fig 2.12, which also indicates how the methane being formed. As for the formation of C_2 species, it could be the pathway A or the pathway B (Fig 2.13).

In the Fig 2.14, the chain propagation pathways were shown. During the chain propagation, it forms the C-C bond with the hybridization change from sp^2 to sp^3 on growing chain and hybridization change from sp to sp^2 on monomer. Therefore, as shown in Fig 2.14, the deuterium will be enriched during the chain growing steps.
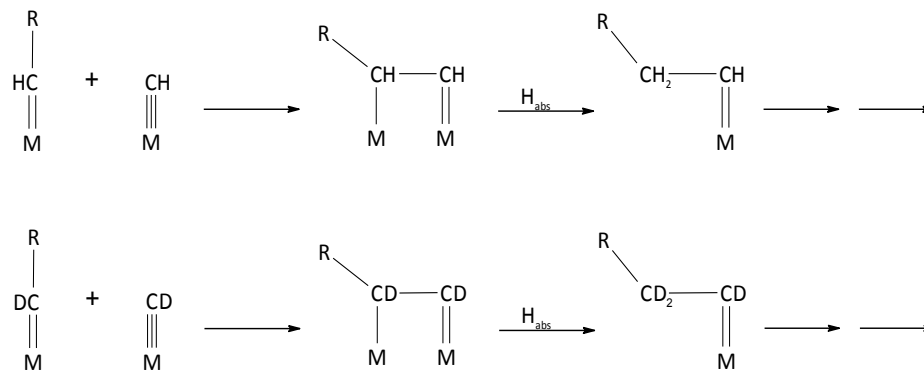
Figure 2.14: Catalyst surface long chain C-C formation

2.4.3 Further Insight of The Modified Alkylidene Mechanism

Since the FTS is a polymerization reaction, it involves rate of chain initiation (r_i),

rate of chain propagation (r_p), and rate of chain termination (r_t). This indicates that the

rate determining step of FTS must be originated from one of these three steps.

Previously, the Anderson Schulz Flory (ASF) equation has been used to describe the rate

of production of products[60]. ASF equation describes the distribution of polymers

based on the molecular weight of compounds[61]. Under most of the reaction

conditions, the Fischer-Tropsch type hydrocarbon products follow the ASF distribution

with increasing carbon chain length [62, 63].The ASF equation involves one carbon atom

addition at a time at one end of the growing chain at the end or penultimate

carbons[61].

In the ASF equation, carbon n compound (r_n) production rate has been

introduced by the equation $r_n = r_1 \alpha^{n-1}$, in which r_1 represents the formation rate of C_1

initiator, α represents the chain growth probability [52]. The chain growth probability α,

in the polymerization reaction represents the C_n species will add another C_1 species to become C_{n+1} on the catalyst surface, instead of leaving the catalyst surface as product. Subsequently, the chain growth probability α can be defined as eq. 2.3.

$$\alpha = \frac{r_p}{(r_p + r_t)} \qquad (2.3)$$

For the reactions that use CO/H_2 as the syngas, $r_n^H = C_1^H(\alpha_H)^{n-1}$. Under exactly the same reaction conditions, for the reaction that use CO/D_2 as the syngas, $r_n^D = C_1^D(\alpha_D)^{n-1}$. Thus we have eq. 2.4.

$$\frac{r_n^H}{r_n^D} = \frac{C_1^H}{C_1^D}\left(\frac{\alpha_H}{\alpha_D}\right)^{n-1} \qquad (2.4)$$

It has been reported that the $(\alpha_H/\alpha_D)^{n-1}$ can be hypothesized as the formation rate of C_n, which has the average molecular weight of FT alkane products[64]. It has been known that in the cabalt catalyzed FTS, it mainly produces the linear paraffin and some 1-alkene and 2-alkene products[65, 66] and water, but the water-gas-shift reaction was inactive with cobalt catalysts. This indicates that the CO conversion is mainly contributed to the linear alkane hydrocarbon product formations, and the α_H/α_D can be expressed as eq. 2.5 by considering the n as a carbon number of an alkane, which has average molecular weight of alkanes.

$$\frac{\alpha_H}{\alpha_D} = \sqrt[n-1]{\frac{CO_{conv}^H}{CO_{conv}^D}} \qquad (2.5)$$

The ratio of α_H/α_D can be evaluated by CO conversion because the change of reaction rate was displayed by the change of CO conversion. The $[CO_{conv}]^H/[CO_{conv}]^D$

varies with changing in CO conversion level and they have wide range of 0.68-0.95 as

shown in Table 2.3. The α_H/α_D has been calculated for each H_2/D_2 switch experiments as

shown in Table 2.3. The α_H/α_D values range from 0.93-0.98 and they were calculated by

assuming that the average molecular weight of the reaction could be calculated based

on the molecular weight of alkanes from methane to C_{40} alkane[65].

Table 2.3 Results of α_H/α_D calculation values

Run	Catalyst/T(^{o}C)	$[CO_{conv}]^H/[CO_{conv}]^D$	α_H/α_D
1	20%CoSi/215	0.83±0.01	0.96±0.01
2	20%CoSi/230	0.93±0.01	0.98±0.01
3	16%CoSiPt/215	0.68±0.02	0.93±0.01
4	16%CoSiPt/230	0.77±0.02	0.98±0.01
5	16%CoAlPt/215	0.91±0.01	0.98±0.01
6	16%CoAlPt/240	0.95±0.01	0.98±0.01

The kinetic isotope effect was quantitatively defined as the ratio of rate constant

k_H/k_D, and it was derived from the Arrhenius equation, in which the rate constant k is

depended on the temperature[67]. Upon the isotope effect, it was displayed as a

change of reaction rate with the isotopic substitution, and there are three major types

of isotope effects. They are the primary isotope effect, the secondary isotope effect, and

inverse isotope effect[68], respectively.

The primary isotope effect is generally defined as: during the isotopic

substitution, the primary isotope effect involves C-H (C-D) bond breakage, and the

reaction rate over hydrogen is faster than the reaction rate over deuterium, which can be expressed as $k_H/k_D \approx 6.0$.

The secondary isotope effect is defined as; during the isotopic substitution, the compound does not involve bond breakage in the reaction, it has a hybridization change from sp^3 to sp^2 during C-C bond formation and the reaction rate over hydrogen is also faster than the reaction rate over deuterium, which can also be expressed as $k_H/k_D \approx 1.4$.

The inverse isotope effect is an inverse type of secondary isotope effect. In other words, it can be defined as: during the isotopic substitution, the compound does not involve bond breakage in the reaction. Additionally, the heavier substrate reacts faster than the lighter one during the hybridization change from sp^2 to sp^3 or from sp to sp^2, leading to $k_H/k_D < 1$. The inverse isotope effect has also been illustrated quantitatively by bending vibrations as shown in the Fig 2.15[69].
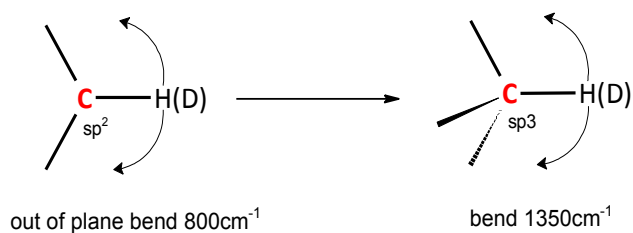
Figure 2.15: C-H vibration changes from sp^2 to sp^3

The stretch-stretch and the in-plane bend to bend vibrations were not taken into account because their contribution to the isotope effect was small enough to be

neglected[68]. The inverse isotope effect can be evaluated by the following eq. 2.6 according to the equation of the secondary isotope effect[67]:

$$\frac{k_H}{k_D} \approx \exp[-\frac{0.1865}{T}(v_{rH} - v_H)]$$
(2.6)

At 298K, the transition state is more close to sp^3 hybridized product, and the theoretically obtained ratio of k_H/k_D is 0.71 as shown in the eq. 2.7 when the inverse isotope effect exist in a reaction. However, the experimental values are usually in between 0.8 to 0.9[70]. According to the experimental value, the difference of vibration value during the transition state has been calculated, which is in the range of $168cm^{-1}$ ~ $356cm^{-1}$ as shown in the eq. 2.8. These numbers indicate that there exist hybridization change, but the change is smaller than the change from sp^2 conformation to sp^3 conformation. Based on the experimental transition state vibration values and our FT reaction temperature 493K ($220°C$), the ratio of rate constant range 0.87-0.94 were obtained as shown in the eq. 2.9. In other words, if there is inverse isotope effect in the cobalt catalyzed FT reaction, the ratio of rate constant should fall into the range of 0.87-0.94. The detailed calculations were shown in eq. 2.7-2.9. The α_H/α_D ratios in Table 2.3 are consistent with the result of inverse isotope effect.

$$\frac{k_H}{k_D} = \exp\left[-\frac{0.1865}{298K}(1350 - 800)\right] = 0.71 < 1 \quad x = 550cm^{-1}$$
(2.7)

$$\frac{k_H}{k_D} = \exp\left[-\frac{0.1865}{298K} * x\right] \approx 0.8{\sim}0.9 \quad x = 168cm^{-1}{\sim}356cm^{-1}$$
(2.8)

$$T = 493K\ (220°C), \text{and } x = 168{\sim}356cm^{-1} \quad \frac{k_H}{k_D} = 0.87{\sim}0.94$$
(2.9)

2.5   CONCLUSION

During the investigation of cobalt catalyzed FT mechanism, H_2/D_2 switching experiments and H_2/D_2 competition experiments were undertaken. The results of switching experiment in the Table 2.1 implied that the reaction rate is faster with deuterium reagent than the hydrogen reagent, which indicate the inverse isotope effect exists as rate determining step through the hybridization change. Additionally, the results of competition experiments in the Fig 2.8 implied that the deuterium got enriched during the carbon-carbon formation steps, which revealed the inverse isotope effect was generated by both of the growing chain and the monomer, and lead to the deuterium enrichment with increasing carbon number.

Most of the previously reported mechanisms can explain the result of inverse isotope effect, but they are only relating to the hybridization change over the monomer that the H/D ratio will remain as a constant. The H_2/D_2 competition experiment results implied that the inverse isotope effect is present along with the deuterium enrichment with increasing carbon number under cobalt catalyzed FTS.

Based on the results of inverse isotope effect and deuterium enrichment, the modified alkylidene mechanism has been proposed[59], and this mechanism has provided more reliable explanation over the mechanism of cobalt catalyzed FTS. However, how the C_2, C_3 initiator structure were originated is still under debating, and new method were need to find the information over the structure of initiators.

CHAPTER 3

THE STRUCTURE OF C_2 AND C_3 SPEICIES DURING COBALT CATALYZED FISCHER-

TROPSCH SYNTHESIS

3.1   INTRODUCTION

In order to understand the formation of long chain hydrocarbons in the Fischer-

Tropsch reaction, ^{14}C tracer studies have been performed under different reaction

conditions with iron and cobalt catalysts. During the mechanism studies of the FTS,

radioactive alcohols and alkenes have been used as the tracer. Among the tracer

addition experiment, the C^{13} and C^{14} [12, 71-76] labeled alcohol and alkene additions

have been conducted. The mechanisms, such as the hydroxylmethylene mechanism [13,

77], alkyl mechanism[15, 16], and alkenyl mechanism[17], were proposed mainly based

on the isotope tracer studies.

Through the addition of C^{13} and C^{14} [12, 71-76] labeled C_2 and C_3 tracer species,

the constant radioactivity of the hydrocarbon products on a per molar basis was

observed by adding 2, 3, or 4 carbon atom alcohols and alkenes. These results indicate

that the C_2 or C_3 species derived from C_2 or C_3 tracers are acted as the initiators.

In the addition of radioactive carbon atom alcohols with iron catalyzed FTS, it has

been reported that constant molar radioactivity was observed in the hydrocarbons.

Therefore, they concluded that the alcohols acted as chain initiators in the propagation

steps[78, 79]. However, in the addition of radioactive carbon atom alkenes under iron catalyzed FT reaction conditions, constant molar radioactivity was also observed. They reported that the ethylene acted as the C_2 initiator of the long chain hydrocarbon products[80]. Obviously, these contradictory results do not afford an adequate explanation over the structure of the C_2 initiator promoted by the metal catalyst.

The addition of deuterated ethanol has been performed as tracer under iron catalyzed FT reaction[81] conditions. Based on the liquid product analysis, it has been observed that the deuterated ethanol was incorporated into the FT hydrocarbon products, and the number of deuterium showed nearly constant values of atoms per molecule at 1.3-1.5. These results of deuterium labeled alcohol addition experiments under iron catalysts led authors to conclude that the ethanol undertaken deuterium/hydrogen exchange before it had been incorporated into the growing chain, and they also reported that both of the ethanol and ethylene have the possibility to be derived as the C_2 initiator.

The investigation over the C_2 initiator also has been conducted by the addition of ethanol in the absence of a syngas reagent under the Co/TiO_2 catalyzed FTS conditions, and it was reported that ethanol was incorporated into the FT hydrocarbon products[82]. In order to have a deeper understanding over the detailed structure of the C_2 and C_3 initiator, and the FT propagation pathways, we conducted Co/SiO_2 catalyzed alcohol-addition experiments.

3.2 EXPERIMENTAL

3.2.1 Alcohol Addition Reagents and Catalysts

Ethanol-d_6, 1-Propanol and 2-Propanol-d_8, n-Hexane, Al_2O_3, ethanol, and cobalt (II) nitrate hexahydrate were all purchased from Sigma-Aldrich Co. The silica dioxide (SiO_2) was purchased from the PQ Corporation. The catalyst used in the alcohol tracer studies were our 16% Co/SiO_2 (w/w) catalyst, and it was synthesized by the same method in the literature[55]. Two type of synthesis gas reagents were used in the alcohol addition experiments, which were purchased from the Scott-Gross Company, Inc. They are: (1). H_2, 60±1%; CO, 30±1%; N_2, 10%. (2). D_2, 60±1%; CO, 30±1%; N_2, 10%. The hydrogen synthesis gas reagent was used during the addition of deuterated alcohols, and deuterium synthesis gas reagent was used during the addition of non-deuterated alcohol addition experiments.

3.2.2 Alcohol Addition Procedure

Alcohols were added into FTS reactions under two conditions, one was conducted only with the 16%Co/ SiO_2 catalyst, and the other one is conducted with 16%Co/ SiO_2 catalyst and Al_2O_3 dehydration catalyst. In the second type of addition experiments, the Al_2O_3 dehydration catalyst was placed 5cm above the 16%Co/ SiO_2 catalyst. The detailed information was listed in the Table 3.1.

Table 3.1 Addition experiment conditions, catalyst, and incorporation results

Run	FT catalyst	Tracer	Synthesis Gas	Concentration of Alcohol in hexane (%)	Flow Rate	Al_2O_3	Incorporation
1	Co/SiO_2	Ethanol-d6	$H_2/CO/N_2$	10%	0.03ml/min	No	No
2	Co/SiO_2	2-Propanol-d8	$H_2/CO/N_2$	10%	0.05ml/min	No	No
3	Co/SiO_2	Ethanol-d6	$H_2/CO/N_2$	15%	0.04ml/min	Yes	Yes
4	Co/SiO_2	Ethanol	$D_2/CO/N_2$	30%	0.04ml/min	Yes	Yes
5	Co/SiO_2	1-Propanol	$D_2/CO/N_2$	20%	0.04ml/min	Yes	Yes
6	Co/SiO_2	2-Propanol-d8	$H_2/CO/N_2$	30%	0.04ml/min	Yes	Yes
7	Co/SiO_2	Propionaldehyde	$D_2/CO/N_2$	15%	0.04ml/min	No	No

Evenly mixed 1g of cobalt catalyst and 8g of white quartz sand mixture was placed in the center of the fixed bed reactor (FBR). Finely crushed 1g of Al_2O_3 catalyst and 3g of white quartz sand was evenly mixed, and the mixture was placed around 5 cm above the cobalt catalyst when the Al_2O_3 catalyst was used. Above the aluminum catalyst, between the aluminum and cobalt catalyst and below the cobalt catalyst, 10g of white quartz sand was placed. The top and bottom space of the reactor was filled with glass wool, and the detailed reactor setup picture for FTS reaction was shown in Fig 2.1. The reaction temperature was measured by a thermocouple, which was placed in the middle of the cobalt catalyst. The catalyst was activated with hydrogen gas under 623K for 12hours.

After the catalyst was activated, the reactor temperature was lowered to 373K and the syngas was introduced into the reactor. Subsequently, the reactor temperature and partial pressure were gradually increased to 503K, 250psi, respectively, and the

cooling system for the oil trap has been turned on. The reaction was carried out in a 90% gas flow of syngas. In addition, the hot trap temperature was increased to 333K from room temperature.

Once the reaction condition has reached a steady state (around 12hours), the hot trap (333K) and cool trap (273K) were emptied. The mixture of n-hexane and alcohols were introduced into the FT reactor through the HPLC pump at the desired flow rate and pressure. Gas samples were collected every one hour since the reaction started, and carbon monoxide conversion was calculated. Wax and oil samples were collected after 8 hours of alcohol added experiments.

3.2.3 Addition Experiment Product Analysis

Gas samples, and liquid samples were analyzed by the Agilent 3000 Micro 4 channel gas chromatograph and GC/MS instrument, respectively. Two types of GC/MS instruments have been used, one is Perkin Elmer GC-MS equipped with a 30m SPB-5 capillary column, and the other is HP 5890 GC-MS equipped with a 60m SPB-5 capillary column. The relative amounts of the isotopic isomers were determined based on the relative abundances of molecular ions after adjusted for contribution from M+1 and M+2 ions. The hydrogen (deuterium) distribution was determined by GC/MS from the recovered alcohols.

3.3   RESULTS AND DISCUSSION

3.3.1   Addition of Ethanols over Co/ SiO_2 Catalyzed FT reactions

According to the reported results of iron[73-76, 78, 79] and Co/TiO_2

catalyzed[82] ethanol and alkene tracer addition studies, it is reasonable to assume that

the C_2 initiator resembles either ethanol or ethylene, and could incorporate into Co/SiO_2

catalyzed hydrocarbon products. If this hypothesis is correct, the products by the

addition of the deuterated alcohols over Co/SiO_2 catalyzed FT reactions should also

contain deuterium. However, no dueterated alkane isomers were observed in the

GC/MS analysis of oil products obtained from ethanol-d_6 and 2-Propanol-d_8 addition

experiments in the run No. 1 and No. 2, respectively (Table 3.1). This result led us to

conclude that alcohol cannot incorporate into the Co/SiO_2 catalyzed FT hydrocarbon

product, and the ethanol did not act as the C_2 initiator in the Co/SiO_2 catalyzed FT

reaction. It led us to assume that the C_2 initiator was derived from ethene, which is

possibly derived from ethanol by the dehydration process.

3.3.2   Addition of Ethanol during FT reaction over Co/ SiO_2 and Al_2O_3 Dehydration

Catalyst

Unlike the results of runs No. 1 and No. 2, ethanol was incorporated into the FT

products after the addition of the Al_2O_3 dehydration catalyst. This result indicates that C_2

initiator is derived from ethene but not from ethanol, and it can be shown as Fig 3.1:
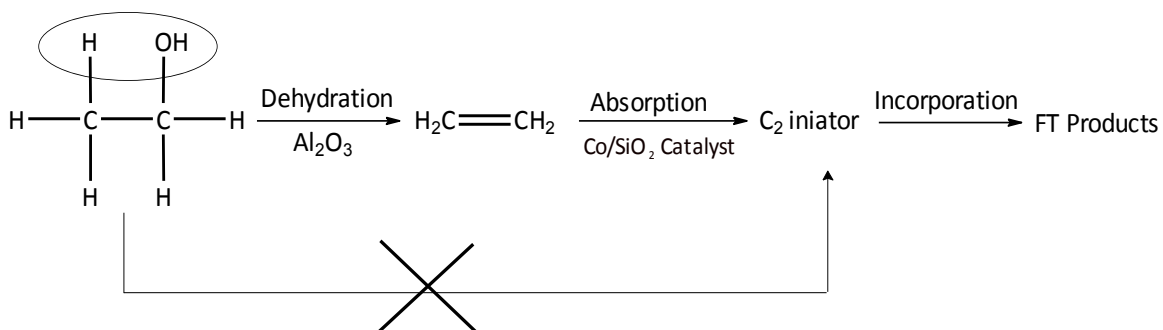
Figure 3.1: Pathway of alcohol addition into the cobalt catalyzed FT product

Two ways of ethanol tracer experiments were performed as shown in Table 3.1 (run No. 3 and run No. 4). In run No. 3, deuterated ethanol-d_6 was used as a tracer with H_2/CO (2:1) as the synthesis gas. In run No. 4, ethanol-h_6 was used as tracer with D_2/CO (2:1) as the synthesis gas. More detailed experiment conditions were shown in the Table 3.1.

In run No. 3, ethanol incorporation was observed in the C_7-C_{15} alkane products through the GC/MS analysis based on the deuterium distribution in alkanes. The results of run No.3 were shown in Fig 3.2 and Table 3.2.

Table 3.2 Deuterium distribution in alkanes from the ethanol-d_6 tracer addition experiment oil product analysis

Carbon Number	Deuterium Number/mol%					D/molecule
	0	**1**	**2**	**3**	**4**	
7	80.3	13.8	4.6	1.3	0	1.4
8	82.5	11.9	4.5	1	0	1.4
9	83.2	10.7	4.6	1.5	0	1.4
10	80.4	12.2	5.5	1.9	0	1.5
11	80.3	11.7	5.7	2.4	0	1.5
12	79.6	11.8	6.1	2.5	0	1.5
13	82.5	9.8	5.5	2.2	0	1.6
14	87.8	7.5	4.7	0	0	1.4
15	92.9	4.7	2.4	0	0	1.3

Addition Run No. 3 (table header spanning)
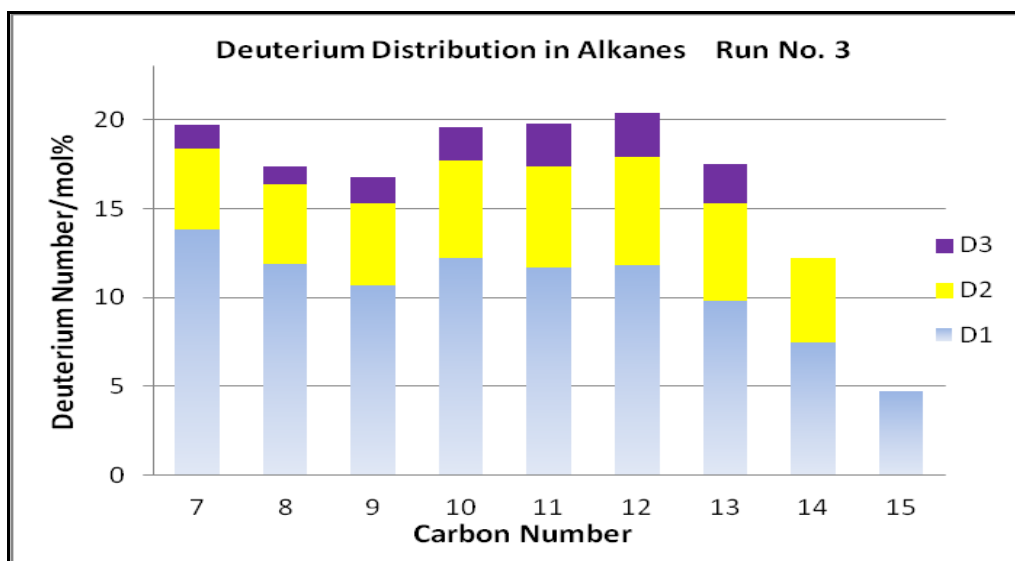
Figure 3.2: Deuterium distribution in alkanes from the ethanol-d_6 tracer addition experiment oil product analysis

The result of deuterium distribution in the Table 3.2 shows that the highest deuterium number in the alkane is 3, and relative amount of d_1, d_2, d_3 isotopic isomer in each alkane were about the same (Fig 3.2). This result indicated that the labeled ethanol went through the dehydration process and generated ethene before it incorporated into the FT products, and the C_2 initiator derived from ethene incorporated into the FT products. In other words, the C_2 initiator was derived from ethene, which can be obtained from ethanol through dehydration process by the Al_2O_3 dehydration catalyst. Additionally, the result of relatively constant deuterium number in each molecule was obtained. The deuterium number 1.5±0.1 in each molecule indicates that the C_2 species derived from ethene acted as an initiator.

In the previous iron catalyzed ethanol-d_5 tracer studies[81], it has been reported the similar result of deuterium number per molecule in alkane is 1.3-1.5, and it has been explained as the deuterium/hydrogen exchange during the formation of initiator or the propagation steps. However, if the ethanol-d_6 tracer underwent a significant deuterium/hydrogen exchange during the propagation steps, the maximum deuterium number in the alkane product should be much higher than 3. Since the result in Table 3.2 shows slightly different amount of d_1, d_2, d_3 species in each alkane, a small amount of hydrogen/deuterium exchange do exist.

The addition of ethanol-h_6 tracer during the FTS experiment (Run No. 4) was performed with D_2/CO as synthesis gas, and ethanol incorporation was observed in the C_8-C_{18} alkanes through the GC/MS analysis based on the hydrogen distribution in alkanes. The results of addition experiment run No.4 were shown in the (Fig 3.3, Table 3.3).

Table 3.3 Hydrogen distribution in alkanes from the ethanol tracer addition experiment oil product analysis

Carbon Number	Addition Run No. 4										
	Hydrogen Number/mol%										H/molecule
	0	1	2	3	4	5	6	7	8	9	
8	39.6	26.3	14.5	6.3	6.7	3.5	1.7	0.6	0.6	0.2	2.3
9	43.1	27.7	16.3	8.2	2.3	0.7	0.4	0	0	0	1.8
10	40.3	25.4	16.2	8	6.2	3.8	0.2	0	0	0	2.1
11	38.5	24.5	16.8	9.4	5.4	3.1	1.1	0.9	0	0	2.2
12	38.6	23.6	16.9	10	5.7	2.9	1.1	0.5	0	0	2.3
13	38.5	22.7	18	9.9	6.1	3.5	1.3	0	0	0	2.3
14	39.7	20.5	17.2	13	4	3.4	1.4	0.9	0	0	2.3
15	38.4	19.2	19.7	14.1	4.3	0.9	1.5	1.1	0	0	2.4
16	43.2	20.7	19.6	8.5	5.3	2.6	0.2	0	0	0	2.1
17	49.8	18.1	13.4	9.5	5.8	3.4	0	0	0	0	2.3
18	50.7	14.8	16.8	8.2	5.7	2.5	1.4	0	0	0	2.4
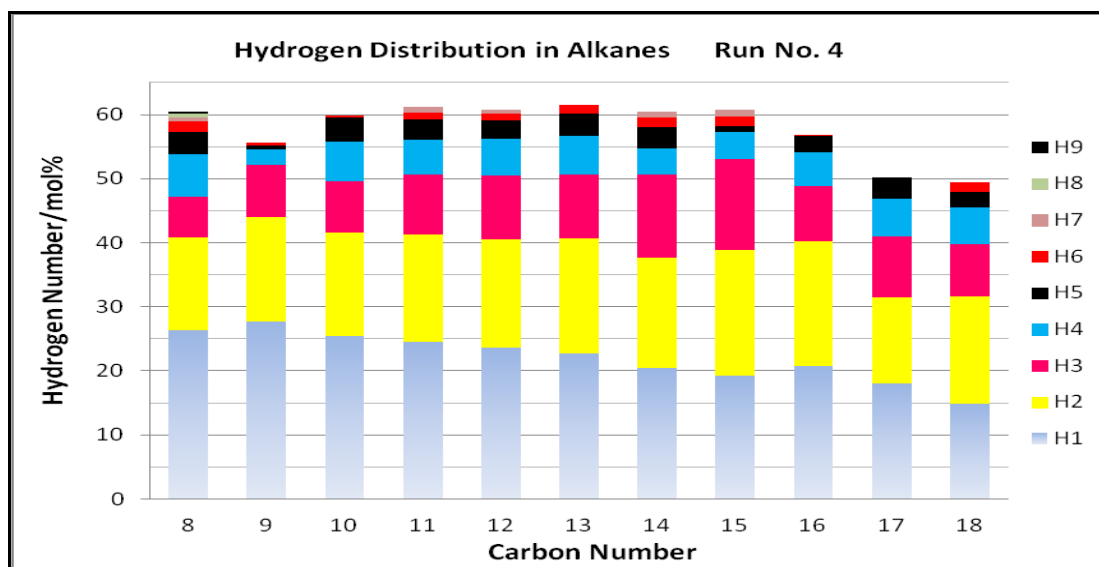
Figure 3.3: Hydrogen distribution in alkanes from the ethanol tracer addition experiment oil product analysis

Unlike the result of ethanol-d_6 addition experiment, the maximum hydrogen number in the paraffin product is higher than 3. In this experiment, large amount of ethanol (30% and 0.04ml/min) was added. Significant amount of H_2O was produced in this run and the H_2O acted as the source of H_2, resulting in the products with more than 6H atoms.

However, the result of hydrogen number per molecule in alkanes in the Table 3.3 shows a relatively constant number of 2.3±0.1. This result indicates that the hydrogen in alkane is mainly generated from ethene.

Unlike the previous studies over the iron and Co/TiO_2 catalyzed isotope tracer addition FT experiments, with and without dehydration catalyst Al_2O_3 and the Co/SiO_2 catalyzed the alcohol-addition experiment results (Run No. 1 –No. 4) indicated that the

C_2 initiator is derived from ethene but not ethanol, and the ethene was obtained from ethanol through the elimination reaction by Al_2O_3 dehydration catalyst. According to this result and the modified alkylidene mechanism, the C_2 initiator incorporation pathway can be obtained. As the addition of ethanol-d_6 (a) as an example, the ethene incorporation pathway has been shown in the Fig 3.4.

According to the Fig 3.4, six ethene isomers (b, b1, b2, b3, b4, b5) can be obtained from the dehydration/hydration of added ethanol-d_6. Obviously, the isotopic isomer d_4 should be generated from the incorporation of the ethene isomer (b). In the case of b isomer, it can be absorbed on the cobalt catalyst surface (M) to form a π-complex (c), which can form (d). The intermediate d can undergo α-elimination[83, 84] to produce the C_2 iniator, ethylidene (e). During the formation of ethylidene, the maximum number of deuterium in the alkane product will be 3 with the loss of one deuterium via the incorporation of e. The e can under to C-C bond formation with the C_1 monomer M≡CH to produce f. Through the hydrogenation of the intermediate f, it can generate propylidene structure (g). According to previous studies, the formation of g is irreversible under FT reaction conditions[9].
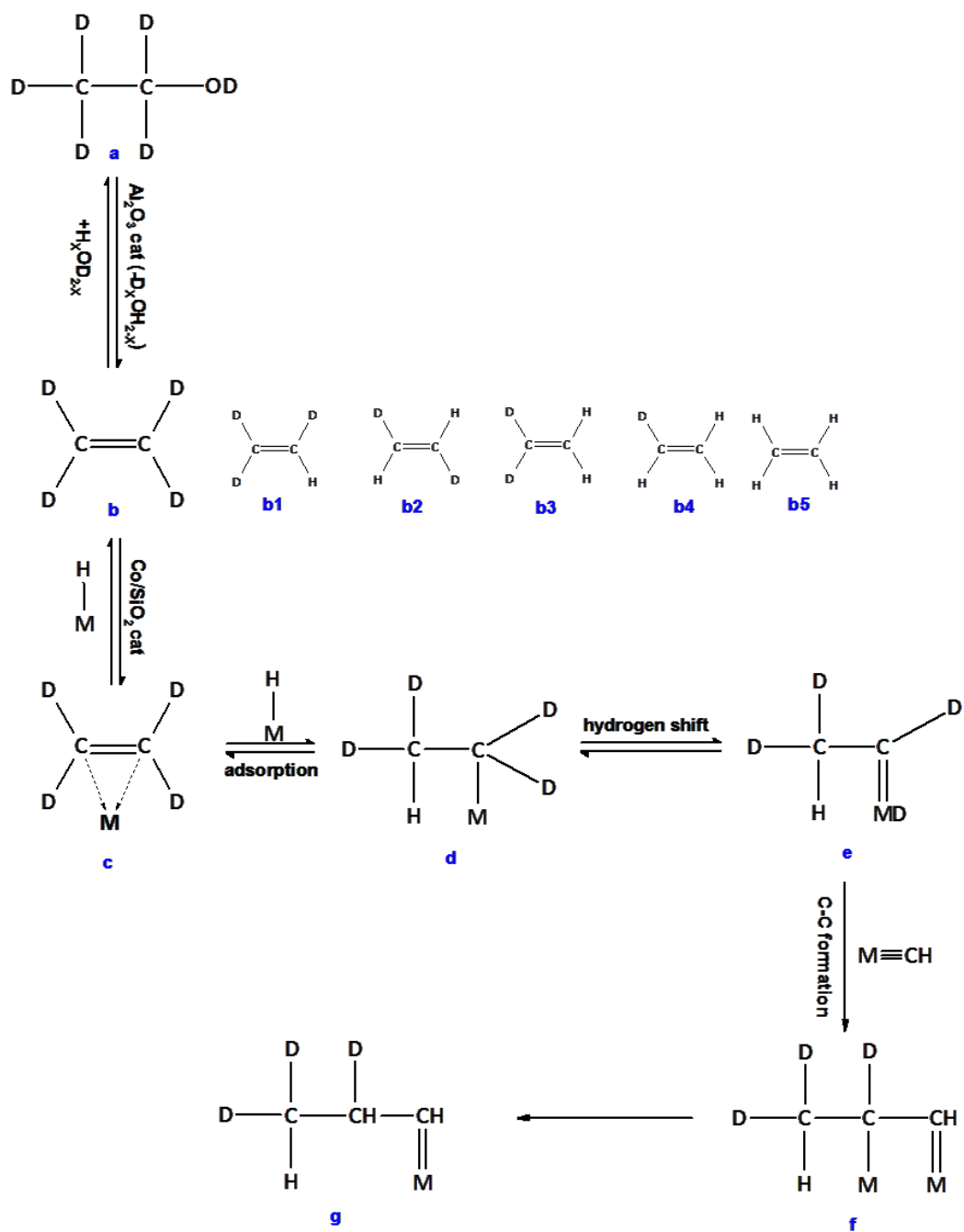
Figure 3.4: Mechanism of the ethanol-d$_6$ tracer addition based on the modified alkylidene mechanism

3.3.3 Addition of Propanol over Co/ SiO$_2$ Catalyst with Al$_2$O$_3$ Dehydration Catalyst

In run No. 5, 1-propanol-h$_8$ and D$_2$/CO synthesis gas were used. In the addition experiment of run No. 6, 2-propanol-d$_8$ was used with H$_2$/CO synthesis gas.

According to the results of ethanol tracer addition, propanols should form propene, and the C$_3$ initiator derived from propene will incorporate into the FT hydrocarbon products, which means, addition of 1-propanol and 2-propanol will result in similar results. In order to confirm the alkylidene incorporation pathway, addition of 1-propanol-h$_8$ (Run No. 5) and 2-propanol-d$_8$ (Run No. 6) were conducted during the Al$_2$O$_3$ and cobalt catalyzed FT reaction.

The product analysis shows that the 1-propanol-h$_8$ (Table 3.4), 2-propanol-d$_8$ (Table 3.5) were incorporated into the FTS products. The isomer distribution from (h$_1$-h$_7$ or d$_1$-d$_7$) in alkanes was observed. These results suggest that the small amount of D$_2$O (H$_2$O) produced from propanol also incorporated into the growing chain because the labeled atom numbers of d$_7$ (h$_7$) in alkanes are higher than the possible D (H) number in propene.

Table 3.4 Hydrogen distribution in alkanes from 1-propanol-h$_8$ tracer addition experiment oil product analysis

Addition Run No. 5									
Carbon Number	Hydrogen Number/mol%								H/molecule
	0	1	2	3	4	5	6	7	
8	57.7	23.6	7	2.3	3.8	4.2	1.1	0.2	2.1
9	60	25.5	4.8	2.3	4.5	2.1	0.6	0.2	1.9
10	60	25.5	7.6	2.2	2.6	1.5	0.5	0.1	1.7
11	63.5	22.1	8.5	2.7	1.8	1	0.4	0.1	1.7
12	56.4	30.7	7.3	3.3	1.3	0.7	0.3	0.1	1.5
13	55.8	27.2	11.6	3.3	1.5	0.4	0.1	0	1.6

Table 3.5 Deuterium distribution in alkanes from 2-propanol-d_8 tracer addition experiment oil product analysis

Addition Run No. 7									
Carbon Number	**Deuterium Number/mol%**								**D/molecule**
	0	**1**	**2**	**3**	**4**	**5**	**6**	**7**	
7	65.6	14.6	10.2	5.7	2.5	0.9	0.3	0.1	2
8	75.2	10	6.9	4.6	2.1	1	0.2	0.1	2.1
9	81.2	6.2	5.7	3.7	2	0.9	0.2	0	2.3
10	78.5	6	6.1	4.6	2.8	1.4	0.5	0.1	2.5
11	81.8	4.5	4.9	3.9	2.7	1.4	0.6	0.2	2.7
12	89.5	2.3	2.7	2.3	1.6	1	0.4	0.2	2.8
13	94.3	1.6	1.4	1.4	0.6	0.4	0.1	0.1	2.6
14	97.8	0.8	0.6	0.6	0.1	0	0	0	2.1

The deuterium distribution (Fig 3.5) indicated that the relative amounts of isotopic isomers in alkanes are about the same, suggesting that they are formed from the same C_3 initiator.
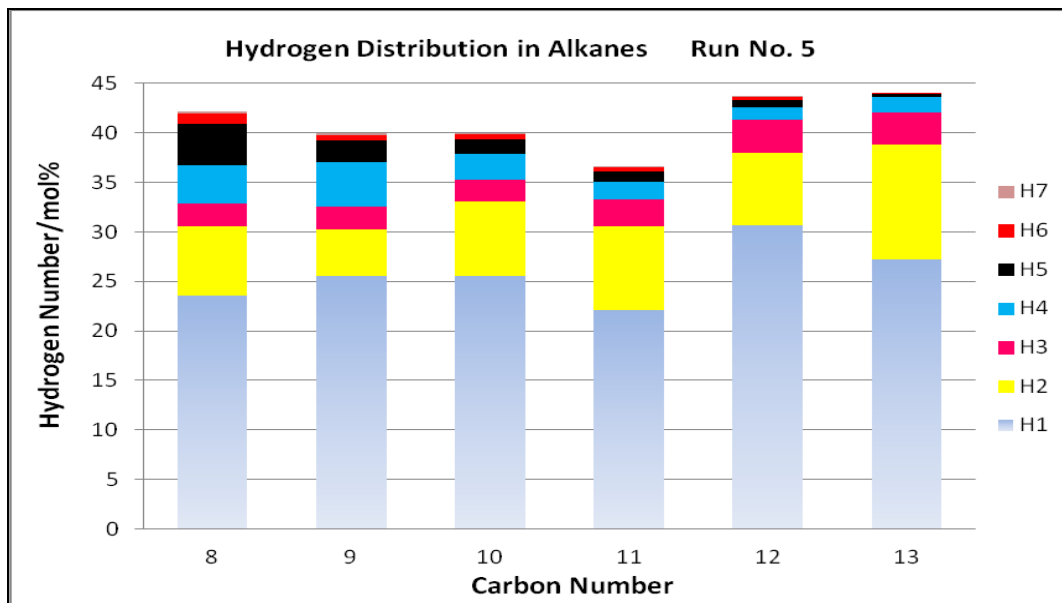

Figure 3.5: Hydrogen distribution in alkanes from the 1-propanol-h_8 tracer addition experiment oil product analysis

Additionally, the results of D/molecule≈2.0-2.8 (H/molecule≈ 1.5-2.1) in Table 3.5 (Fig 3.6) and Table 3.4 (Fig 3.7) display that the addition of 2-propanol contributed higher amount of deuterium than addition of 1-propanol. This result can be explained by the secondary alcohol dehydration reaction is much faster than the primary alcohol dehydration reaction. In other words, higher amount of 2-propanol was eliminated into the propene than 1-propanol, and higher amount of propene derived from 2-propanol was incorporated into the FT paraffin products. It also means, the large amount of 1-propanol did not participate in the dehydration process and it was directly recovered into the water layer of FT product.
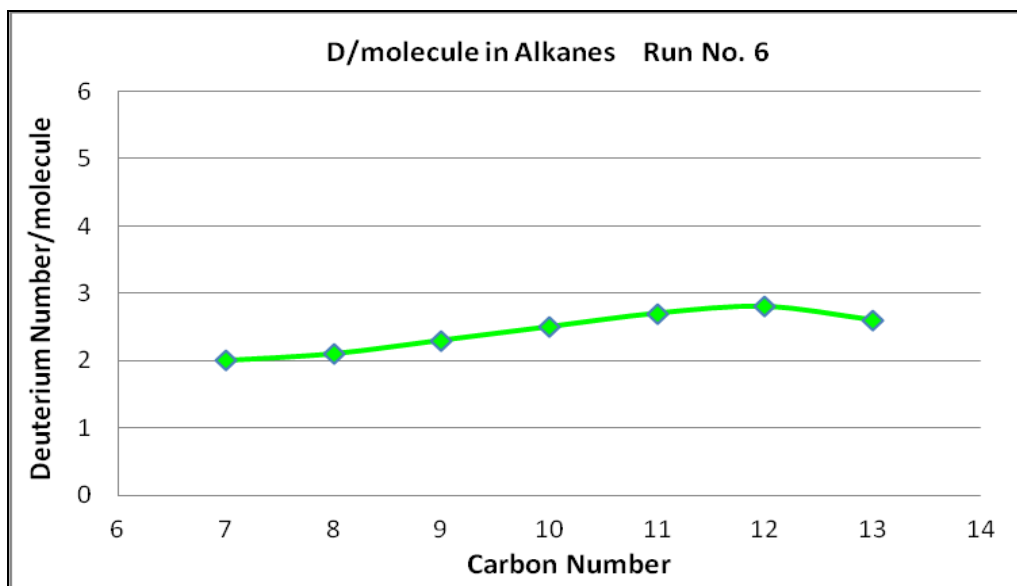

Figure 3.6: Deuterium number per molecule distribution in alkanes from the 2-propanol-d_8 tracer addition experiment oil product analysis
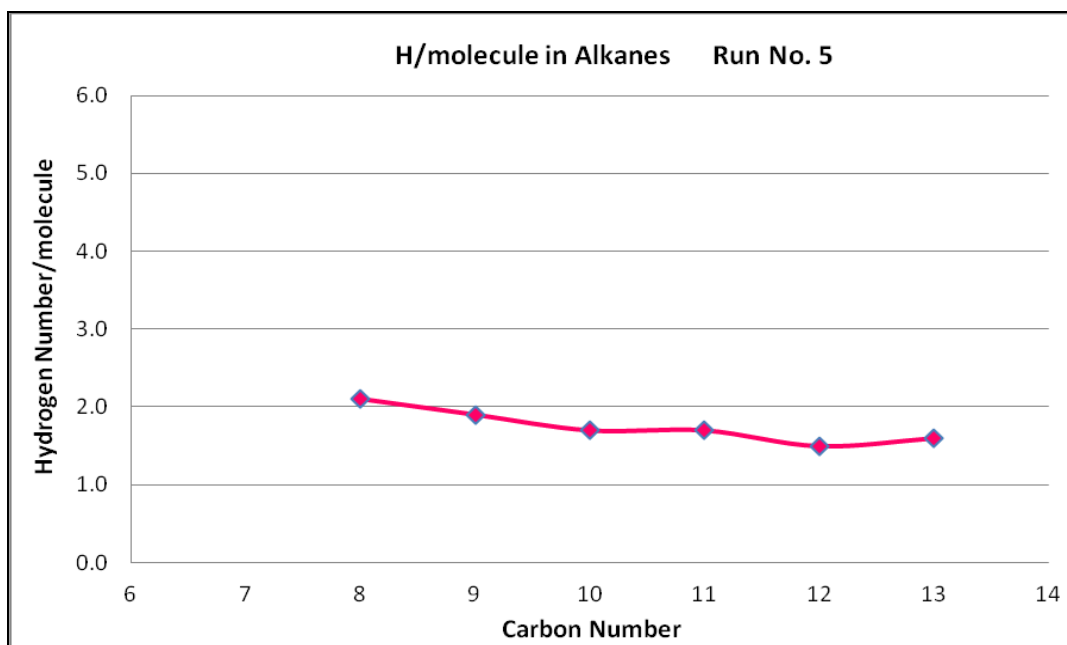
Figure 3.7: Hydrogen number per molecule distribution in alkanes from the 1-propanol-h_8 tracer addition experiment oil product analysis

The analysis results of water product analysis from the addition experiment run No. 5 (Fig 3.8) and run No. 6 (Fig 3.9) show that about 10% d_7 and d_8 isomers of 2-propanol was recovered and about 50% h_7 and h_8 isomers of 1-propanol was recovered, respectively. This result indicates less amount of 1-propanol-h_8 underwent dehydration and incorporation process.

Figure 3.8: Deuterium distribution in water from the recovered 2-propanol-d_8 analysis

Figure 3.9: Hydrogen distribution in water from the recovered 1-propanol-h_8 analysis

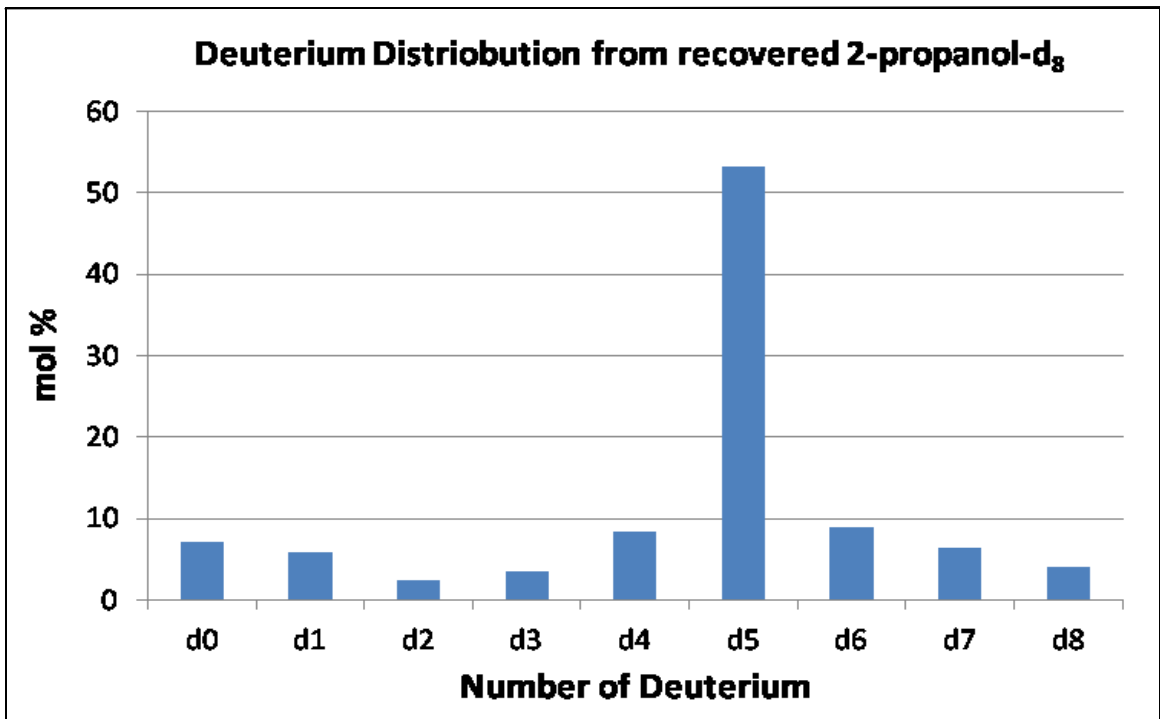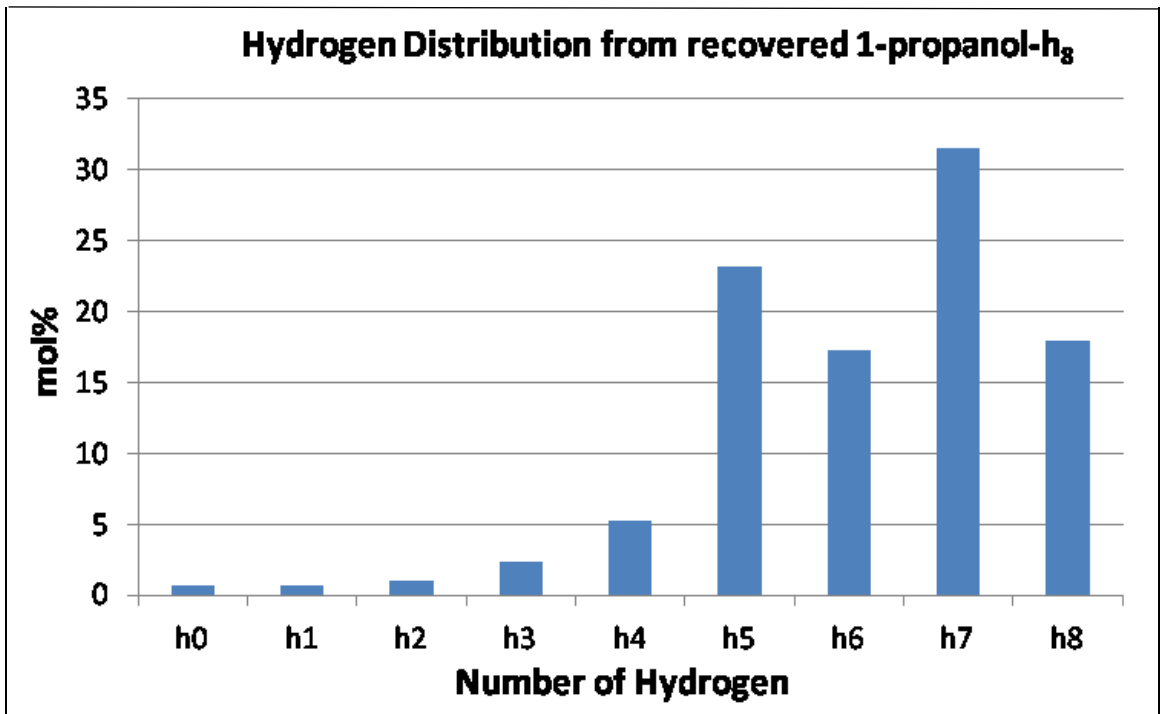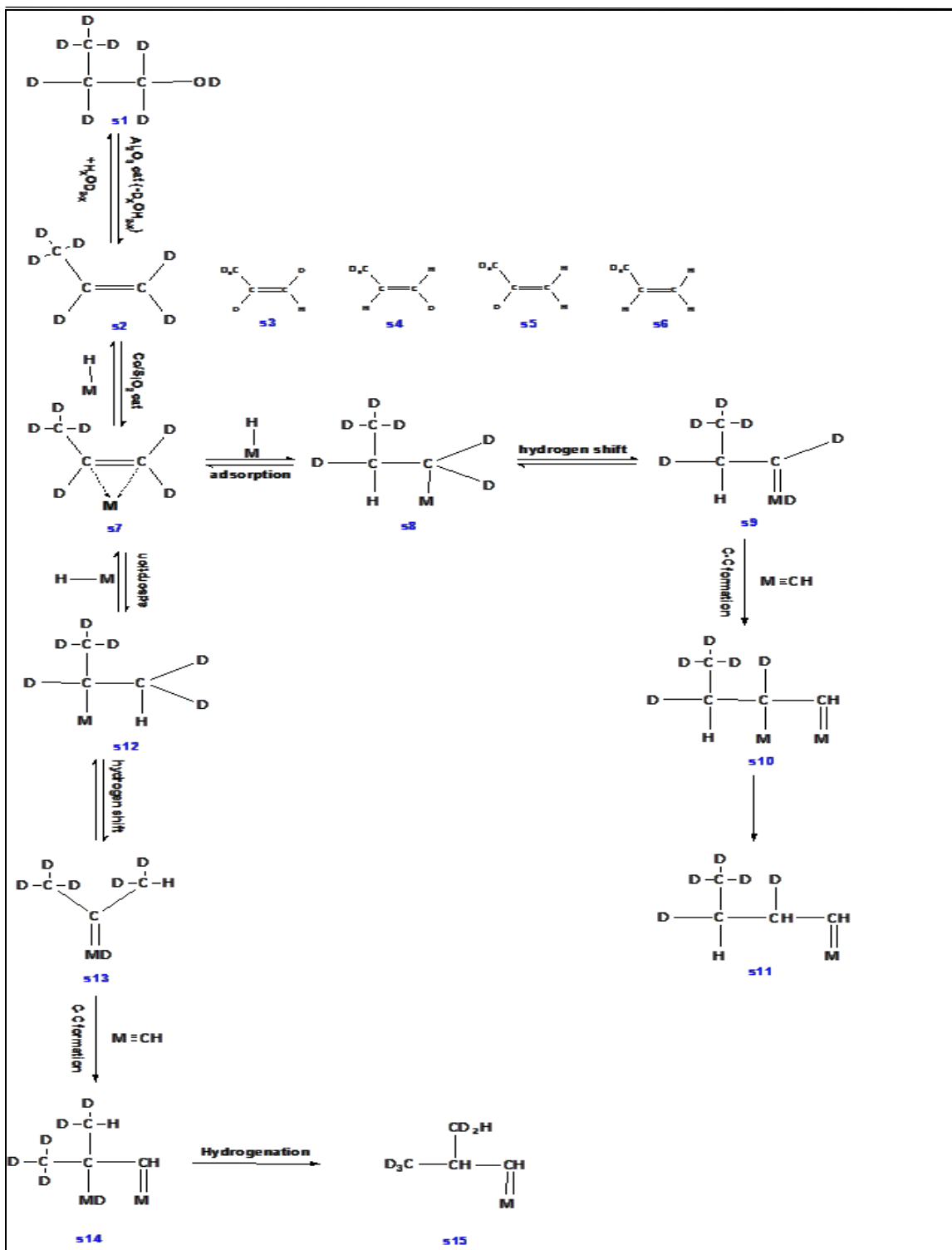**Figure 3.10:** Mechanism of the 1-propanol-d_8 tracer addition based on the modified alkylidene mechanism

3.4   CONCLUSION

The results of ethanol addition experiments during the cobalt catalyzed FT reaction with and without Al_2O_3 dehydration catalyst implied that the C_2 and C_3 species are derived from ethene or propene but not from ethanol or propanol. Plus, the no-incorporation result (Table 3.1, run No. 7) of propionaldehyde addition with D_2/CO synthesis gas implied that the C_3 initiator does not resemble the propionaldehyde.

The similar incorporation results of 1-propanol, 2-propanol-d_8 over Al_2O_3 and cobalt catalysts provided further support of alkylidene incorporation pathway, in which the C_2 and C_3 initiator derived from ethene and propene, respectively.

These results can be explained by the modified alkylidene mechanism. The incorporation of readsorped propene indicated that the branched hydrocarbons could be formed through the iso-alkylidene intermediates.

CHAPTER 4

FORMATION OF BRANCHED COMPOUNDS IN THE COBALT CATALYZED FTS

4.1   INTRODUCTION

The C-C formation pathways and the structure of C_2 and C_3 initiator for the

cobalt catalyzed FTS mechanism have been proposed in the chapter 2 and chapter 3.

However, the structure of branched hydrocarbon products and the formation pathways

of branched compounds are remain uncertain. It has been known that the FT reaction is

producing the branched hydrocarbon compounds. Therefore, identify the structure of

branched FT hydrocarbon products and understand how they were formed should

provide further supporting evidence of the FT mechanism.

Previously, several branched FT hydrocarbon products related reports have

been recorded over iron and cobalt catalyzed FT reactions. For the iron catalyzed FT

reaction, the product has been reported that it can produce monomethyl-, dimethyl-,

and ethyl-branched hydrocarbon products[86, 87]. For the cobalt catalyzed FT reaction,

it has been reported that the monomethyl- branched hydrocarbon compounds are the

primary branched products[10, 88].

In order to know the structure of the branched hydrocarbon compounds, the key

step is to understand how the branched compounds are. According to many reports ,

the alkenes were considered as primary products because the olefins and paraffins have

same skeleton and the alkenes transformed into alkanes through further hydrogenation[10]. In addition, it also has been observed that the 1-alkene has much higher concentration than the 2-alkene that the 1-alkene was assumed to be primary products of FTS[89]. Furthermore, it has been reported that the 1-alkene can undergo secondary reaction to produce 2-alkene, linear alkanes and methyl-branched hydrocarbons[10], and the produced alkenes can readsorb on the surface of the catalysts and regrown. These reports implied that the branched compounds could be obtained via the re-adsorption of alkenes.

Prior to identify the cobalt catalyzed branched FT products, the possible branched hydrocarbon formation pathways can be predicted based on the proposed modified alkylidene mechanism[59], pathway of alcohol addition[90] and previous reports. The predicted branched hydrocarbon formation pathways over cobalt catalyzed FTS has been shown in the Fig 4.1.

According to the modified alkylidene mechanism, the ethylidene C_2 initiator could be hydrogenated to produce ethene or ethane product, or it also can be readsorped on the metal catalyst surface and incorporate into long chain hydrocarbons. The readsorped ethene transforms into ethylidene, which can then react with M≡CH to form propylidene. The propylidene can be completely hydrogenated to produce propane, or it can be hydrogenated and eliminated to form propenes. Before the propene leaves the catalyst surface as a product, part of propene compound can readsorb on the catalyst surface to regrown as straight-chain propylidene or

isopropylidene. The straight-chain propylidene can be grown to produce straight-chain

butylidene, and the isopropylidene can be grown to produce 2-methylbranched

hydrocarbon products.

The straight-chain butylidene can be completely hydrogenated to produce

butane or hydrogenated and eliminated to form the 1-butene. The 1-butene can be

readsorbed on the catalyst surface, and go back to the form of the straight-chain

butylidene, or form the isobutylidene. The isobutylidene can produce the 3-methyl

branched hydrocarbons. Similar to the propagation pathway of butylidene, the 4-methyl

branched hydrocarbons also can be produced through the readsorption of 1-pentene.

According to the modified alkylidene mechanism, it can be predicted that the C-C

bond has been formed through the hybridization change from sp^2 to sp^3 on alkylidene

growing chain and sp to sp^2 on M≡CH monomer on the surface of metal catalyst. The

alkylidene chain can be further hydrogenated to leave the catalyst surface as alkane

product or it also can be eliminated to form the alkene. Prior to the step of alkene

readsorption, it has two options. One, it can be readsorbed on the less sterically

hindered carbon to regrow as straight chain FT product. The other one, it can be

readsorped on the sterically hindered penultimate carbon to regrow as mono-methyl

branched FT hydrocarbon products. The general methyl branched hydrocarbons
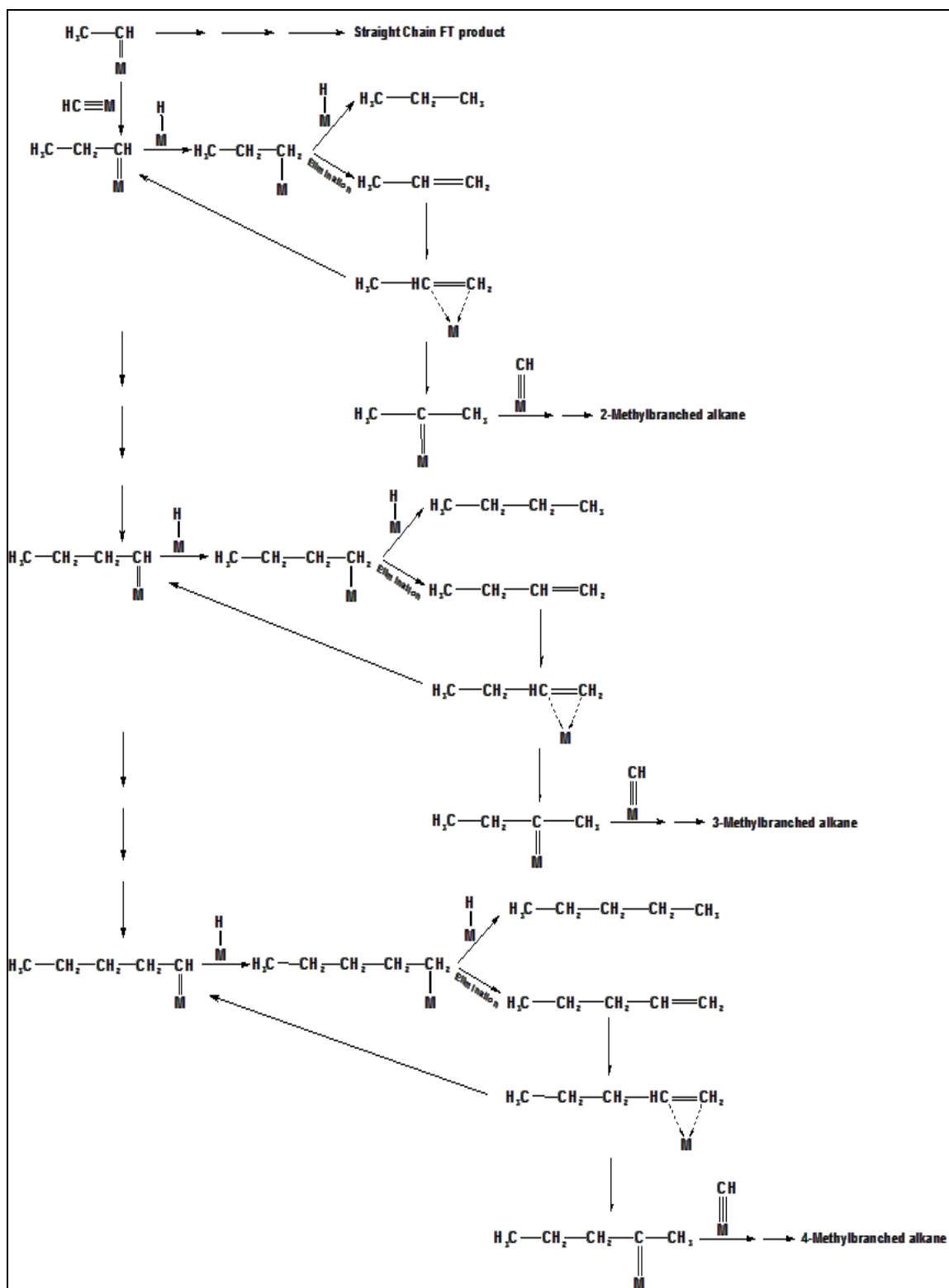
formation pathways were shown in the Fig 4.1.

Figure 4.1: Formation pathway of methyl branched hydrocarbons based on the Modified Alkylidene Mechanism

In the Fig 4.2, the formation pathway of n-propane, formation pathway of straight chain hydrocarbons (HC) and formation pathway of 2-Methylbranched HC products were shown. The carbon-carbon bond was formed by coupling of the sp^2 carbon in the ethylidene and sp carbon in the M≡CH. By the adsorption of hydrogen, the unsaturated metal-carbon bond gets saturated and leaves the metal surface. Before the propyl- structure leaves the metal surface, it also can perform the elimination reaction to form the 1-propene. The 1-propene could readsorb on the metal surface and regrown also. During this re-adsorption process, depends on the adsorbed carbon, it can produce two type of hydrocarbons: it can readsorped on C_1 to produce the n-propylidene (e) or readsorped on C_2 to produce the 2-propylidene, which will regrow as 2-methyl branched HC products.
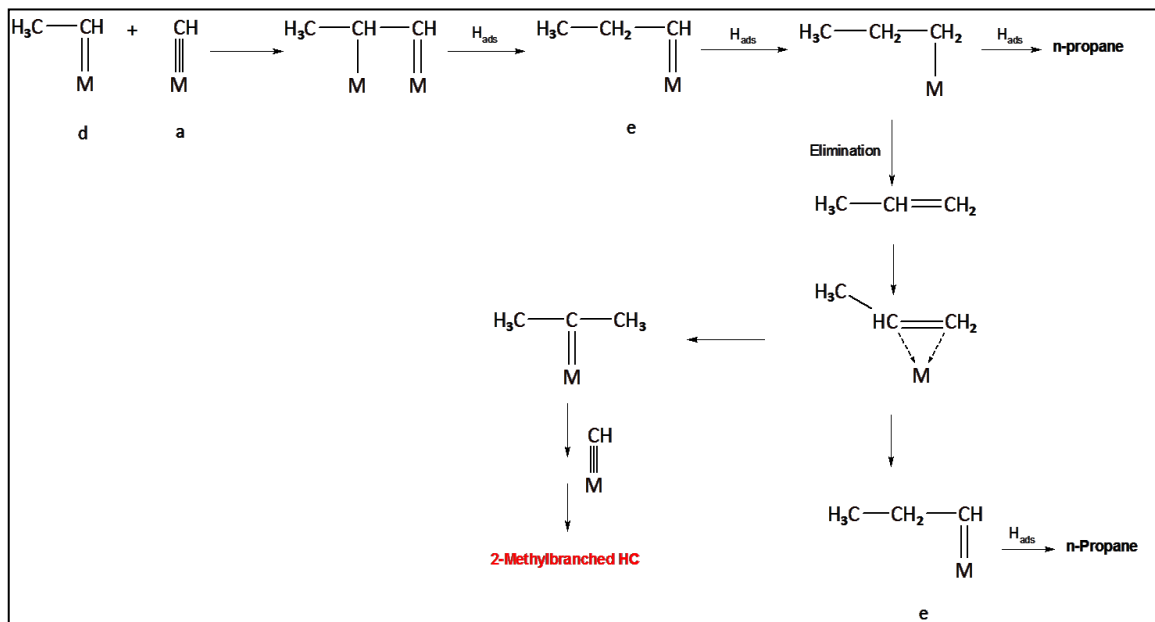

Figure 4.2: Formation of 2-Methylbranched FT hydrocarbon products

60

Similar to the 2-Methylbranched hydrocarbon formation pathway, the formation pathway of 3-methybranched products has been predicted in Fig 4.3. After the 1-butene is formed, it can leaves the catalyst surface as FT product, or can be re-adsorbed on the catalyst surface and regrown to straight chain or branched chain FT products. Depends on the choice of the re-adsorbed carbon, it can produce normal-butylidene with the formation of π-complex on C_1 carbon, and it gets further hydrogenated to generate straight chain hydrocarbon products; it also can produce 3-Methylbranched butylidene with the formation of π-complex on C_2 carbon to generate 3-Methylbranched hydrocarbon products.

In the Fig 4.4, the formation pathway of 4-methylbranched hydrocarbon products has been shown, and in the Fig 4.5, the formation pathway of 5-methylbranched HC products has been shown. Based on above analysis, the branched hydrocarbons in FTS are produced from the re-adsorption of 1-alkene and they are methyl branched hydrocarbons. For example, the branched C_8 hydrocarbons should be 2-methylheptane or 3-methylheptane but cannot be 3-ethylhexane.
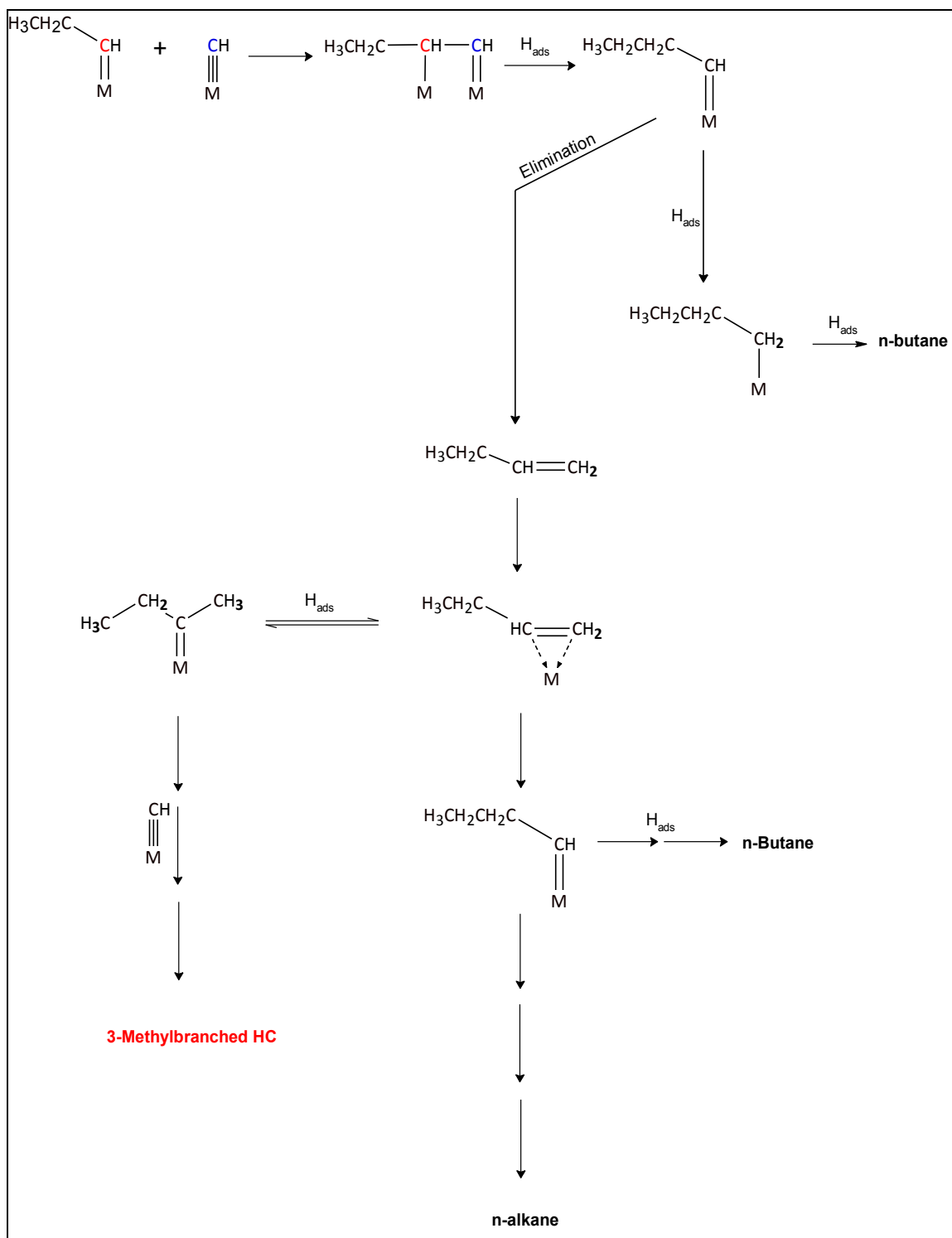
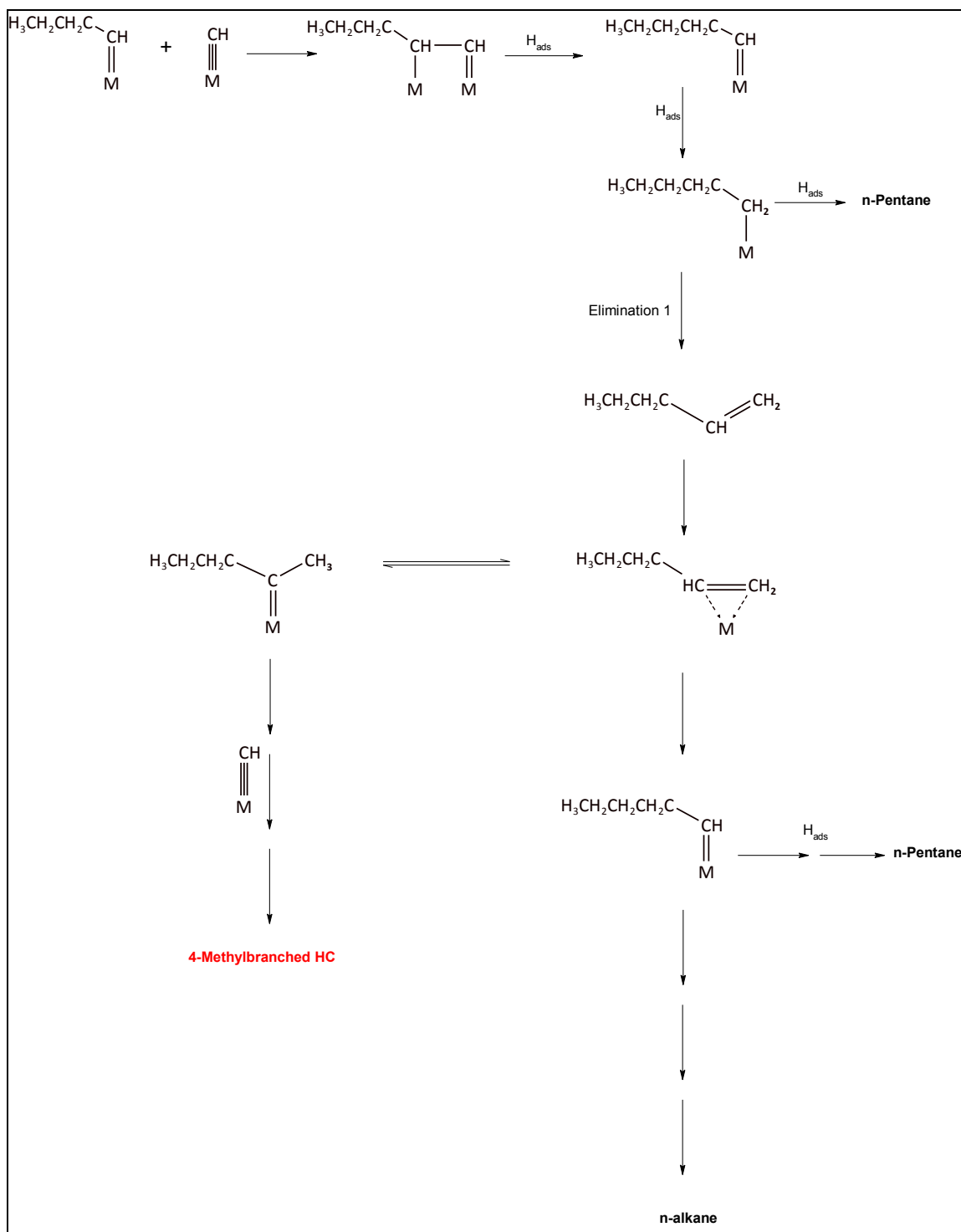**Figure 4.3:** Formation of 3-Methylbranched FT hydrocarbon products

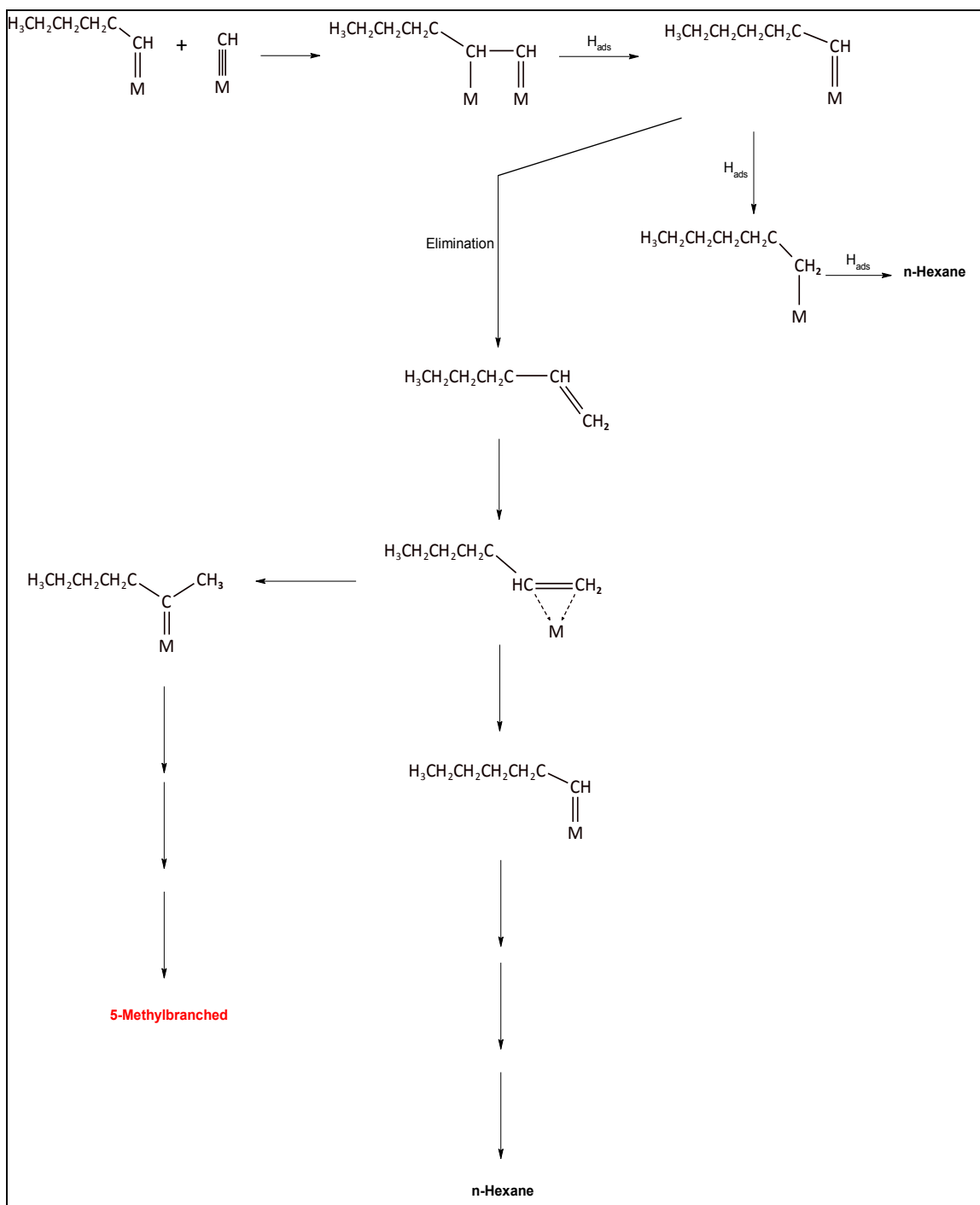**Figure 4.4:** Formation of 4-Methylbranched FT hydrocarbon products

Figure 4.5: Formation of 5-Methylbranched FT hydrocarbon products

4.2   EXPERIMENTAL

4.2.1   Reagents and Catalysts

Dry Diethyl Ether, 2-Butanone (≥99.7%), 2-Pentanone (98%) were purchased from Sigma-Aldrich. Inc. Platinum on Activated Carbon (5% wt. on activated carbon), Methylmagnesium Bromide (3.0M solution in diethyl ether), 2-Nonanone (99%), 3-Nonanone (99%), 1-Bromononane (98%) were purchased from Aldrich, Inc. 1-Chlorooctane (99%),   1-Bromoheptane (99%), 2-Methylheptane(99%) were purchased from Acros, Inc. 3-Methylheptane (98%) was purchased from Alfa Aesar, Inc. The contents of compounds are provided according to the manufacturer.

4.2.2   Synthesis of Branched Alkanes

The original FT products of C_{10} compounds were shown in Fig B-17. In the Fig B-17, it can be seen that there are two branched peaks in the left side of the n-decane peak. They are possibly the branched C_{10} alkanes or branched-chain C_{10} alkenes. Based on the modified alkylidene mechanism, the branched hydrocarbon compounds were predicted, and it has been shown in the Fig 4.1. The prediction Fig 4.1 shows clearly that the most possible branched compounds should be 2-Methyl, 3-Methyl, 4-Methyl branched alkanes.

In order to confirm the prediction of branched compound formation pathway, 2-Methylnonane, 3-Methylnonane, 2-Methyldecane, 3-Methyldecane, 2-Methylundecane,

, 4-Methylundecane were synthesized through the Grignard, Elimination, Hydrogenation reactions, but the 2-Methylheptane, 3-Methylheptane, and 4-Methylheptane were directly purchased. Each reaction products were analyzed by the Focus GC (FID), and the data were shown in the Fig B18-B30. Example of detailed amount of each reagent was described.

Synthesis of 3-Methyl-3-decanol

0.81g of magnesium pieces was prepared, and the magnesium pieces, two iodine crystals, and a stir bar were placed into a three neck around bottom flask. 15ml of dry anhydrous diethyl ether was added into the flask, and started stirring. The 5ml bromoheptane and 10ml of dry ether was completely mixed in a pressure equalizing funnel. The bromoheptane-ether mixture was slowly added into the magnesium-ether mixture. After the addition was completed, the mixture was warmed to reflux and it was kept for additional 60 minutes. When the reaction mixture was cooled to room temperature, 3.50ml of butanone and 10ml of dry ether was mixed and the mixture was transferred into the pressure equalizing funnel. The butanone-ether mixture was added dropwise into the synthesized heptalmagnesium bromide. After the addition was completed, the mixture was warmed to refluxing and kept for additional 60 minutes. When the reaction mixture was cooled to room temperature, 10% HCl was added until all precipitation was dissolved. The organic layer was separated out, and the water layer was extracted with 15ml of diethyl ether 4times.The organic fractions were combined into one flask and acid compounds were washed out with the 0.5ml of distilled water

4times. Then the organic solution was dried with anhydrous $MgSO_4$ for 5minutes. After the organic solution was dried, the ether solvent was evaporated, and the obtained products were analyzed. 2-Methyl-2-nonanol, 3-Methyl-3-nonanol, 2-Methyl-2-decanol, 2-Methyl-2-undecanol, 4-Methyl-4-undecanol were prepared in a similar manner.

Synthesis of 3-Methyl-decene

4ml of Grignard product and 25ml of 6M sulfuric acid were added into a three neck round bottom flask. A stir bar was placed into the flask. After the addition was completed, the mixture was warmed up, and it was refluxed for one hour at the temperature of 70°C. The reaction mixture was cooled to room temperature, it was placed in an ice bath. Afterwards, the solution was diluted with 5ml of distilled water. The organic layer was separated out, and the water layer was extracted with 10ml of diethyl ether 4 times. The organic fractions were combined and washed with 0.5ml distilled water multiple times until the aqueous layer become neutral. Then the organic solution was dried with anhydrous $MgSO_4$. The ether solvent was evaporated out with the Rotavapor, and products were determined by GC (FID). 3-Methyl-2-decene, 3-Methyl-3-decene, 2-Methyl-1-nonene, 2-Methyl-2-nonene, 3-Methyl-2-nonene, 3-Methyl-3-nonene, 2-Methyl-1-undecene, 2-Methyl-2-undecene, 4-Methyl-3-undecane, 4-Methyl-4-undecane were synthesized in the same methods.

Synthesis of 3-Methyldecane

Four metal balls, 0.02g of Pt/C catalyst were placed into a metal reaction bottle. The 3ml of 3-Methyl-decene product and 3ml of diethyl ether were added into the

reactor. Tightly sealed the cap of the reactor, and provided pressure of 175psi into the reactor. The reaction bottle was shaken periodically for 12hours. Released the pressure, filtrated the solution, and the products were determined by GC (FID). 2-Methylnonane, 3-Methylnonane, 2-Methyldecane, 3-Methyldecane, 2-Methylundecane, 4-Methylundecane were synthesized in the similar manner.

4.2.3 Analysis of Synthesized Alcohol, Alkene, and Alkanes

Original Fischer-Tropsch liquid samples, synthesized Grignard products, Elimination products, Hydrogenation products, and standard branched alkane compounds were analyzed using a Focus gas Chromatograph with flame ionization detector. Branched C_8 compounds were directly purchased from Acros and Alfa Aesar companies, respectively. The unknown branched FT products can be determined by running the mixture of FT product with standard compounds, this is based on the principle of same compounds have the same retention time on the GC (FID) instrument with the same operation method.

4.3 RESULTS AND DISCUSSION

4.3.1 Identification of the Branched C_8 Compounds

The original FT products of C_8 compounds were showed in Fig B-14. From the Fig B-14, it can be seen that there are two small peaks with a shorter retention time than

the n-Octane, and one other small peak is with longer retention time than the n-Octane. According to the previous report, the peak has the highest retention time should be the trans-octene compound[91]. For the peaks in the left side of the major n-octane in Fig B-14, it could be branched C_8 alkanes or alkenes.

By running the mixture of FT product and the authentic 3-Methylheptane, the GC data has been shown that the second small peak was increased, which indicates that the second small peak is the 3-Methylheptane. This data has been shown in the Fig B-15.

The 2-Methylheptane was added into to the mixture of FT product and 3-Methylheptane. By running the mixture of this sample, the GC data has been shown that the first small peak was increased, which indicates that the first small peak is 2-Methylheptane. This data has been shown in the Fig B-16.

4.3.2   Identification of the Branched C_{10} Compounds

In the original C_{10} FT sample data of Fig B-17, it can be seen that the first branched peak is higher than the second branched peak. After the addition 3-methylnonane into the original FT sample, the second branched peak is clearly increased as shown in the Fig B-26.

Subsequently, 2-Methylnonane was added into the previous mixture of original FT sample and 2-Methylnonane and the analysis result of this mixture has been shown

69

in the Fig B-27. With the addition of 2-Methylnonane, the first branched peak is

significantly increased compared to the result in the Fig B-26.

The analysis results in the Fig B-26 and Fig B-27 indicate that the first branched

peak is 2-Methylnonane and the second branched peak is 3-Methylnonane. Beside

these two branched peak, no other type of branched peaks were detected for the C_{10}

products.

4.3.3   Identification of the Branched C_{11} Compounds

The original FT products of C_{11} compounds were shown in Fig B-28. In the Fig B-

28, it can be seen that there are two branched peaks in the left side of n-Undecane

peak. Based on the branched C_8, C_{10} identification results, the branched C_{11} compounds

were estimated to be in the order of 2-Methyl and 3-Methyl in the C_{11} analysis result.

Based on the estimation, 2-Methyldecane was added into the FT product, and

the analysis result of the mixture was shown in the Fig B-29 for C_{11} products. If compare

the branched peaks in Fig B-28 and Fig B-29, it can be clearly seen that the first

branched peak was increased with the addition of 2-Methyldecane.

After addition of the 3-Methyldecane, the 2-Methyldecane was also added into

the same FT product, and the mixture was analyzed by the same analysis method in GC

(FID). The analysis result of 2-Methyldecane added mixture was shown in the Fig B-30.

With the comparison of Fig B-30 and Fig B-29, the second branched peak was increased

followed by the addition of 3-Methyldecane.

Overall, the addition of 2-Methyldecane and 3-Methyldecane analysis result in the Fig B-29 and Fig B-30 implied that the first branched peak is 2-Methylbranched C_{11}, and the second branched peak is 3-Methylbranched C_{11}. In addition, no other type of branched peak was detected in the cobalt catalyzed C_{11} FT products.

4.4   CONCLUSION

Recently, with our identification of branched compounds in the cobalt catalyzed C_8, C_{10}, C_{11} FT product, it has been observed that the cobalt catalyzed branched compounds were 2-methyl, 3-methyl branched FT hydrocarbon product. However, no other type of branched C_8, C_{10}, C_{11} compounds were detected in the cobalt catalyzed FT product, such as dimethyl or ethyl branched hydrocarbon compounds. The identification result of C_8, C_{10}, C_{11} FT product was shown in the Fig 4.6.
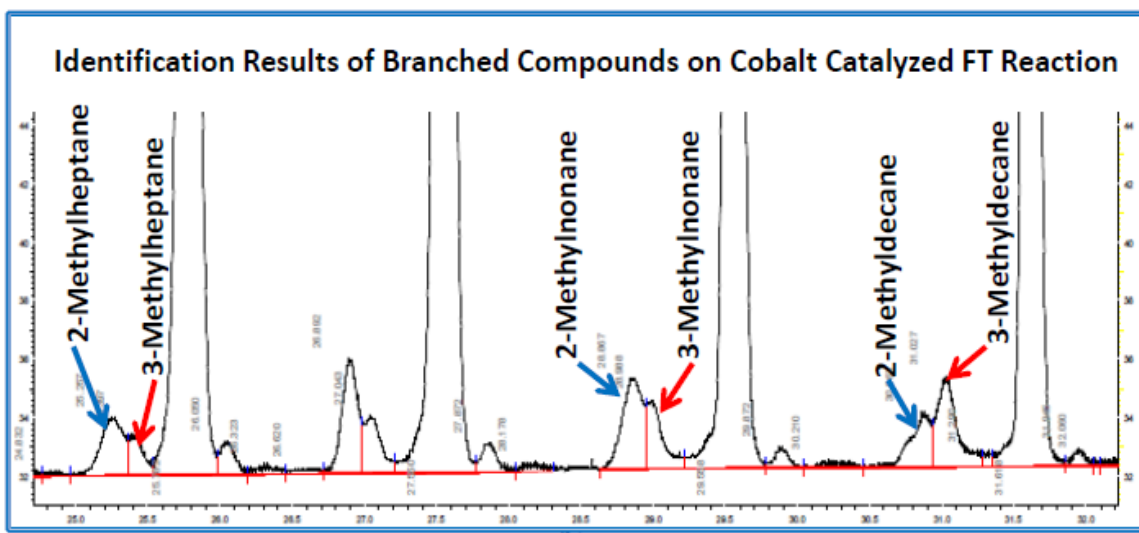

Figure 4.6: Branched hydrocarbon compound identification results

The identification results of 2 or 3 monomethyl- branched hydrocarbon

compounds in C_8, C_{10}, C_{11} provided further support over prediction of branched carbon

formation pathway as shown in the Fig 4.1. Since the prediction of branched

hydrocarbon formation pathways were obtained based on the modified alkylidene

mechanism, the identification result also provided a support over the proposal of

modified alkylidene mechanism for the cobalt catalyzed FT reaction.

CHAPTER 5

SUMMARY AND POSSIBLE FUTURE DIRECTIONS

5.1   SUMMARY

- Higher CO conversion with deuterium syngas compared to the CO conversion with hydrogen syngas during the H_2/D_2 switch experiments have proven that there exists the inverse isotope effect during the Co catalyzed FT reaction.

- The decreasing H/D ratio with increasing carbon number during the H_2/D_2 competition experiments indicates that the deuterium was enriched with increasing carbon number. The H/D ratio is always smaller than 1 and decreasing ratio with increasing carbon number revealed the inverse isotope effect is originated from both of the growing chain and monomer during the carbon-carbon formation.

- The deuterium labeled ethanol addition experiments with and without Al_2O_3 catalyst suggested that the C_2 initiator of FT long chain hydrocarbon products are derived from ethene, but not ethanol. The isotope labeled isopropanol and 1-propanol addition experiment results suggested that the C_3 initiator of FT long chain hydrocarbon products are derived from propene.

- The isotopic distribution in alkane product from ethanol-d_6 experiments indicated that the dehydration/hydration process and deuterium/hydrogen exchange was occurred before it incorporated into the FT hydrocarbon products.

- The recovered isopropanol and 1-propanol isotopic distribution in water product suggested that the isopropanol is more likely to undergo elimination reaction and incorporate into the FT products.

- The isotope labeled propionaldehyde addition experiment result with no incorporation implied that the C_3 initiator does not resemble the propionaldehyde.

- The identification of branched C_8, C_{10}, C_{11} hydrocarbons provided that only mono-methyl branched hydrocarbons in the Co/SiO_2 catalyzed FT products were formed.

- The mono-methyl branched hydrocarbon formation during the Co/SiO_2 catalyzed FTS provided further support over the proposed modified alkylidene mechanism.

5.2   POSSIBLE FUTURE DIRECTIONS

- In order to provide a complete mechanism of FTS, the further experimental results are needed with other FT catalysts, such as iron, since all of our experimental results were obtained only based on cobalt catalysts.

- In our branched compound identification experiments, only carbon 8, 10, and 11 branched FT products were identified that additional identification of branched compounds are needed to elucidate the trend of branched hydrocarbon formation to support the cobalt catalyzed modified alkylidene FT mechanism.

LIST OF REFERENCES

1. Fischer, F.; Tropsch, H., *Brennst Chem* **1926,** *7* (59), 830-836.

2. Anitescu, G.; Bruno, T. J., Liquid Biofuels: Fluid Properties to Optimize Feedstock Selection, Processing, Refining/Blending, Storage/Transportation, and Combustion. *Energ Fuel* **2012,** *26*, 324-348.

3. Steubing, B.; Zah, R.; and Ludwig,C., Heat, Electricity, or Transportation? The Optimal Use of Residual and Waste Biomass in Europe from an Environmental Perspective. *environmental Science & Technology* **2011,** *46*, 164-171.

4. Leckel, D., Diesel Production from Fischer-Tropsch: The Past, the Present and New Concepts. *Energ Fuel* **2009,** *23*, 2342-2358.

5. Gupta, M.; Smith, M. L. and Spivey, J. J., Heterogeneous Catalytic Conversion of Dry Syngas to Ethanol and Higher Alcohols on Cu-Based Catalysts. *ACS Catalysis* **2011,** *1*, 641-656.

6. Anderson, R. B., The Fischer-Tropsch Synthesis. *New york: Academic Press* **1984**.

7. Dry M. E.; Anderson J. R.; Boudan, M. Eds.; *Catalysis Science and Technology* **1981,** *1*, 160.

8. Bartholomew, C. H., Recent Developments in Fischer-Tropsch Catalysis, New Trends in CO Activation. In: studies in Surface Science and Catalysis. **1991,** 64.

9. Davis, B. H., Synthetic lubricants: Advances in Japan up to 1945 based on Fischer-Tropsch derived liquids. *Appl Catal a-Gen* **1991,** *73* (2), 237-248.

10.   Henrici-Olive, G.; Olive, S., The Fischer-Tropsch Synthesis: Molecular Weight

        Distribution of Primary Products and Reaction Mechanism. *Angew. Chem* **1976,**

        88, 144.

11.   Turner, M. L.; Marsih, N.; Mann, B. E.; Quyoum, R.; Long, H. C.; Maitlis, P. M.,

        Investigations by C-13 NMR spectroscopy of ethene-initiated catalytic CO

        hydrogenation. *J Am Chem Soc* **2002,** *124* (35), 10456-10472.

12.   Fridel, R. A.; Sharkey, A. G.; Shultz, J. L., Similar Compositions of Alkanes from

        coal, petroleum, natural gas, and Fischer-Tropsch Product. *J Am Chem Soc* **1966,**

        55 (102), 32-42.

13.   Storch, H. H.; Golumbic, N.; Anderson, R. A., The Fischer-Tropsch and Related

        Synthesis. *Wiley* **1951**.

14.   Teng, B.; Zhang, C.; Yang, J.; Cao, D.; Chang, J.; Xiang, H.; Li, Y., Oxygenate

        Kinetics in Fischer-Tropsch synthesis over an industrial Fe-Mn catalyst. *Fuel* **2005,**

        84 (7-8), 791-800.

15.   Brady III, R.C.; Pettic, R., On the mechanism of the Fischer-Tropsch reaction -

        the chain propagation step. *J Am Chem Soc* **1981,** 103, (5), 1287-1289.

16.   Brady III, R. C.; Pettic, R., Reactions of diazomethane on transition-metal surfaces

        and their relationship to the mechanism of the Fischer-Tropsch reaction, *J Am

        Chem Soc* **1980,** 102, 1287-1289.

17.   Turner, M. L.; Long, H. C.; Shenton, A.; Byers, P. K.; Maitlis, P. M., The Alkenyl

        Mechanism for Fischer-Tropsch Surface Methylene Polymerization - the

Reactions of Vinylic Probes with Co/H-2 over Rhodium Catalysts. *Chem-Eur J* **1995,** *1* (8), 549-556.

18.   Akita, M.; Musashi, H.; Akanishi, N. S.; Moro-oka, Y., Photochemical C-H bond activation of diruthenium bridging alkylidene complexes: Interligand H-exchange on Cp_2Ru_2(mu-CH_2)(mu-CHR)(CO)(2)(R= H, Me). *Journal of Organometallic Chemistry* **2001,** *617* (1), 254-260.

19.   Ekstrom, A.; Lapszewicz, J. A., Reactions of cobalt surface carbides with water and their implications for the mechanism of the Fischer-Tropsch reaction. *Journal of Physical Chemistry* **1987,** *91* (17), 4514-4519.

20.   Akin, A.N.; Onsan, Z. I., Kinetics of CO hydrogenation over coprecipitated cobalt-alumina. *Journal of Chemical Technology and Biotechnology* **1997,** 7(3), 304-310.

21.   Wang, Y.D.; Davis, B. H., Fischer-Tropsch synthesis. Conversion of alcohols over iron oxide and iron carbide catalysts. *Appl Catal a-Gen* **1999,** *180* (1-2), 277-285.

22.   Deng, B. L.; Campbell, T. J.; Burris, D. R., Hydrocarbon formation in metallic iron/water systems. *Environmental Science & Technology* **1997,** *31* (4), 1185-1190.

23.   Duprat, J.; Dobrica, E.; Engrand, C.; Aleon, J.; Marrocchi, Y.; Mostefaoui, S.; Meibom, A.; Leroux, H.; Rouzaud, J. N.; Gounelle, M.; Robert, F., Extreme Deuterium Excesses in Ultracarbonaceous Micrometeorites from Central Antarctic Snow. *Science* **2010,** *328* (5979), 742-745.

24.   Alexander, C. M. O.; Fogel, M.; Yabuta, H.; Cody, G. D., The origin and evolution of chondrites recorded in the elemental and isotopic compositions of their

macromolecular organic matter. *Geochim Cosmochim Ac* **2007,** *71* (17), 4380-

4403.

25.   Bradley, J. P.; Brownlee, D. E., Carbon compounds in the Interplanetary Dust:

Evidence for Formation by Heterogeneous Catalysis. *Science* **1984,** *223 (4631),*

56-58.

26.   Christoffersen. R.; Buseck, P. R., *Epsilon Carbide:* A low-Temperature Component

of Interplanetary Dust Particles. *Science* **1983,** *222 (4630),* 1327-1329.

27.   Taran, Y. A.; Kliger, G. A.; Cienfuegos, E.; Shuykin, A. N., Carbon and hydrogen

isotopic compositions of products of open-system catalytic hydrogenation of

CO(2): Implications for abiogenic hydrocarbons in Earth's crust. *Geochim*

Cosmochim Ac **2010,** *74* (21), 6112-6125.

28.   Lollar, B. S.; Westgate, T. D.; Ward, J. A.; Slater, G. F.; Lacrampe-Couloume, G.,

Abiogenic formation of alkanes in the Earth's crust as a minor source for global

hydrocarbon reservoirs. *Nature* **2002,** *416* (6880), 522-524.

29.   Foustoukos, D. I.; Seyfried, W. E., Hydrocarbons in hydrothermal vent fluids: The

role of chromium-bearing catalysts. *Science* **2004,** *304* (5673), 1002-1005.

30.   Horita, J.; Berndt, M. E., Abiogenic methane formation and isotopic fractionation

under hydrothermal conditions. *Science* **1999,** *285* (5430), 1055-1057.

31.   Kelley, D. S.; Karson, J. A.; Fruh-Green, G. L.; Yoerger, D. R.; Shank, T. M.;

Butterfield, D. A.; Hayes, J. M.; Schrenk, M. O.; Olson, E. J.; Proskurowski, G.;

Jakuba, M.; Bradley, A.; Larson, B.; Ludwig, K.; Glickson, D.; Buckman, K.; Bradley,

A. S.; Brazelton, W. J.; Roe, K.; Elend, M. J.; Delacour, A.; Bernasconi, S. M.; Lilley,

M. D.; Baross, J. A.; Summons, R. T.; Sylva, S. P., A serpentinite-hosted ecosystem: The lost city hydrothermal field. *Science* **2005,** *307* (5714), 1428-1434.

32. McCollom, T. M.; Lollar, B. S.; Lacrampe-Couloume, G.; Seewald, J. S., The influence of carbon source on abiotic organic synthesis and carbon isotope fractionation under hydrothermal conditions. *Geochim Cosmochim Ac* **2010,** *74* (9), 2717-2740.

33. Proskurowski, G.; Lilley, M. D.; Seewald, J. S.; Fruh-Green, G. L.; Olson, E. J.; Lupton, J. E.; Sylva, S. P.; Kelley, D. S., Abiogenic hydrocarbon production at Lost City hydrothermal field. *Science* **2008,** *319* (5863), 604-607.

34. Lollar, B. S.; Lacrampe-Couloume, G.; Voglesonger, K.; Onstott, T. C.; Pratt, L. M.; Slater, G. F., Isotopic signatures of CH4 and higher hydrocarbon gases from Precambrian Shield sites: A model for abiogenic polymerization of hydrocarbons. *Geochim Cosmochim Ac* **2008,** *72* (19), 4778-4795.

35. McCollom, T. M.; Seewald, J. S., Abiotic synthesis of organic compounds in deep-sea hydrothermal environments. *Chem Rev* **2007,** *107* (2), 382-401.

36. Kress, M. E.; Tielens, A. G. G. M., The role of Fischer-Tropsch catalysis in solar nebula chemistry. *Meteorit Planet Sci* **2001,** *36* (1), 75-91.

37. Patzlaff, J.; Liu, Y.; Graffmann, C.; Gaube, J., Studies on product distributions of iron and cobalt catalyzed Fischer-Tropsch synthesis. *Appl Catal a-Gen* **1999,** *186* (1-2), 109-119.

38.   Schulz, H., Special issue: Recent advances in Fischer-Tropsch synthesis - Preface. *Appl Catal a-Gen* **1999,** *186* (1-2), 1-1.

39.   Dry, M., The Fischer-Tropsch process: 1950-2000. *Catalysis Today* **2002,** *71* (3-4), 227-241.

40.   Steynberg, A. P.; Dry, M. E.; Davis, B. H., Breman, B. B., Fischer-Tropsch reactors. *Fischer-Tropsch Technology* **2004,** *152*, 64-195.

41.   Davis, B. H., Fischer-Tropsch Synthesis: Reaction mechanisms for iron catalysts. *Catalysis Today* **2009,** *141*, 25-33.

42.   O. Evans; Nash, A., *Nature* **1926,** *118*, 1954.

43.   Westgate, T. D. W.; J. A.; Slater, G. F.; Lacrampe-Couloume, G.; Sherwood Lollar, B. , Abiogenic formation of alkanes in the earth's crust as a minor source for global hydrocarbon reservoirs. *Nature* **2002,** *416*, 522-524.

44.   Friedel, R. A.; Sharkey, A. G. Jr., Similar Compositions of Alkanes from Coal, Petroleum, Natural Gas, and Fischer-Tropsch Product. *Advances in Chemistry* **1966,** *55*, 32-42.

45.   Glasby, G., Abiogenic origin of hydrocarbons: An historical overview. *Resource Geology* **2006,** *56* (1), 83-96.

46.   Mendeleev, D., L' origine du petrole. *Review. Science* **1877,** *13*, 409-416.

47.   Katz, B. J.; Mancini, E. A.; Kitchka, A. A., A review and technical summary of the AAPG Hedberg Research Conference on "Origin of petroleum - Biogenic and/or abiogenic and its significance in hydrocarbon exploration and production". *AAPG Bulletin* **2008,** *92* (5), 549-556.

48.   Sangely, L.; Chaussidon, M.; Michels, R.; Brouand, M.; Cuney, M.; Huault, V.; Landais, P., Micrometer scale carbon isotopic study of bitumen associated with Athabasca uranium deposits: Constraints on the genetic relationship with petroleum source-rocks and the abiogenic origin hypothesis. *Earth and Planetary Science Letters* **2007,** *258* (3-4), 378-396.

49.   Konn, C.; Charlou, J. L.; Donval, J. P.; Holm, N. G.; Dehairs, F.; Bouillon, S., Hydrocarbons and oxidized organic compounds in hydrothermal fluids from Rainbow and Lost City ultramafic-hosted vents. *Chemical Geology* **2009,** *258* (3-4), 299-314.

50.   Graser, G.; Potter, J.; Kohler, J.; Markl, G., Isotope, major, minor and trace element geochemistry of late-magmatic fluids in the peralkaline llimaussaq intrusion, South Greenland. *LITHOS* **2008,** *106* (3-4), 207-221.

51.   Potter, J.; Rankin, A. H.; Treloar, P. J., Abiogenic Fischer-Tropsch synthesis of hydrocarbons in alkaline igneous rocks; fluid inclusion, textural and isotopic evidence from the Lovozero complex, N.W Russia. *LITHOS* **2004,** *75* (3-4), 311-330.

52.   Sherwood Lollar, B.; Westgate, T. D.; Ward, J. A.; Slater, G. F.; Lacrampe-Couloume, G., Abiogenic formation of alkanes in the Earth's crust as a minor source for global hydrocarbon reservoirs. *Nature* **2002,** *416* (6880), 522-524.

53.   Hosgormez, H.; Etiope, G.; Yalcin, M. N., New evidence for a mixed inorganic and organic origin of the Olympic Chimaera fire (Turkey): a large onshore seepage of abiogenic gas. *Geofluids* **2008,** *8* (4), 263-273.

54.   Lollar, B. S.; Lacrampe-Couloume, G.; Voglesonger, K.; Onstott, T. C.; Pratt, L. M.; Slater, G. F., Isotopic signatures of CH4 and higher hydrocarbon gases from Precambrian Shield sites: A model for abiogenic polymerization of hydrocarbons. *Geochim Cosmochim Ac* **2008,** *72* (19), 4778-4795.

55.   Bian, G.; Mochizuki, T.; Fujishita, N.; Nomoto, H.; Yamada, M., Activities and Microstructure of Co/SiO_2 Catalysts for FT Synthesis. *Fuel Chem. Division preprints*, **2002,** *47* (2), 494-495.

56.   Davis, B. H.; Jacobs, G.; Das, T. K.; Patterson, P. M.; Li, J. L.; Sanchez, L., Fischer-Tropsch synthesis XAFS XAFS studies of the effect of water on a Pt-promoted Co/Al2O3 catalyst. *Appl Catal a-Gen* **2003,** *247* (2), 335-343.

57.   Lowry, T. H.; Richardson, K. S., *Mechanism and theory in organic chemistry*, 3rd ed.; Harper & Row: New York, **1987**, p 748.

58.   Storch, H. H.; Golumbic, N.; Anderson, R. A., The Fischer-Tropsch and Related Synthesis. *John Wiley & Sons, Inc., New York,* **1951**.

59.   Shi, B.; Jin, C., Inverse kinetic isotope effects and deuterium enrichment as a function of carbon number during formation of C-C bonds in cobalt catalyzed Fischer-Tropsch synthesis. *Appl Catal a-Gen* **2011,** *393* (1-2), 178-183.

60.   Dictor, R.; Bell, A., *Ind. Eng. Chem. Process Des. Dev* **1983,** *22*, 678-681.

61.   Anderson, R. B., Schulz-Flory Equation. *Chemistry of Petrochemical Processes* **1978,** 55 (1), 114-115.

62. Schulz, G. V., Über die Beziehung zwischen Reaktionsgeschwindigkeit und usammensetzung des Reaktionsproduktes bei akropolymerisationsvorgängen'. *Zeit. Physikal. Chemie.* **1935,** (B30), 379.

63. Flory, P. J., Molecular-size distibution in linear condensation polymers. *J Am Chem Soc* **1936,** *58*, 1877.

64. *The α value of an FT reaction using CO/H$_2$ as the synthesis gas is used to determine the average molecular weight of the reaction since the small change in α when switched to CO/D$_2$ will not significantly change the value of n, which equals to (average molecular weight)/14.*

65. Sarup, B.; Wojciechowski, B. W., The effect of time on stream and feed composition on the selectivity of a cobalt Fischer—Tropsch catalyst. *Can, J. Chem, Eng* **1984**, *62 (2)*, 249-256.

66. Hirsa, M. T.; Johannes, H. B.; Chaitanya, B. K.; Matthijs R.; Iulian Dugulan, A.; Krijn P. de Jong, Supported Iron Nanoparticles as Catalysts for Sustainable Production of Lower Olefins. *Science* **2012,** *335*, 835.

67. Halevi, E. A., For a Review of secondary isotope effect. *Prog. Phys. Org. Chem* **1963,** *1*, 109.

68. Lowry, T. H.; Richardson, K. S., *Mechanism and theory in organic chemistry*. 2d ed.; Harper & Row: New York, N.Y., **1981**; p 901.

69. Streitwieser, A. Jr.; Jagow, R. H.; Fahey, R. C.; Suzuki, S., Kinetic Isotope Effects in the Acetolyses of Deuterated Cyclopentyl Tosylates. *J Am Chem Soc* **1958,** *80 (9),* 2326-2332.

70. Strausz, O. P.; Safarik, I.; O' Callaghan, W. B.; Gunning, H. E., Streitwieser's treatment as applied to addition to double bonds has been criticized as being oversimplified. However, a calculation including an important isotope-sensitive vibration of the transition state not present in reactants (a CH_2 twist) and also including the effect of moment-of-inertia changes on going to the transition state gives k_H/k_D= 1/ 1.38=0.72, only a small change from Streitwieser's value. *J Am Chem Soc* **1972,** *94*, 1828.

71. Michael L. T.; Peter, K. B.; Helen, C. L.;Peter M. M., Vinyl Initiation of Fischer-Tropsch Polymerization over Rhodium. *J Am Chem Soc* **1993,** *115*, 4417-4418.

72. Emmett, P. H., Fischer-Tropsch Synthesis Mechanism Studies. The addition of Radioactive Ketene to the Synthesis Gas. *Journal of Physical Chemistry* **1959,** *63* (6), 962-965.

73. Tau, L. M.; Dabbagh, H. A.; Davis, B. H., Fischer-Tropsch Synthesis: carbon-14 tracer study of alkene incorporation. *journal of Energy Fuels* **1990,** *4* (1), 94-99.

74. Kummer, J. T.; Podgurski, H. H.; Spencer, W. B.; Emmett, P. H., Mechanism Studies of the Fischer-Tropsch Synthesis. The Addition of Radioactive Alcohol. *J Am Chem Soc* **1951,** *73* (2), 564-569.

75.   Hall, W. K.; Kokes, R. J.; Emmett, P. H., Mechanism Studies of the Fischer-Tropsch Synthesis: The Incorporation of Radioactive Ethylene, Propionaldehyde and Propanol. *J Am Chem Soc* **1960,** *82* (5), 1027-1037.

76.   Tau, L. M.; Dabbagh, H. A.; Davis, B. H., Fischer-Tropsch synthesis: comparison of carbon-14 distributions when labeled alcohol is added to the synthesis gas. *Journal of Energy Fuels* **1991,** *5* (1), 174-179.

77.   Hayashi, K.; Isomura, K.; Taniguchi, H., *Chem. Lett.* **1975**, 1011.

78.   Emmett, P.H.; Kummer, B. J. T., Fischer-Tropsch Synthesis Mechanism Studies. The addition of Radioactive Alcohols to the Synthesis Gas. *J Am Chem Soc* **1953,** *75* (21), 5177–5183.

79.   Kokes, B. R. J.; Keith, W.; Emmett, P. H., Fischer-Tropsch Synthesis Mechanism Studies. The addition of Radioactive Ethanol to the Synthesis Gas. *J Am Chem Soc* **1957,** *79* (12), 2989–2996.

80.   Kokes, B. R. J.; Keith, W.; Emmett, P.H., Mechanism Studies of the Fischer-Tropsch Synthesis: The Incorporation of Radioactive Ethylene, Propionaldehyde and Propanol. *J Am Chem Soc* **1960,** *82* (5), 1027–1037.

81.   Muthu, K. G.; Keogh, R. A.; Shafer, W. D.; Shi, B.; Davis, B. H., Fischer-Tropsch Synthesis: Deuterium Labled ethanol tracer studies on iron catalysts. *Appl Catal a-Gen* **2010,** *385* (1-2), 46-51.

82.   Jalama, K.; Coville, N. J.; Hildebrandt, D.; Glasser,D.; Jewell, L. L., Fischer-Tropsch Synthesis over Co/TiO$_2$: Effect of Ethanol Addition. *Journal of Fuel* **2007,** *86* (1-2), 73-80.

83. Schrock, R. R., Catalysis by Transition Metals: metal-carbon double and triple bonds. *Science* **1983,** *219*, 13-18.

84. Tanaka, K.; Imamoglu, i.Y.; Zumreogla-Karam, B.; Amass (Eds), A. J., Olefin Metathesis and Polymerization Catalysis: Synthesis, Mechanism, and Utilization. *Kluwer Academic Publishers* **1990**, 303-333.

85. Shi, B.; Keogh, R. A.; Davis, B. H., Fischer-Tropsch synthesis: The formation of branched hydrocarbons in the Fe and Co catalyzed reaction. *J Mol Catal a-Chem* **2005,** *234*, 85-87.

86. Sharkey, A. G.; Schulz, J. L.; Friedel, R. A., Mass Spectrometric Determination of the Ratio of Branched to Normal Hydrocarbons Up to C_{18} in Fischer-Tropsch Product. *Analytical Chemistry* **1962,** *34* (7), 826-830.

87. Pichler, H.; Schulz, H.; Kuhne, D., *Brennst Chem* **1968,** *49 (11)*, 344.

88. Satterfield, C. N., Yates, I. C., Hydrocarbon Selectivity from Cobalt Fischer-Tropsch Catalysts. *Energ Fuel* **1992,** *6*, 308-314.

89. Anderson, R. B., Friedel, R. A., Composition of synthetic liquid fuels. I. Product distribution and analysis of C5-C8 paraffin isomers from cobalt catalyst. *J Am Chem Soc* **1950,** *72*, 1212.

90. Shi, B. and Jin, C., Deuterium tracer studies on cobalt catalyzed Fischer-Tropsch synthesis: Addition of alcohols. *Appl Catal a-Gen* **2011,** *398* (1-2), 54-58.

91. Subramaniam, B.; Snavely, K., On-Line Gas Chromatographic Analysis of Fischer-Tropsch Synthesis Products Formed in a Supercritical Reaction Medium. *Ind. Eng. Chem. Process Des. Dev* **1997,** *36*, 4413-4420.

APPENDIX A:

TABLES

Table A-1: Measured Mass Flow Control Rate under Different Pressure and Temperatures

P= 150Psi, T= 160 °C			P= 150Psi, T= 180 °C		
Flow Control Rate (%)	Flow Rate (ml/min)	STDEV	Flow Control Rate (%)	Flow Rate (ml/min)	STDEV
100	124.12	6.45	100	135.6	3.88
90	117.29	3.05	90	120.93	6.8
80	93.51	7.22	80	108.32	2.59
70	90.12	3.55	70	91.78	4.38
60	73.04	4.72	60	78.99	1.97
50	62.07	7.01	50	66.82	3.49
40	48.13	3.33	40	48.85	1.99
30	37.28	2.83	30	42.15	7.63
20	25.39	4.45	20	26.31	1.7
P= 150Psi, T= 190 °C			P= 150Psi, T= 200 °C		
100	137.52	4.31	100	136.39	2.26
90	121.85	1.86	90	121.63	1.27
80	109.63	2.36	80	110.62	1.56
70	94.56	2.88	70	98.81	4.64
60	79.64	2.19	60	72.33	1.96
50	68.36	1.95	50	67.74	2.41
40	54.56	3.43	40	50.78	3.55
30	43.75	4.51	30	36.34	2.3
20	26.85	3.31	20	23.76	3.07
P= 150Psi, T= 210 °C			P= 150Psi, T= 220 °C		
100	126.77	7.96	100	129.25	11.35
90	111.62	5.16	90	114.92	4.88
80	95.96	1.65	80	109.92	3.28
70	81.44	3.98	70	96.28	1.56
60	77.29	6.66	60	83.63	7.14
50	63.91	4.27	50	70.66	3.89
40	58.75	4.72	40	46.23	4.11
30	38.65	5.22	30	42.64	4.92
20	28.88	4.03	20	30.24	3.03
P= 180Psi, T= 250 °C			P= 180Psi, T= 270 °C		
100	133.92	2.41	100	138.74	0.73
90	122.76	2.22	90	123.71	4.01
80	111.73	3.77	80	108.3	2.05

Table A-1 (continued)

70	93.72	2.32	70	96.82	2.42
60	84.37	2.45	60	83.84	4.74
50	70.13	3.97	50	67.7	4.13
40	56.92	4.69	40	54.01	5
P= 250Psi, T= 215 °C			**P= 250Psi, T= 220 °C**		
100	140.73	4.31	100	138.15	2.74
90	123.53	2.26	90	125.08	3.39
80	108.92	6.65	80	110.76	3.05
70	97.04	5.62	70	98.26	4.49
60	83.31	5.24	60	85.32	4.66
50	67.7	4.11	50	71.78	3.72
40	56.92	3.97	40	57.06	4.51
P= 250Psi, T= 230 °C			**P= 250Psi, T= 250 °C**		
100	136.37	4.49	100	138.51	2.81
90	125.36	4.62	90	123.93	4.18
80	110.45	1.69	80	110.51	3.18
70	36.46	3.69	70	97.06	3.72
60	85.74	3.64	60	80.03	1.57
50	72.84	3.81	50	72.56	4.02
40	58.14	4.34	40	56.1	4.52

Notes: Each flow rate was measured at least six times, and the standard deviation values were calculated and shown as STDEV. Flow control rate is the machine controlled amount of gas flowed out of the gas tank. Flow rate is the rate of gas flowed out of the reactor.

APPENDIX B:

FIGURES
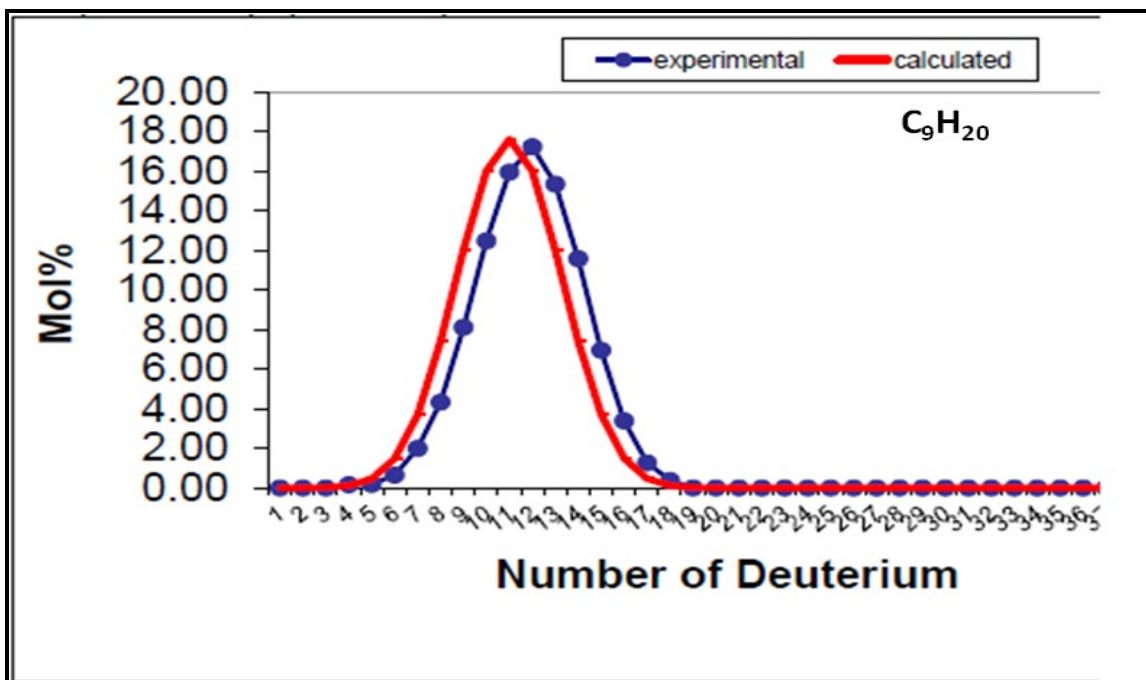
Figure B-1: Deuterium distribution of n-Nonane
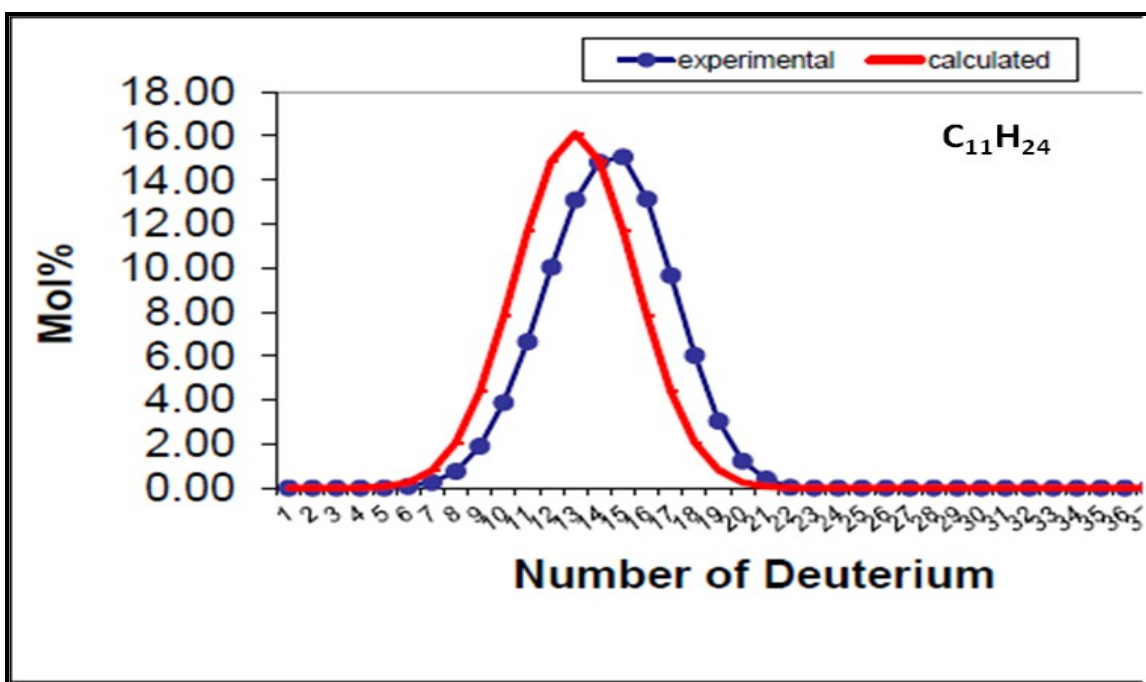
Figure B-2: Deuterium distribution of n-Undecane
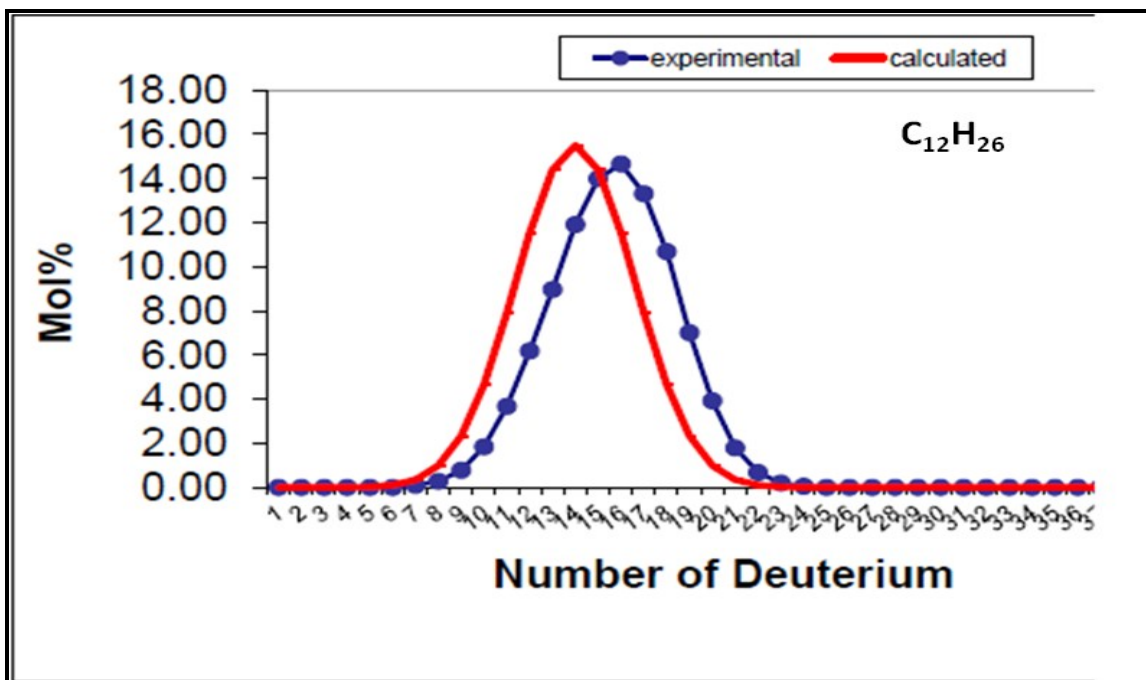
Figure B-3: Deuterium distribution of n-Dodecane
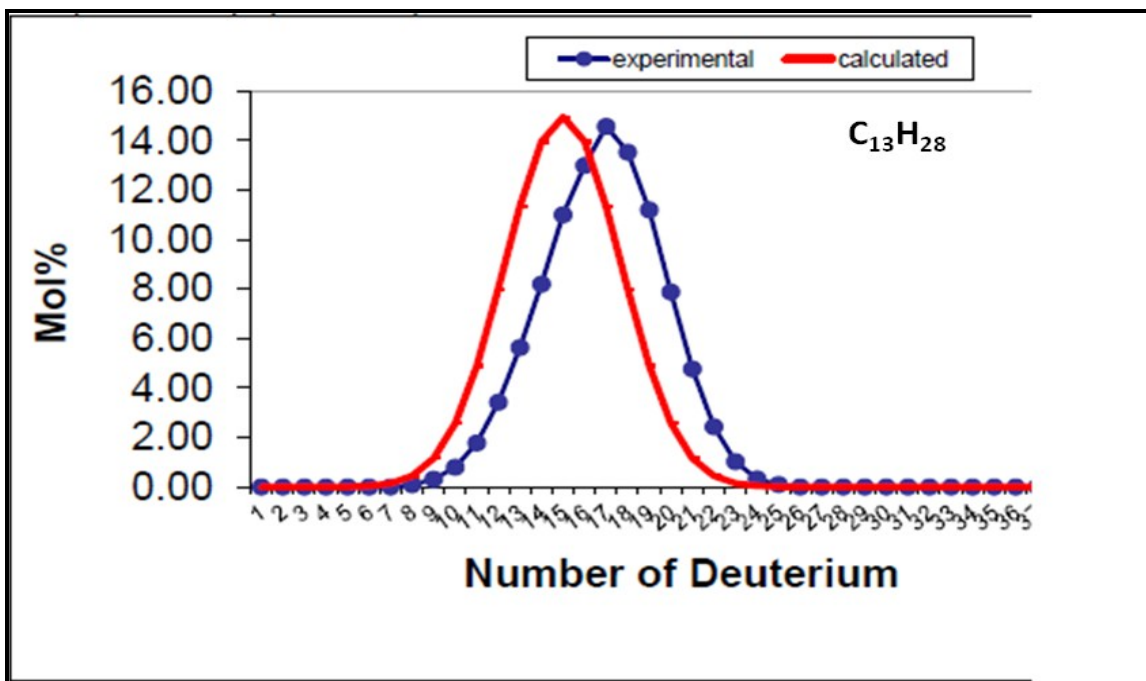
Figure B-4: Deuterium distribution of n-Tridecane
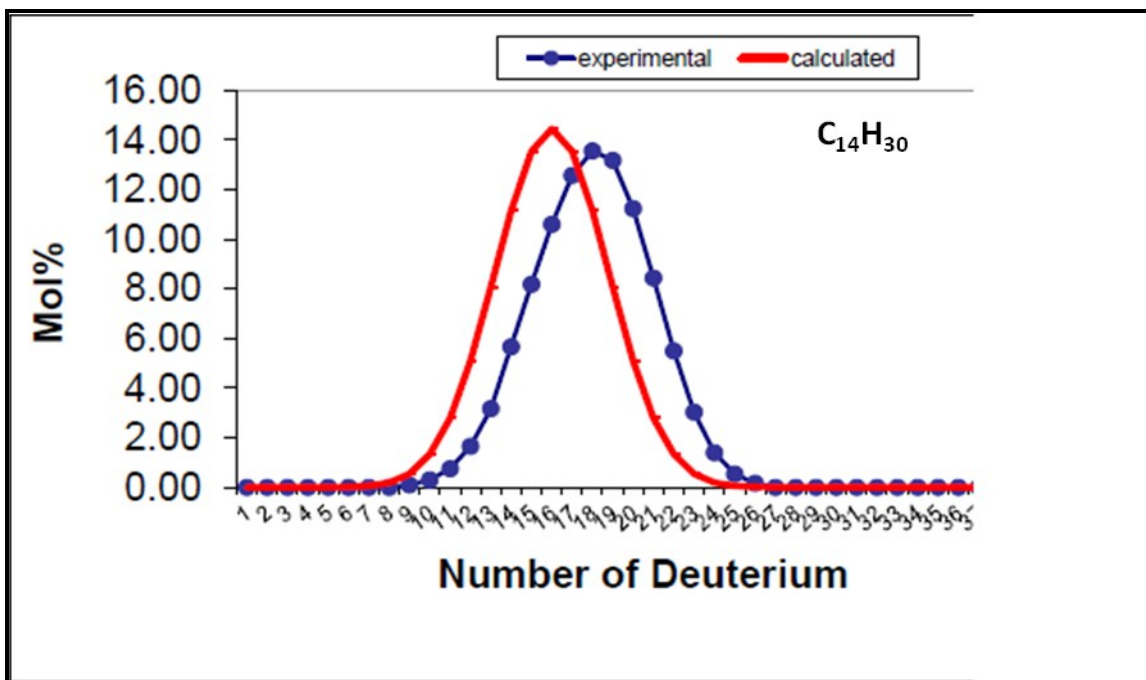
Figure B-5: Deuterium distribution of n-Tetradecane
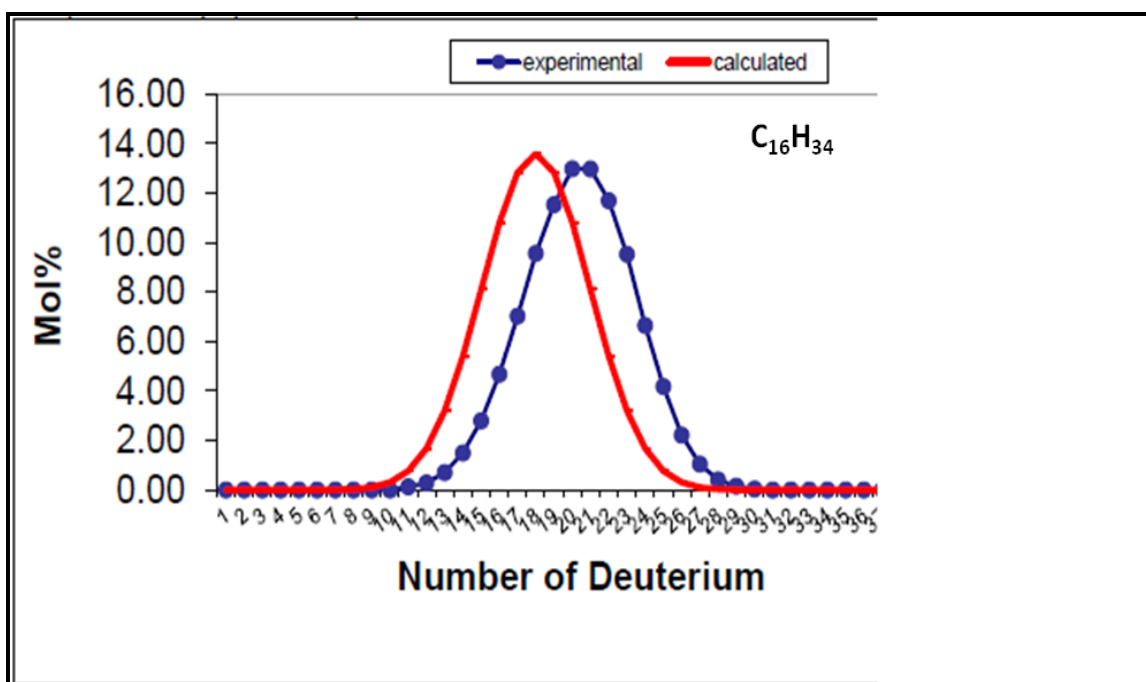
Figure B-6: Deuterium distribution of n-Hexadecane
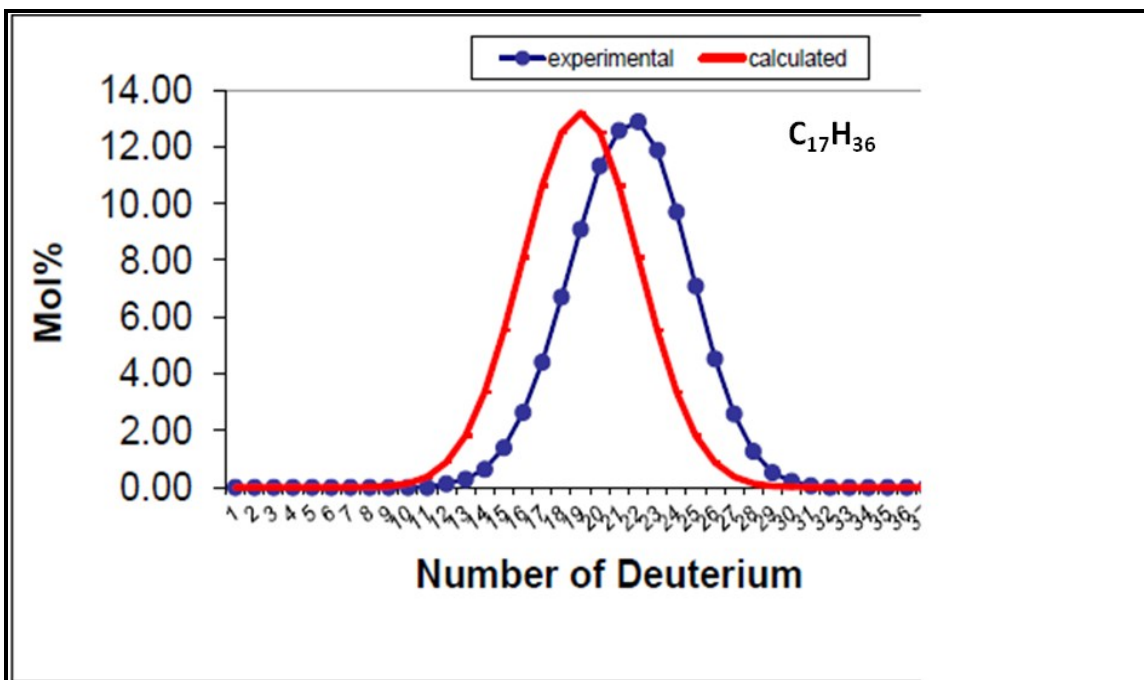
Figure B-7: Deuterium distribution of n-Heptadecane
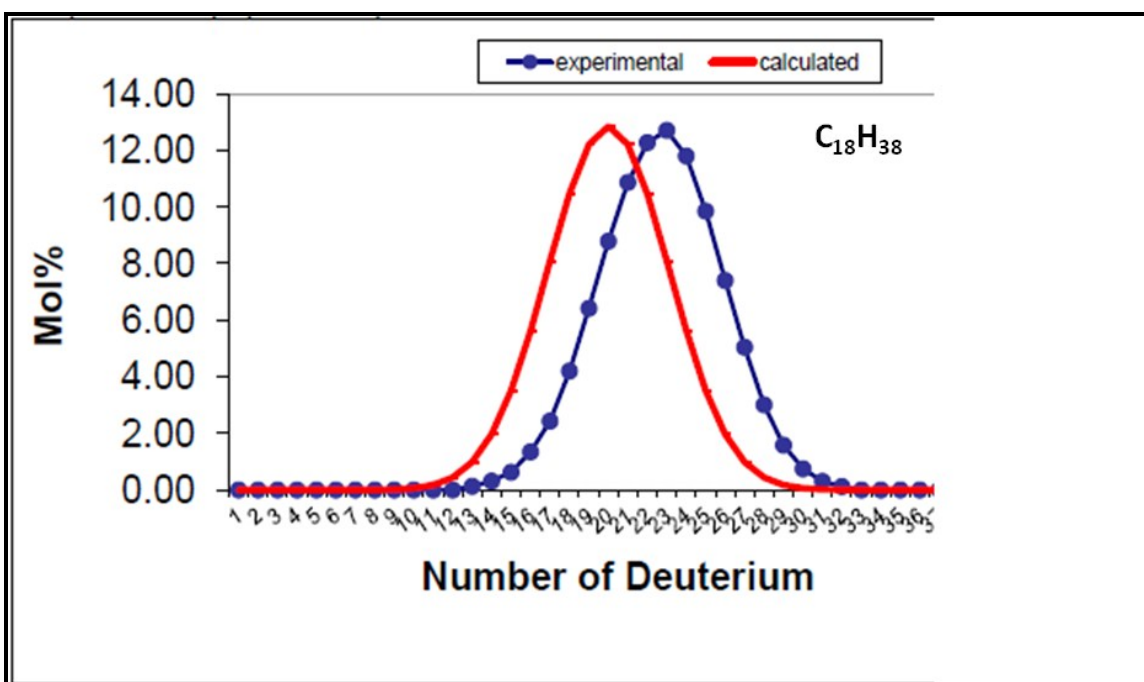
Figure B-8: Deuterium distribution of n-Octadecane
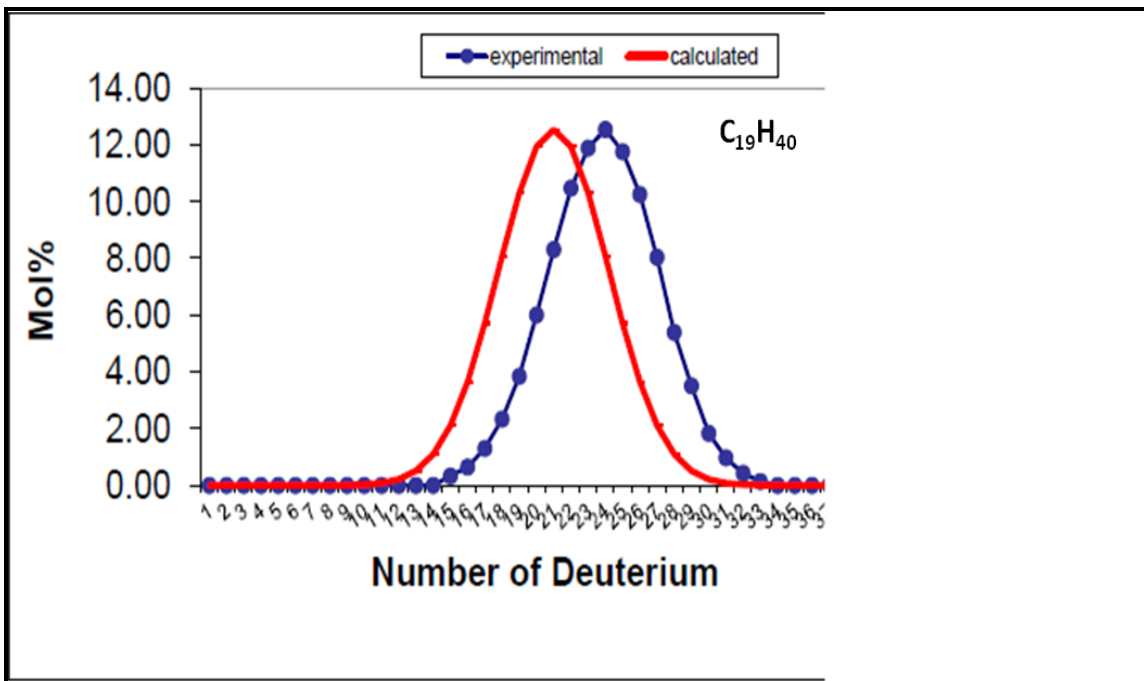
Figure B-9: Deuterium distribution of n-Nonadecane
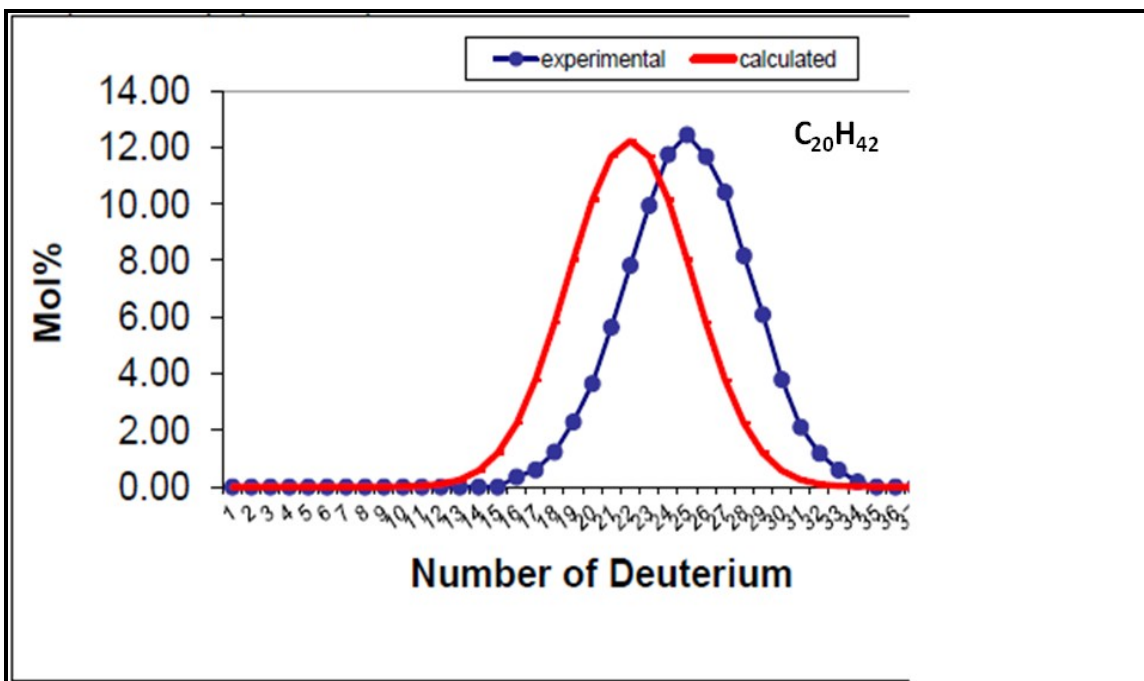
Figure B-10: Deuterium distribution of n-Icosane
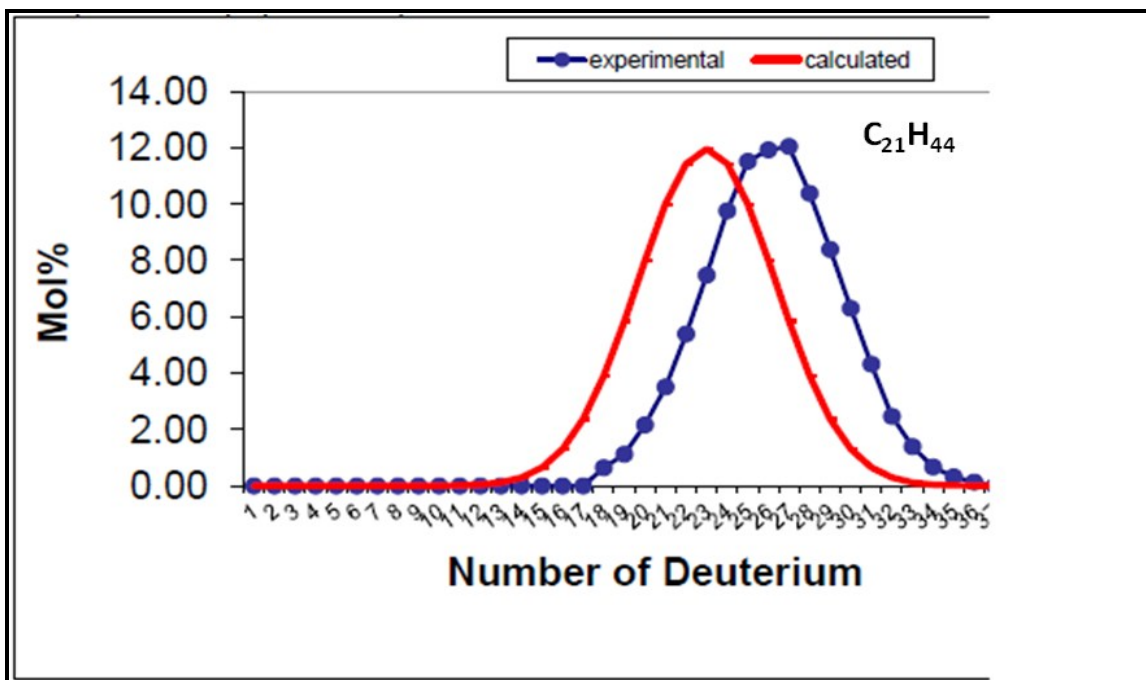
Figure B-11: Deuterium distribution of n-Unicosane
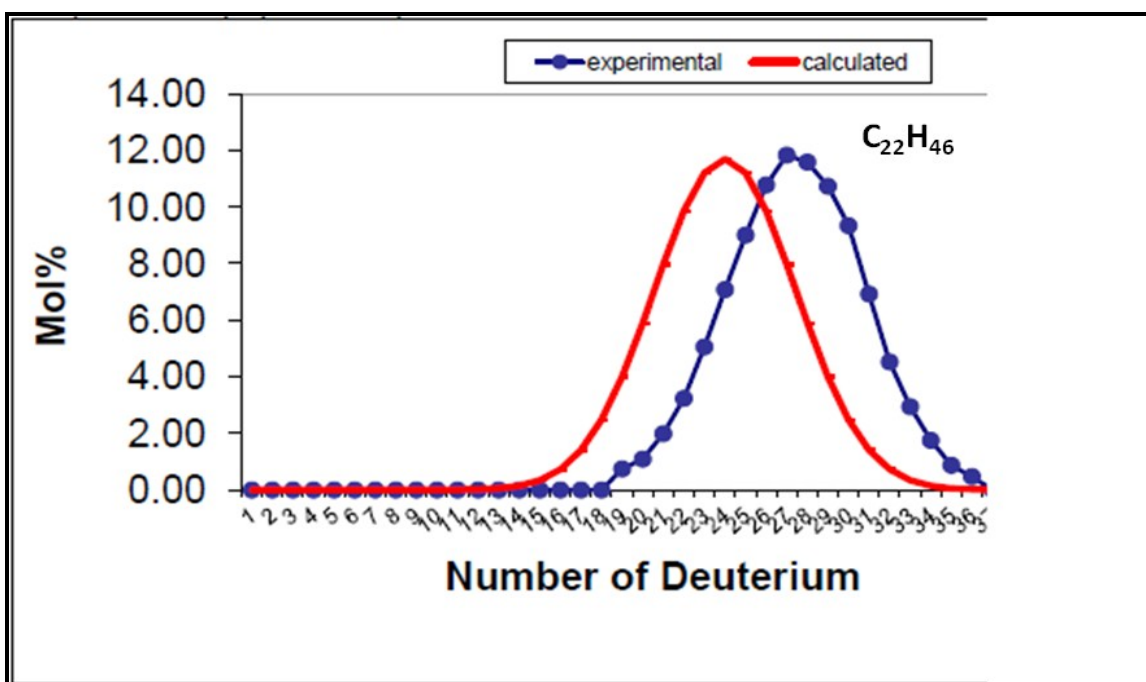
Figure B-12: Deuterium distribution of n-Doicosane
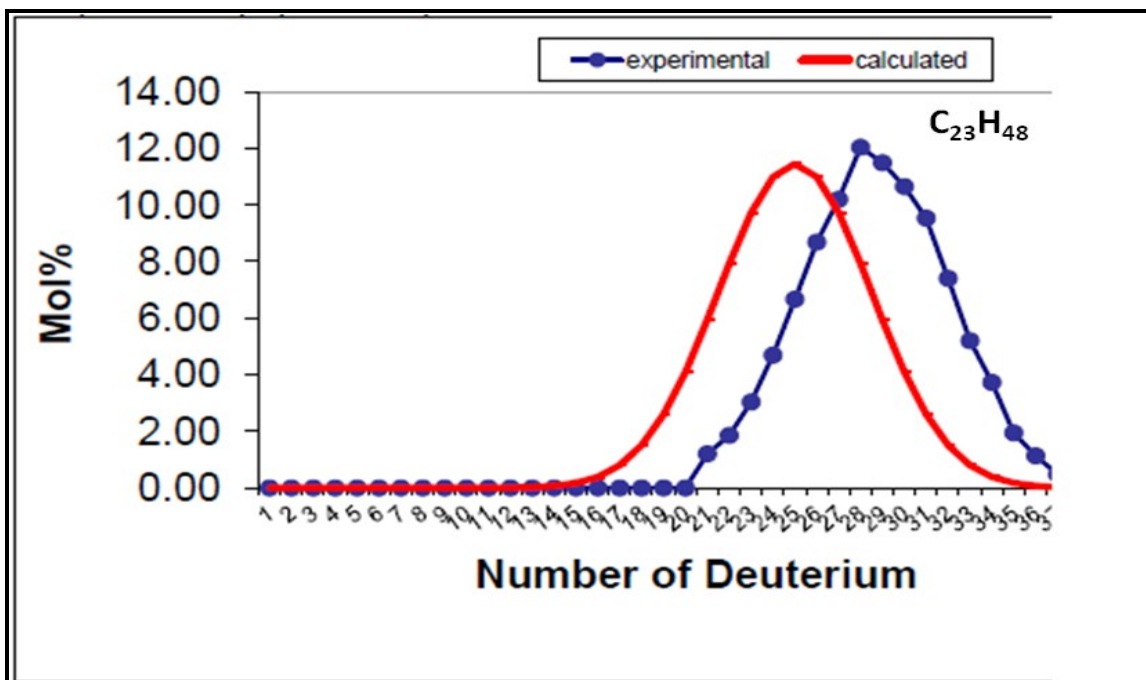
Figure B-13: Deuterium distribution of n-Tricosane
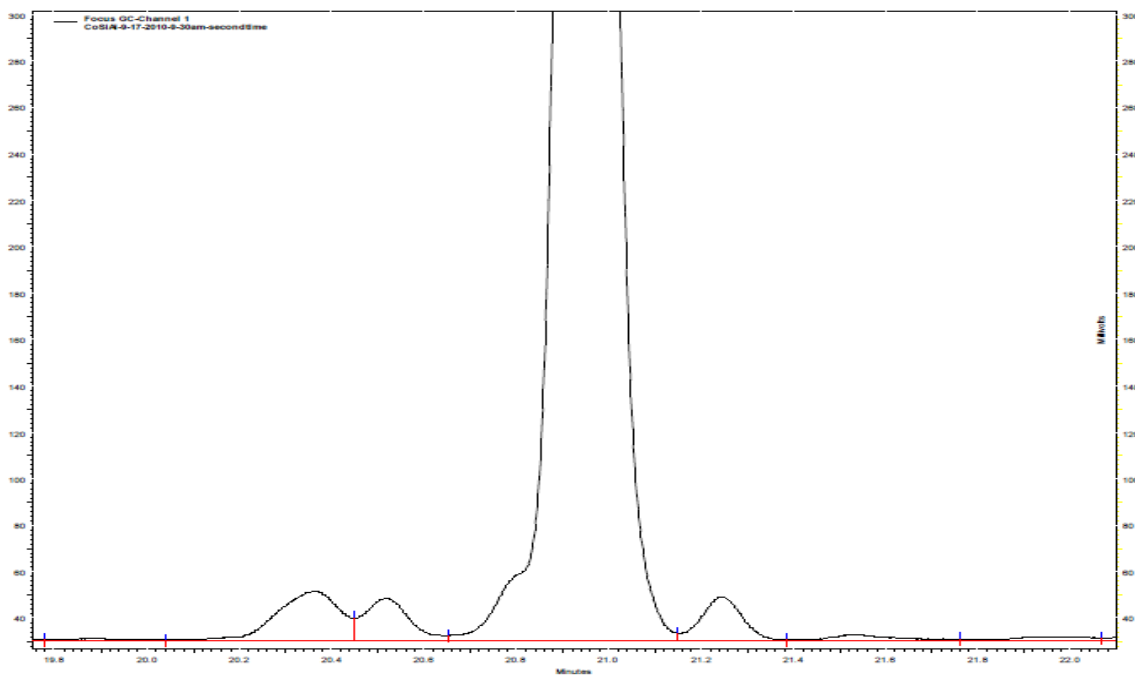
Figure B-14: Gas chromatogram of hydrocarbons with 8 carbon atoms produced by Co catalyzed FT reactions
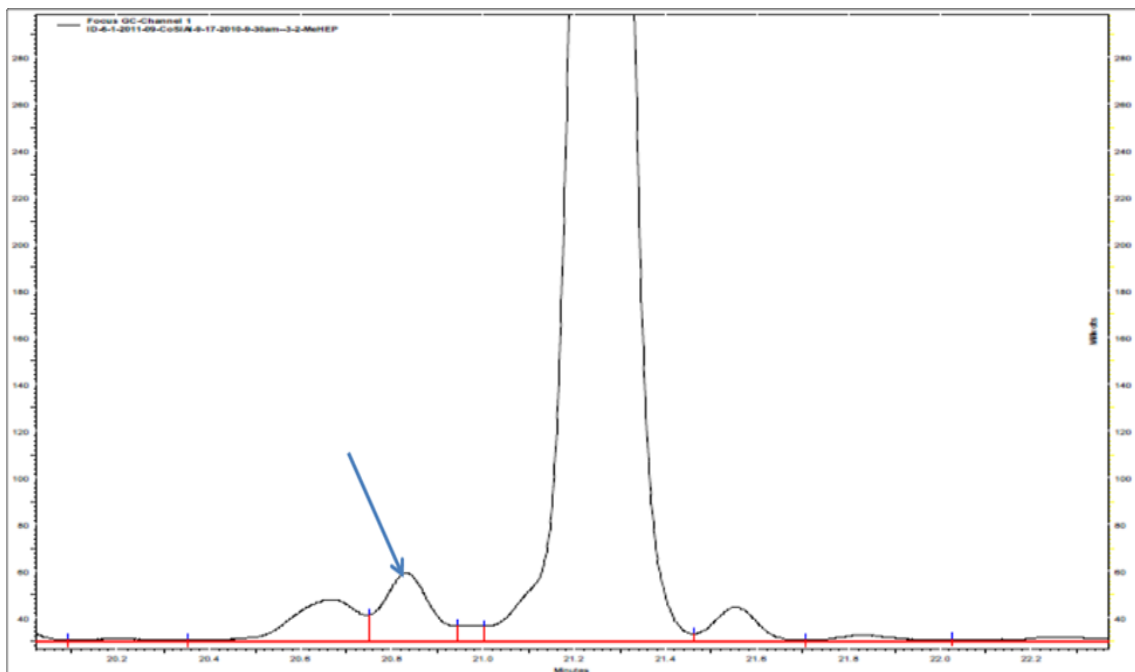
Figure B-15: Gas chromatogram of 3-Methylheptane addition into the Co catalyzed FT products
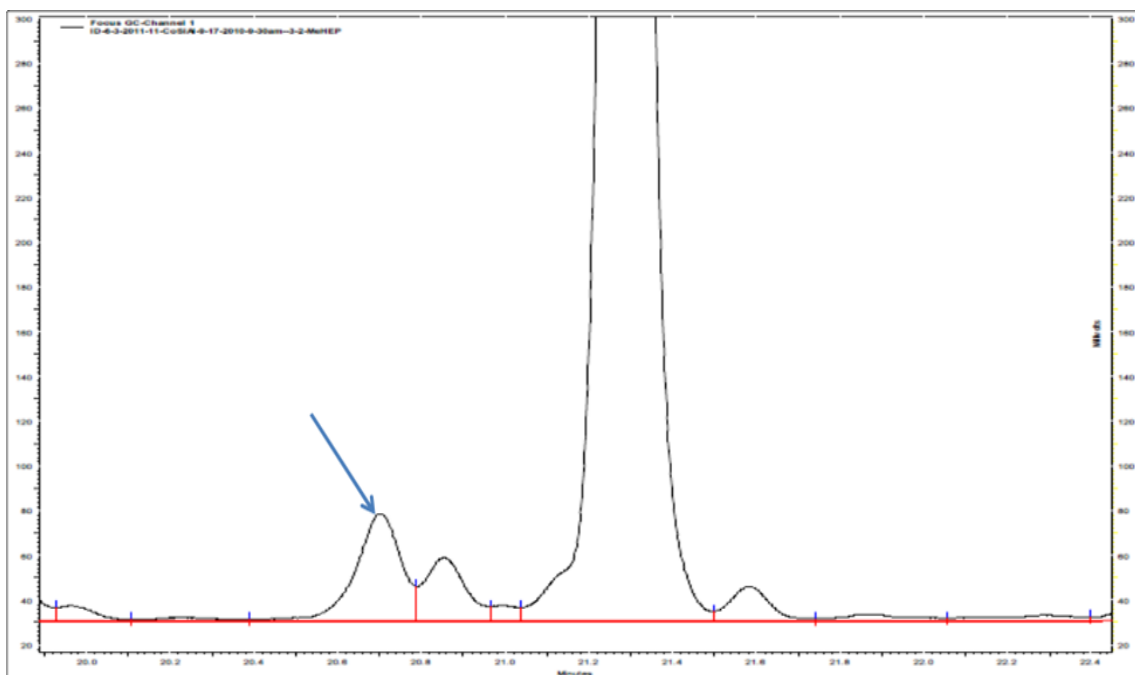
Figure B-16: Gas chromatogram of 2-Methylheptane addition into the Co catalyzed FT products
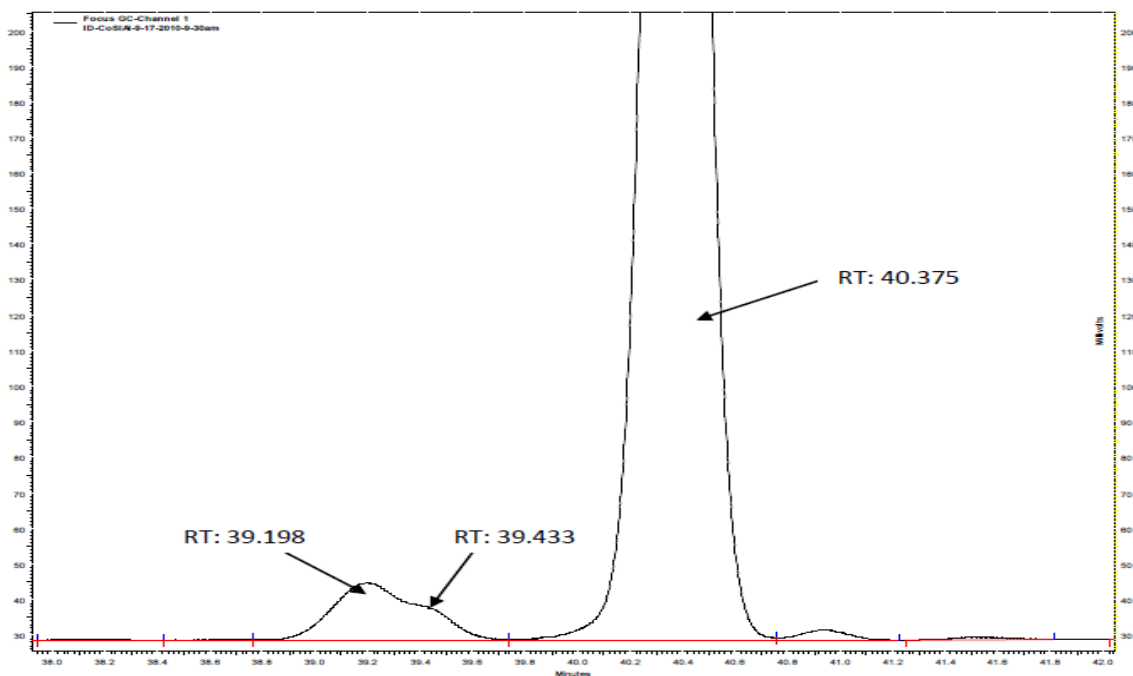
Figure B-17: Gas chromatogram of hydrocarbons with 10 carbon atoms produced by Co catalyzed FT reactions
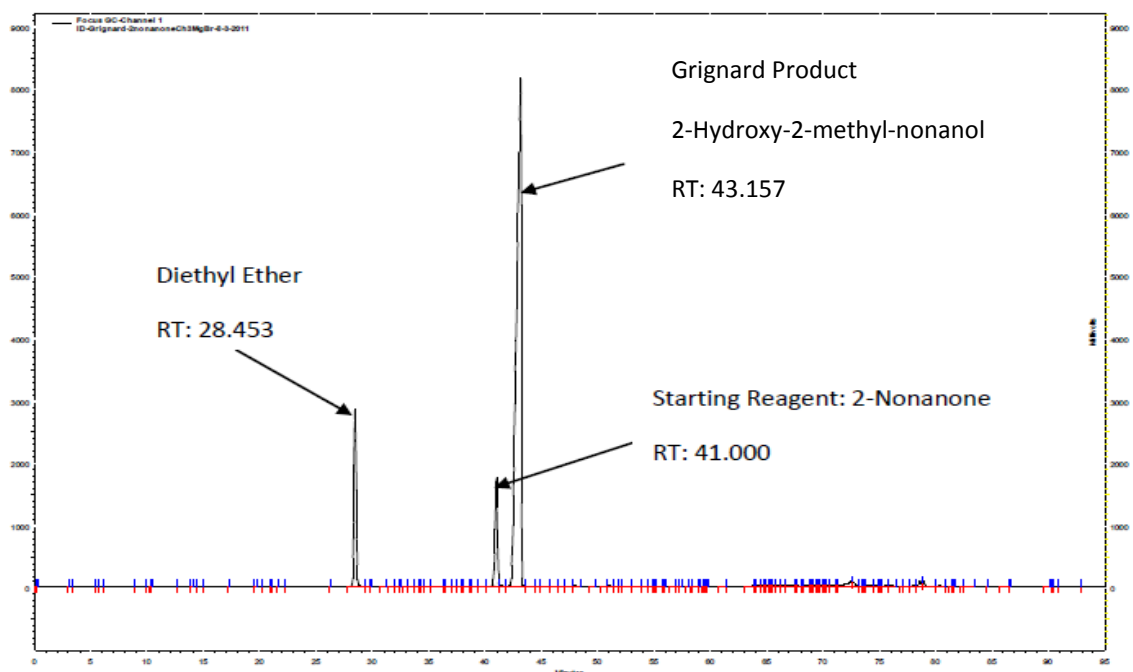
Figure B-18: Gas chromatogram of the synthesized 2-Methyl-2-nonanol
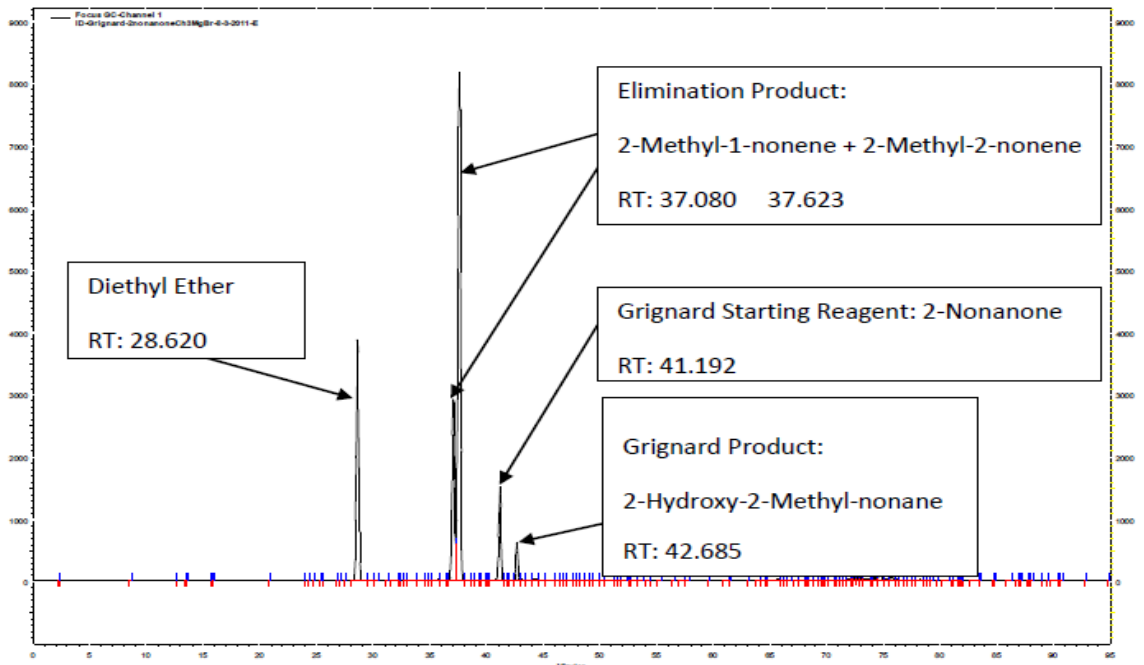
Figure B-19: Gas chromatogram of the synthesized 2-Methyl-nonene
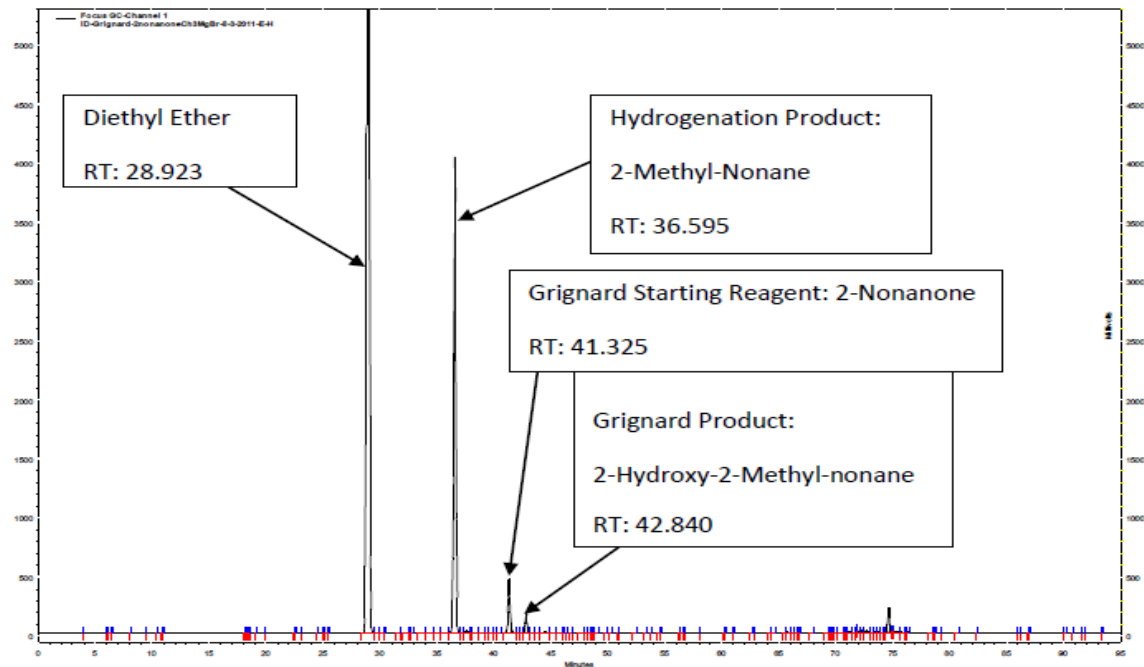
**Figure B-20:** Gas chromatogram of the synthesized 2-Methyl-nonane

101
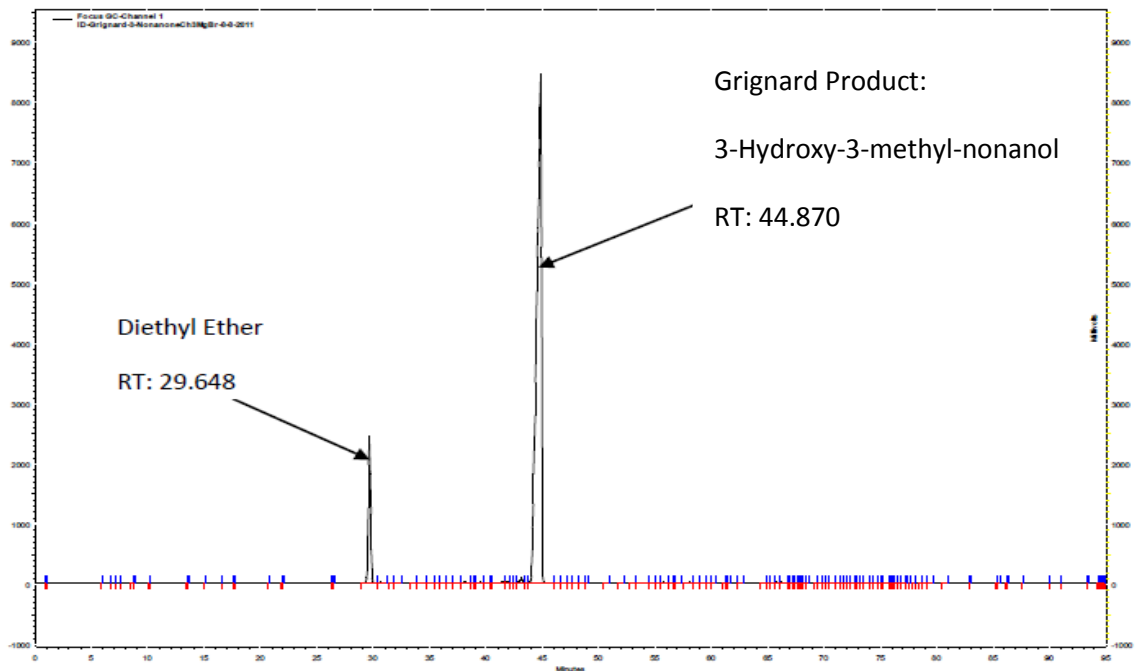
Figure B-21: Gas chromatogram of the synthesized 3-Methyl-3-nonanol
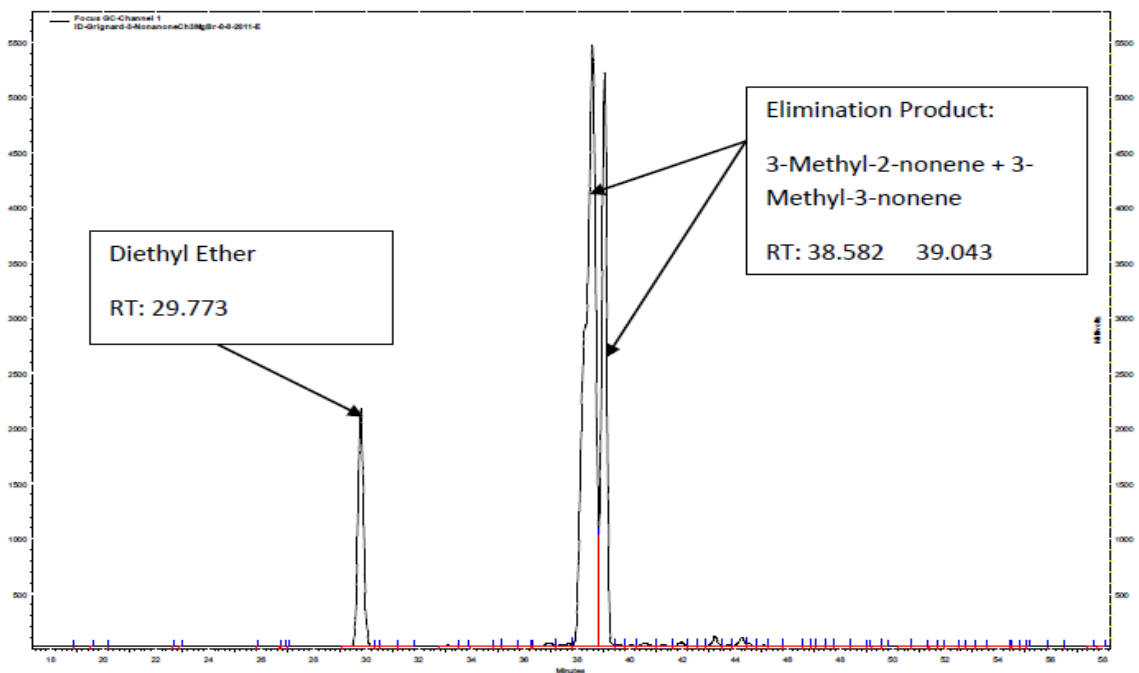
Figure B-22: Gas chromatogram of the synthesized 3-Methyl-nonene
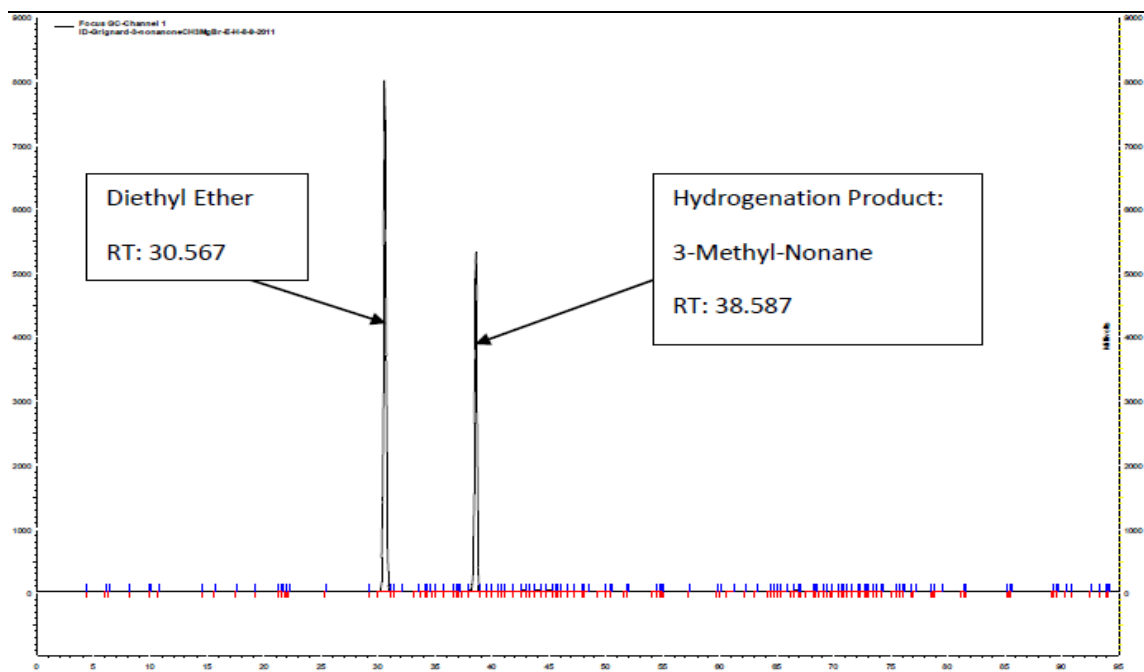
Figure B-23: Gas chromatogram of the synthesized 3-Methyl-nonane
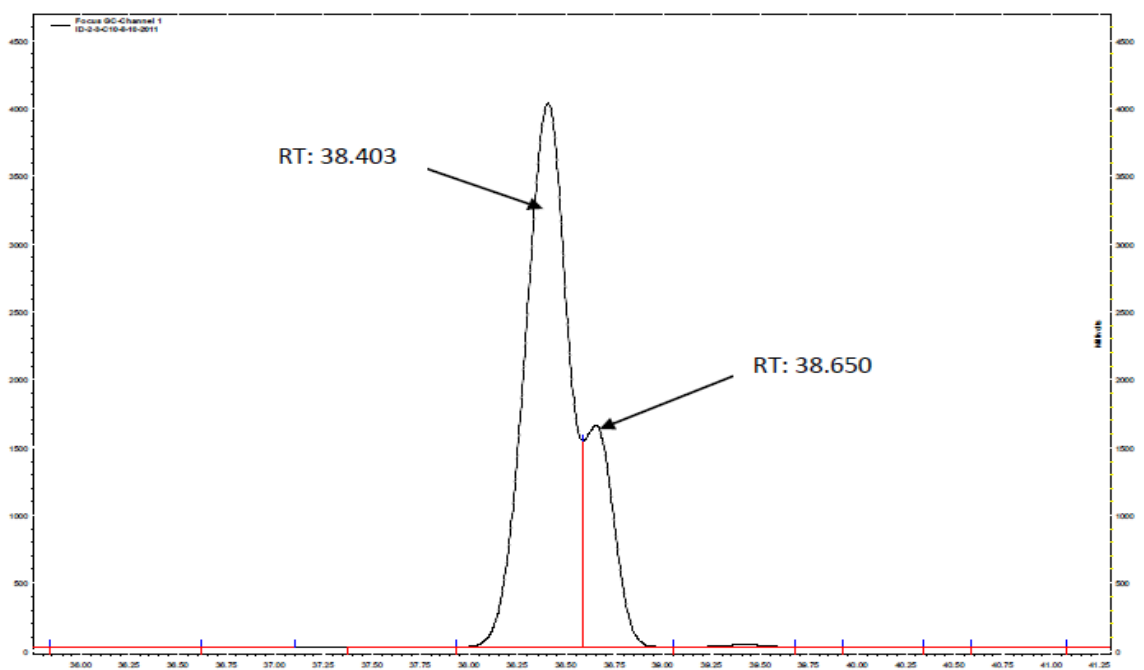
Figure B-24: Gas chromatogram of the synthesized mixture of 2-Methylnonane and 3-Methylnonane
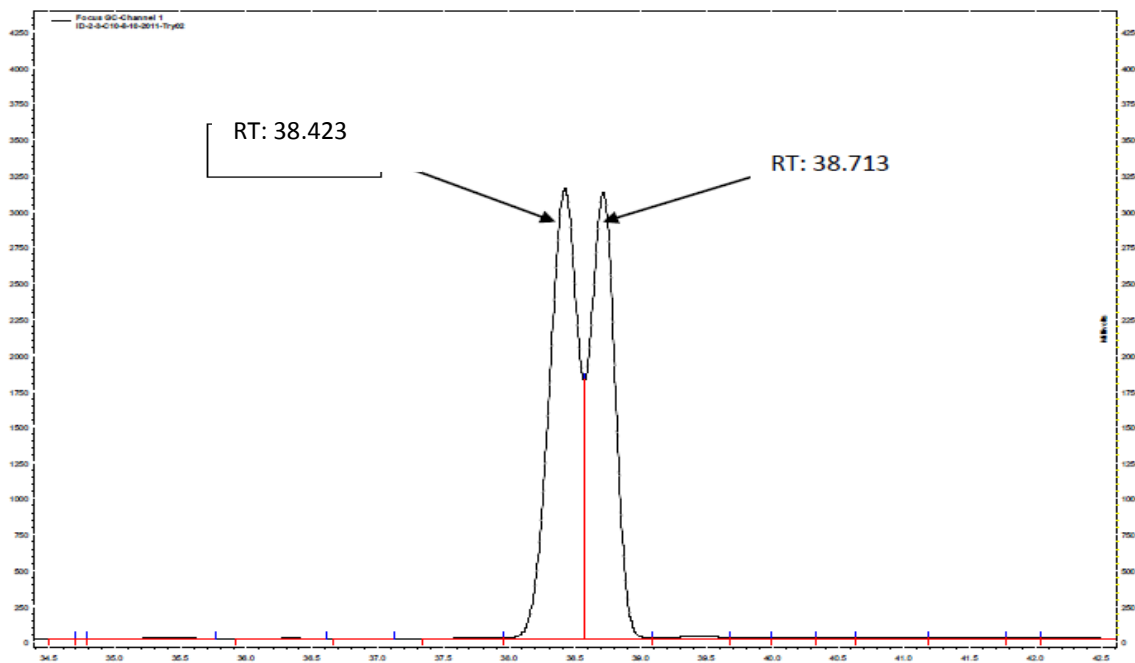
Figure B-25: Gas chromatogram of the synthesized mixture of 2-Methylnonane and additional 3-Methylnonane
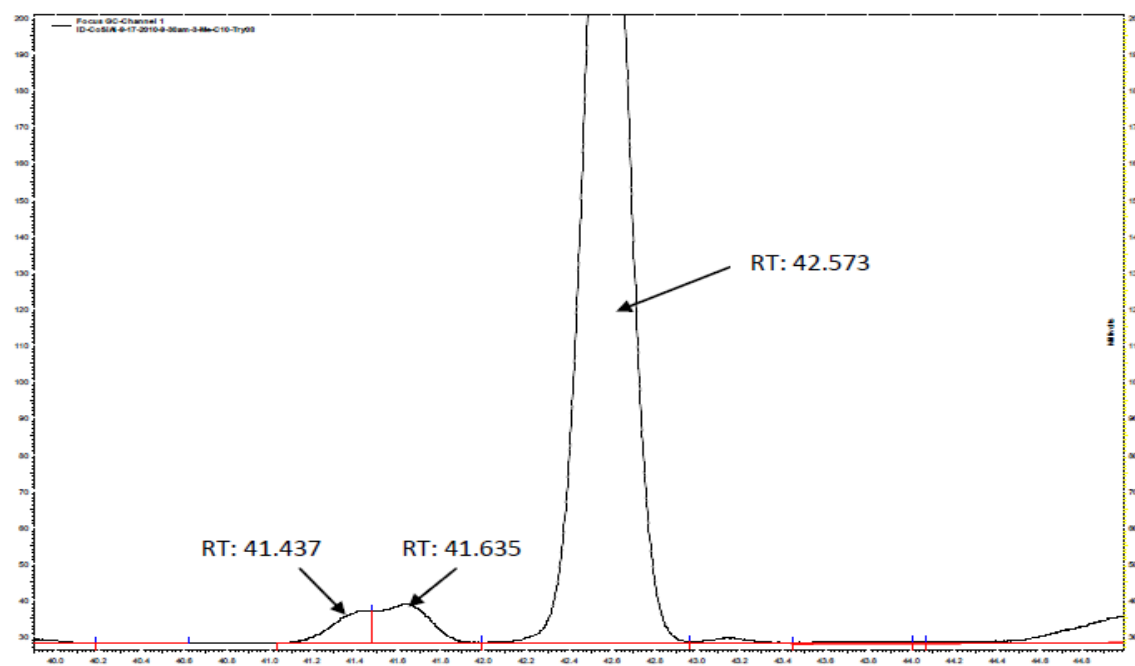
Figure B-26: Gas chromatogram of 3-Methylnonane addition into the Co catalyzed FT products
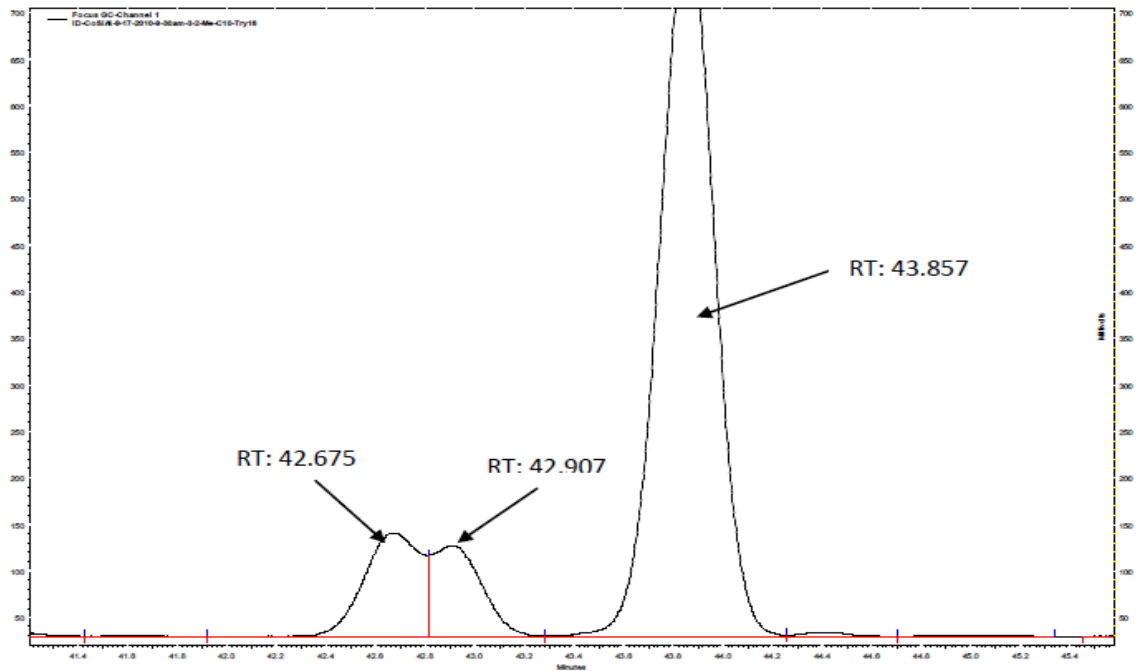
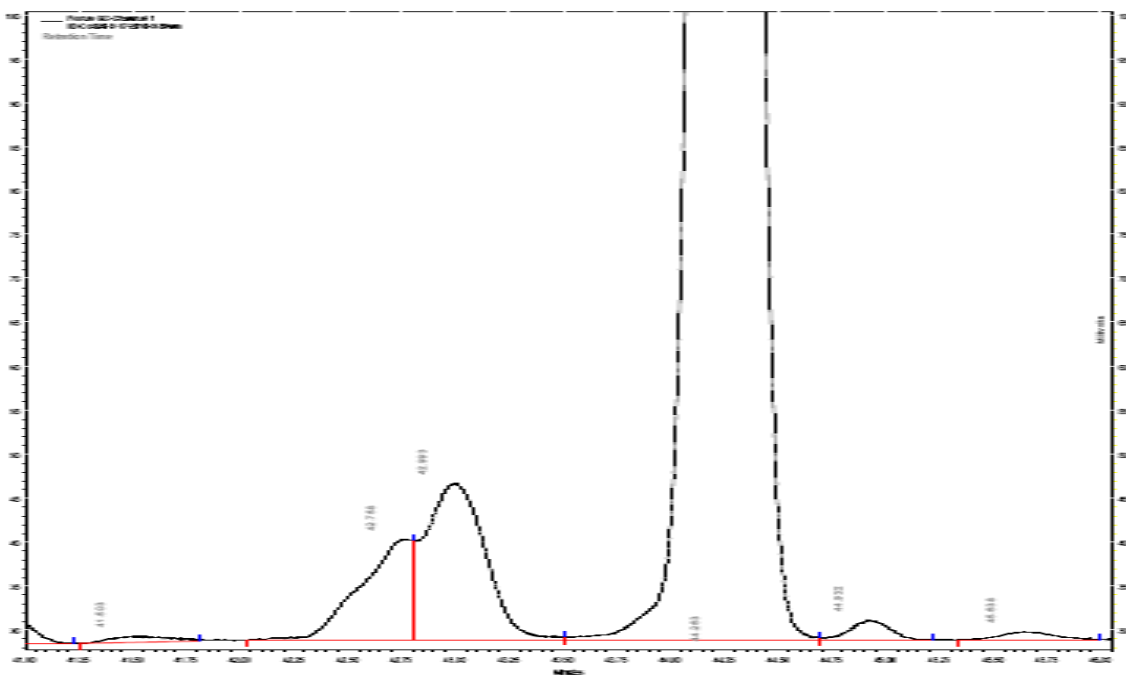**Figure B-27:** Gas chromatogram of 2-Methylnonane addition into the Co catalyzed FT products

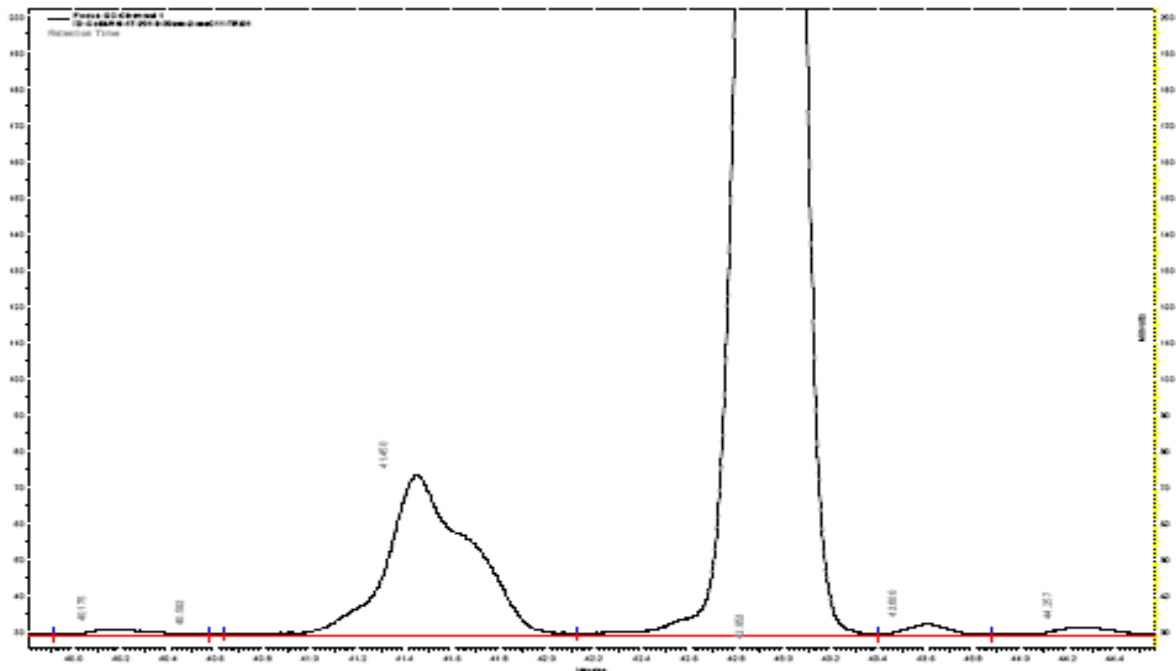**Figure B-28:** Gas chromatogram of hydrocarbons with 11 carbon atoms produced by Co catalyzed FT reactions

Figure B-29: Gas chromatogram of 2-Methyldecane addition into the Co catalyzed FT products
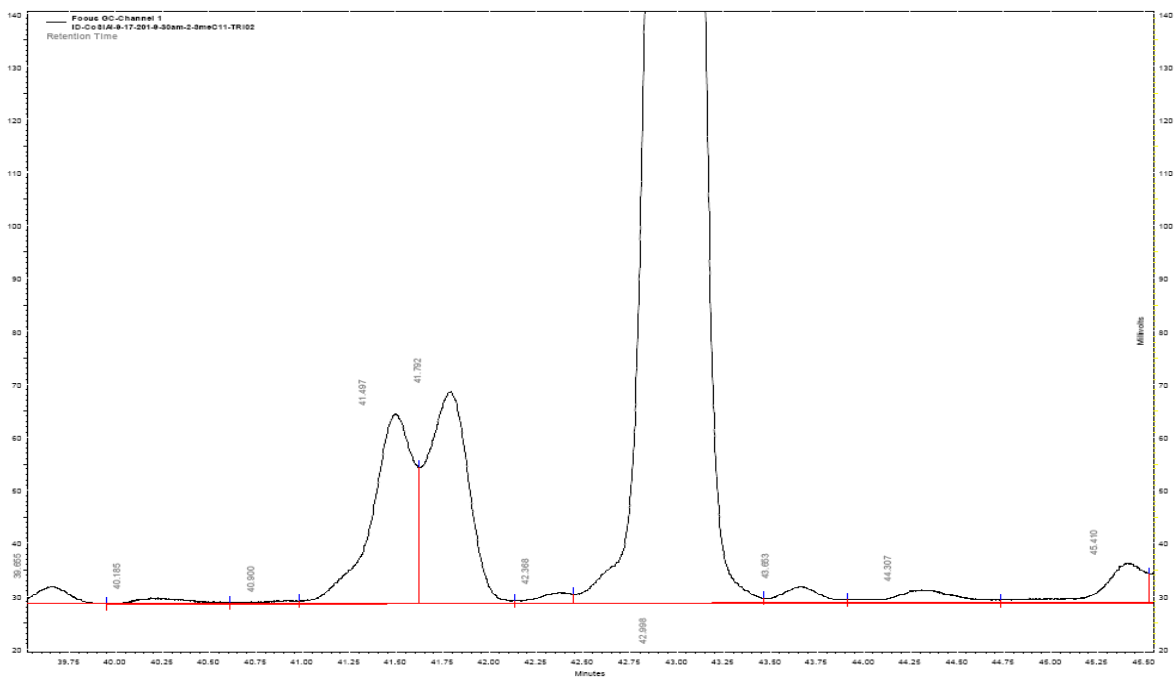

Figure B-30: Gas chromatogram of 3-Methyldecane addition into the Co catalyzed FT products